Study on bio-drying MBT by modelling of moisture removal and evaluation as MSW management system for energy recovery

水分除去モデリング及びエネルギー回収効率評価によるバイオドライング MBT システムの研究

Geun-Yong Ham

A dissertation submitted in partial fulfillment
of the requirements for the degree of
Doctor of Philosophy

Division of Environmental Engineering
Graduate School of Engineering
Hokkaido University
JAPAN

2020

TABLE OF CONTENTS

LIST OF FIGURES

LIST OF TABLES

CHAPTER 1
Introduction

1.1 Background

In hierarchy of waste management, landfilling is the least preferred options for treatment, but most of countries have disposed of municipal solid waste (MSW) into landfill since it is the simplest and cheapest way. When MSW containing high organics and moisture, disposed of landfill without pretreatment, biodegradation of organic matters is kept continuing and thus, it takes long time for stabilization inside the landfill. This lead to long-term management of leachate and landfill gas emission and could be burden on the operator regarding with maintenance cost and at the same time increasing the potential risk to environment by loss of structure and function [1–4].

In Europe, Landfill Directive (99/31/EC) ordered member states for stepwise reduction of organic content in waste destined to landfill. To avoid the landfilling, the most obvious and prevailed technology was incineration but less encouraged due to its negative image. Instead, mechanical biological treatment (MBT) system have emerged to contribute the diversion of the biodegradable waste and to obtain additional value from input waste by the recovery of recyclable materials such as metal, glasses and etc. Since early 1990s, Germany and Austria have already been implemented a simple form of MBT system that consists of low-tech mechanical sorting with low-tech biological stabilization process such as windrow composting [5, 6].

MBT system consists of mechanical sorting and biological stabilization process. Depending on the objective, waste characteristics, products utilization, the mechanical sorting and biological processes can be aligned flexibly in the system. As shown in Fig. 1-1, typical MBT system, aiming on stabilization of organics, begins with mechanical separation of mixed MSW, which is then followed by biological treatment to remove the organics and thermal treatment for the remaining combustible fraction. The biologically and/or thermally stabilized residue from these processes is sent to a landfill for disposal. In biological process, either composting for aerobic or anaerobic digestion (AD) can be applied. Energy also can be recovered as a form of biogas in anaerobic process and refuse-derived fuel (RDF). In solid fuel recovery, separation rate of combustible fraction could be low when moisture content of waste is high. In this case, MSW can be dried first by aerobic process. After reducing moisture content, dried outputs are mechanically separated to recover solid recovered fuel (SRF). This aerobic biological process is called bio-drying and whole process is called bio-drying MBT system that aims on energy recovery as shown in right side of Fig. 1-1. Recovered fuel can be burned in cement kilns or other co-combustion power plants as a fuel, which conserves the conventional energy sources typically used for

those kinds of operations. In early implementation of MBT system, about 85% of operating facility implied a typical MBT system and aims on organic stabilization. As confronting the new era of climate change and transition into low-carbon society, important of energy recovery from solid waste has been increasing. Bio-drying MBT is considered to be practical and economically viable waste treatment option with energy recovery [5, 7–13].

The reactors used in a full-scale bio-drying MBT systems can be divided into three types: dynamic reactors, static reactors, and windrows. Dynamic reactors are used in continuous systems with counter current flow aeration against the waste movement and consist of an inclined rotary drum that is 2-4 m in diameter and a maximum 45 m long (Fig.1-2). Since it is continuous operation, process time takes about 3 to 7 days. But it requires high cost for installation and maintenance. Typical static reactors are enclosed biocell or biocontainer batch-type reactors as shown in Fig.1-3. A biocell is an enclosed rectangular reactor that has a volumetric capacity in the range of 100 to 1000 m^3 and is, at maximum, 50 m long. Waste is charged to the reactor by a wheel loader or conveyor belt. A biocontainer is smaller box reactor with a volume of 20 to 40 m^3 in which waste is loaded from the top of the reactor. A windrow pile system has a pile in a triangular or trapezoidal shape where waste is stacked up to 1.5 or 2.0 m high. In static-type and windrow reactors, forced aeration is accomplished from the bottom. Be contrary to dynamic, static type is advantageous in terms of installation and maintenance cost. But it requires large space for treatment of waste due to long retention time for batch operation. Most full-scale Bio-drying MBT systems in operation are enclosed static-type reactors [5, 14, 15]. Estimation of material flow in a full-scale is important to understand separation rate of fuel material from biodried outputs. However, in previous researches of full-scale bio-drying MBT system, mostly focused on the characteristics of products, such as stabilization, calorific values and methane generation potential [16–19].

In bio-drying process operation, several parameters influence on water removal and biodegradation that are aeration (airflow rate, frequency, and air properties), waste properties (waste time, moisture content, organic content), bulking agent (type, mixing ratio) used to adjust the organic content or moisture content, mixing (interval), and etc. [19–25]. Effects of each parameter on water removal is important to understand drying mechanism in bio-drying process and this can be investigated by lab-scale experiment. Among the various researches studied in lab-scale, aeration has been investigated actively since it is critical in aerobic process. However, most researches focused on effect of one parameter on water removal instead of seeing combined effects of parameters.

1.2 Objectives and methodology

This study aims to understand moisture removal and fuel material recovery from bio-drying MBT system and compare its energy efficiency as a possible option for mixed MSW management by following two approaches.

First, in order to understand the changes in driving force of evaporation and effects of dominant parameters on water removal in bio-drying, lab-scale bio-drying experiment was carried out using simulated waste in column reactor and moisture balance was estimated by using monitored data.

Second, a full-scale bio-drying MBT system was investigated to understand actual water removal and fuel material recovery rate. Then using this measured data and operation data of the system, it has compared with other waste management options that can recover energy to evaluate how energy efficient it is. Environmental impact was also compared by estimation of life cycle CO_2 emission from each system.

1.3 Organization of chapters

This thesis consists of five chapters and the contents of each chapter is as follows:

Chapter 1 describes about the background, objective, methodology and the organization of this research.

Chapter 2 carried out the lab-scale bio-drying experiment to investigate the effect of dominant parameter on water removal in bio-drying. By using the continuously monitored temperature of inlet and outlet air and waste and analyzed CO_2 concentration changes in outlet air, moisture removal model, including metabolic water generation for 15 experimental runs were estimated. Different biodegradation profiles and its limitation caused by different initial condition was discussed. Further, effect of dominant parameters on water removal is evaluated.

Chapter 3 investigated a full-scale bio-drying MBT system, converting mixed MSW into solid fuel by 17-days of bio-drying. Waste samples have collected and analyzed to estimate the material flow by waste component. Based on this, separation rate of fuel materials from biodried outputs and mass changes before and after bio-drying process are discussed. Additionally, by using operation data of bio-drying process and moisture removal model, changes of parameters and resulted water removal under different operation modes were discussed.

Chapter 4 evaluated an energy efficiency of the bio-drying MBT system by comparing it with other waste management options that can recover energy, as incineration, combined system (Anaerobic digestion + Incineration), and RDF production system. Using Asahikawa city data, four systems were compared as possible waste management option with energy recovery there to reflect the reality. Parameters for operation and utilities have referred from different literatures and measured data by the authors were used. Utility consumption and electricity power recovery have calculated based on mass and energy balance. Energy balance and life cycle CO2 emission were estimated and was compared. Sensitivity analysis was carried out and critical operation parameters in each system were discussed.

Chapter 5 summarizes the findings of this research and suggests possible application of the bio-drying MBT system.

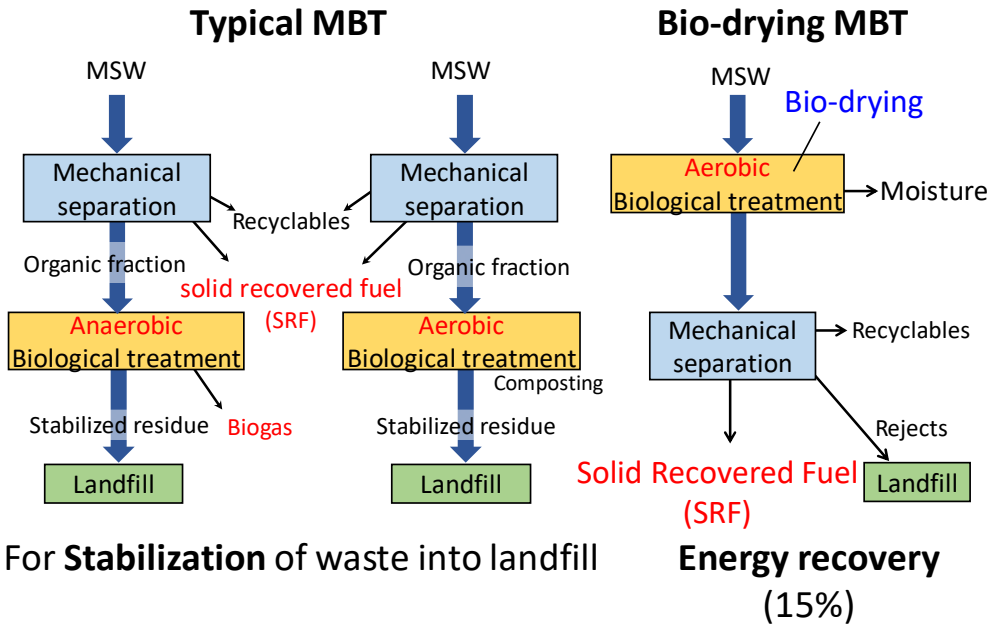

Figure 1-1 Process flow of typical MBT and bio-drying MBT system

Fig.1-1 is referred from Juniper Consultancy Services Ltd (2005) Mechanical-Biological Treatment: A Guide for Decision Makers, Processes, Policies and Markets

(a) Schematic diagram of dynamic reactor

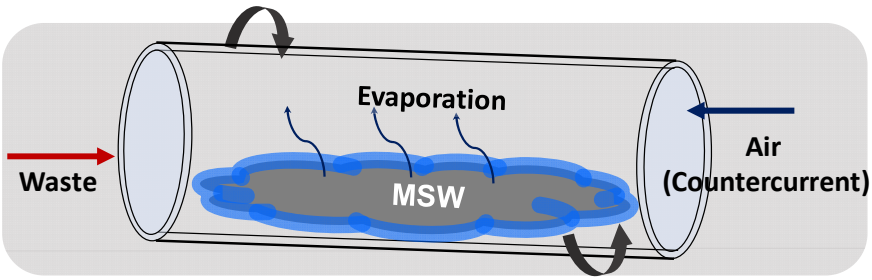

(b) Biodrum (Masias, Spain)

Inner diameter: 2.5 ~ 4.2 m

Length: 25 ~ 50 m

(c) Dano drum (Keppel Seghers, Singapore)

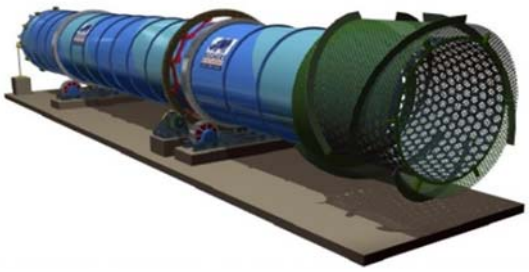

Inner diameter: 3.8 m

Length: 24 ~ 37 m

Figure 1-2 Schematic diagram of dynamic reactor and example of full-scale dynamic reactors

(a) Schematic diagram of static reactor

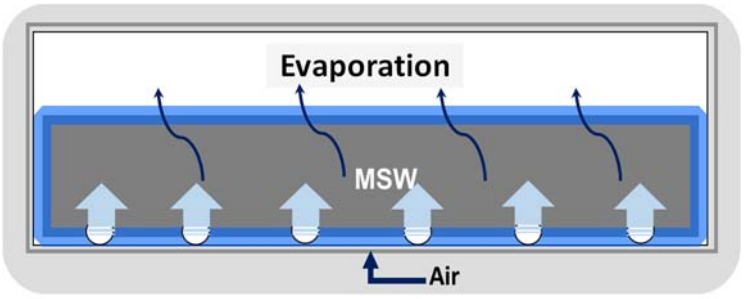

(b) Biocontainer type (Entsorga, Italy)

(c) Biocell type (Ecomaster, Italy)

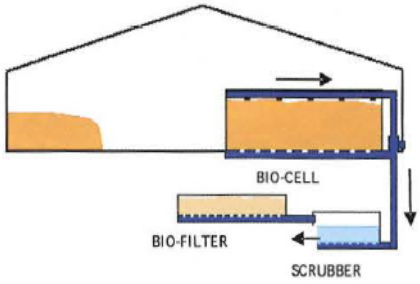

Figure 1-3 Schematic diagram of static reactor and example of full-scale static reactors

All the reactor images in Fig.1-2 and Fig.1-3 are referred from ‘Chiumenti A, Chiumenti R, Diaz L, et al (2005) Modern Composting Technologies. the JG Press Inc.

References

1. Allen A (2001) Containment landfills: The myth of sustainability. Eng Geol 60:3–19. https://doi.org/10.1016/S0013-7952(00)00084-3
2. Hudgins M, Harper S (1999) Operational characteristics of two aerobic landfill systems. Proc Int Conf Solid Waste Technol Manag 358–365
3. Erses AS, Onay TT, Yenigun O (2008) Comparison of aerobic and anaerobic degradation of municipal solid waste in bioreactor landfills. Bioresour Technol 99:5418–5426. https://doi.org/10.1016/j.biortech.2007.11.008
4. Scaglia B, Salati S, Di Gregorio A, et al (2013) Short mechanical biological treatment of municipal solid waste allows landfill impact reduction saving waste energy content. Bioresour Technol 143:131–138. https://doi.org/10.1016/j.biortech.2013.05.051
5. Juniper Consultancy Services Ltd (2005) Mechanical-Biological Treatment: A Guide for Decision Makers, Processes, Policies and Markets
6. Defra (2007) Mechanical biological treatment for municipal solid waste
7. Velis CA, Longhurst PJ, Drew GH, et al (2009) Biodrying for mechanical-biological treatment of wastes: A review of process science and engineering. Bioresour Technol 100:2747–2761. https://doi.org/10.1016/j.biortech.2008.12.026
8. Bayard R, de Araújo Morais J, Ducom G, et al (2010) Assessment of the effectiveness of an industrial unit of mechanical-biological treatment of municipal solid waste. J Hazard Mater 175:23–32. https://doi.org/10.1016/j.jhazmat.2009.10.049
9. Heermann C (2003) Using Mechanical-Biological Treatment for MSW in Europe. Biocycle, 44:58–62
10. Kanning K, Ketelsen K (2013) MBT – Best technology for treatment of moist MSW AD and / or biodrying prior to energy recovery. pp 328–342
11. Velis CA, Longhurst PJ, Drew GH, et al (2010) Production and quality assurance of solid recovered fuels using mechanical-biological treatment (MBT) of waste: A comprehensive assessment. Crit Rev Environ Sci Technol 40:979–1105. https://doi.org/10.1080/10643380802586980
12. Montejo C, Tonini D, Márquez M del C, Fruergaard Astrup T (2013) Mechanical-biological treatment: Performance and potentials. An LCA of 8 MBT plants including waste characterization. J Environ Manage 128:661–673. https://doi.org/10.1016/j.jenvman.2013.05.063
13. Hahladakis J, Purnell P, Iacovidou E, et al (2017) Technical properties of biomass and solid recovered fuel (SRF) co-fired with coal: Impact on multi-dimensional resource recovery value. Waste Manag 73:535–545. https://doi.org/10.1016/j.wasman.2017.07.001

14. Chiumenti A, Chiumenti R, Diaz L, et al (2005) Modern Composting Technologies. the JG Press Inc.
15. Velis CA, Longhurst PJ, Drew GH, et al (2009) Biodrying for mechanical-biological treatment of wastes: A review of process science and engineering. Bioresour Technol 100:2747–2761. https://doi.org/10.1016/j.biortech.2008.12.026
16. Dębicka M, Żygadło M, Latosińska J (2017) The effectiveness of biodrying waste treatment in full scale reactor. Open Chem 15:67–74. https://doi.org/10.1515/chem-2017-0009
17. Evangelou A, Gerassimidou S, Mavrakis N, Komilis D (2016) Monitoring the performances of a real scale municipal solid waste composting and a biodrying facility using respiration activity indices. Environ Monit Assess 188:. https://doi.org/10.1007/s10661-016-5303-6
18. Dziedzic K, Łapczynska-Kordon B, Malinowski M, et al (2015) Impact of aerobic biostabilisation and biodrying process of municipal solid waste on minimisation of waste deposited in landfills. Chem Process Eng - Inz Chem i Proces 36:381–394. https://doi.org/10.1515/cpe-2015-027
19. Tambone F, Scaglia B, Scotti S, Adani F (2011) Effects of biodrying process on municipal solid waste properties. Bioresour Technol 102:7443–7450. https://doi.org/10.1016/j.biortech.2011.05.010
20. Sugni M, Calcaterra E, Adani F (2005) Biostabilization-biodrying of municipal solid waste by inverting air-flow. Bioresour Technol 96:1331–1337. https://doi.org/10.1016/j.biortech.2004.11.016
21. Adani F, Tambone F, Gotti A (2004) Biostabilization of municipal solid waste. Waste Manag 24:775–783. https://doi.org/10.1016/j.wasman.2004.03.007
22. Zhao L, Gu W, Shao L, He P (2012) Sludge Bio-drying Process at Low Ambient Temperature: Effect of Bulking Agent Particle Size and Controlled Temperature. Dry Technol 30:1037–1044. https://doi.org/10.1080/07373937.2012.665113
23. Yang B, Zhang L, Jahng D (2014) Importance of Initial Moisture Content and Bulking Agent for Biodrying Sewage Sludge. Dry Technol 32:135–144. https://doi.org/10.1080/07373937.2013.795586
24. Navaee-Ardeh S, Bertrand F, Stuart PR (2010) Key variables analysis of a novel continuous biodrying process for drying mixed sludge. Bioresour Technol 101:3379–3387. https://doi.org/10.1016/j.biortech.2009.12.037
25. Shao LM, He X, Yang N, et al (2012) Biodrying of municipal solid waste under different ventilation modes: Drying efficiency and aqueous pollution. Waste Manag Res 30:1272–1280. https://doi.org/10.1177/0734242X12462278

CHAPTER 2

Simultaneous effects of airflow rate and biodegradable organic contents on water removal in bio-drying process

2.1 Introduction

In a previous study on bio-drying, the effects of several parameters were examined, including aeration (airflow rate (AFR), frequency), waste properties (waste type, moisture content, organic content (OC)), and bulking agents (type, mixing ratio) used to adjust the OCs or moisture contents. Among them, the AFR and OC have been considered as the primary parameters, and these two parameters were investigated in this study. The simultaneous effects of the AFR and OC were also studied by Huiliñir and Villegas and Colomer-Mendoza et al. [1, 2]. Huiliñir and Villegas used sludge from a wastewater treatment plant used for the slaughterhouse and investigated the AFR (1, 2, and 3 L/min·kg-TS) and OC by changing the ratio of the bulking agents (10%, 23%, and 33%), which resulted in different initial moisture content values of 59%, 68%, and 78%, respectively. Colomer-Mendoza et al. studied AFR (0.88 to 6.42 L/min·kg-TS) and the bulking agent ratio (0% and 15% of mixture) in the bio-drying of garden waste.

Other studies have investigated effects of AFR, OC, and other parameters. Adani et al. studied AFR (0.1–0.4 L/min·kg-TS) in bio-drying of MSW [3], and Navaee-Ardeh et al. investigated AFR (25–75 m^3/h) in a bio-drying process that utilized paper and pulp mill sludge as the feedstock [4]. While other studies have been conducted as batch processes, bio-dried sludge was recirculated in a study by Navaee-Ardeh et al. The effect of OCs was investigated by Yang et al. using different concentration of glucose and ground food waste that were mixed with bio-dried sludge for inoculation [5]. In addition to the AFR and bulking agent ratio, the type of bulking agent, such as sawdust, wood pellets, straw, and corncob [6–8] and initial moisture content for sewage sludge bio-drying [7], and inoculation ratio [6] have also been studied.

In the bio-drying process, moisture is removed by the combined actions of aeration and biodegradation. Generated metabolic heat increases the temperature inside the reactor, and this facilitates the moisture evaporation from the waste. Air then carries the evaporated vapor and discharges it to the atmosphere. Measuring the weight of the waste before and after the experiment is the most common method of determining changes in moisture content. However, this only shows the change in the water amount. To estimate certain ongoing phenomena during the process, temperature, relative humidity in the airflow, and CO_2 concentrations must be continuously measured, and metabolic water generation should be taken into account. Among the previous studies, such continuous monitoring was

performed by Cai et al., Huiliñir and Villegas and Navaee-Ardeh et al. [2, 4, 9]. However, Cai et al. and Huiliñir and Villegas estimated the metabolic water generation through the measurement of VS changes by periodic waste sampling, whereas Navaee-Ardeh et al. estimated metabolic water generation by changes in the CO_2 concentration, but only the AFR was changed as an experimental condition.

Compared with the previously conducted studies that we reviewed, the novelty of our approach is characterized by the monitoring of the simultaneous effects of OC and AFR to balance moisture, including metabolic water generation determined by continuous measurement of the airflow. To establish the moisture balance, inlet and outlet flow of moisture were estimated by continuous measurement of temperature and relative humidity of the air. CO_2 concentrations in the outlet air were periodically analyzed to observe aerobic biodegradation as well as metabolic water generation. Based on the moisture balance, contributions from the AFR and temperature increase on water removal were quantitatively compared.

2.2 Materials and methods

2.2.1 Experimental equipment

As shown in Fig. 2-1, the reactor used in this study was a 25 L acrylic cylindrical reactor with a diameter of 20 cm and a height of 70 cm. The reactor was filled with simulated wastes on a perforated base plate to ensure uniform air distribution from 30 to 60 cm in the reactor. The upper portion was covered with an acrylic lid with a hole for air exhaust. The reactor was insulated with a 5 cm thick layer of styrofoam. A blower was connected to the bottom of the reactor with Teflon tubing. Ambient air was introduced via the blower and moved upward through the reactor toward the exhaust port in the lid. Heat loss through reactor wall by conduction and radiation is negligible referring to the experiment conducted by Zhao (2010) where the loss was less than 1% of energy consumption for evaporation and temperature increase of air and solid materials in lab-scale bio-drying reactor insulated with 100-mm a hollow cotton wall [10, 11].

All the experiments were conducted in a temperature-controlled room at 30 °C ±1 °C. The reactor was placed on an electronic scale (FG-60KBM-H, AND, Korea), and the total weight was measured and manually recorded at 12 h intervals. Each experimental run was terminated when the temperature of outlet air reached that of the ambient air.

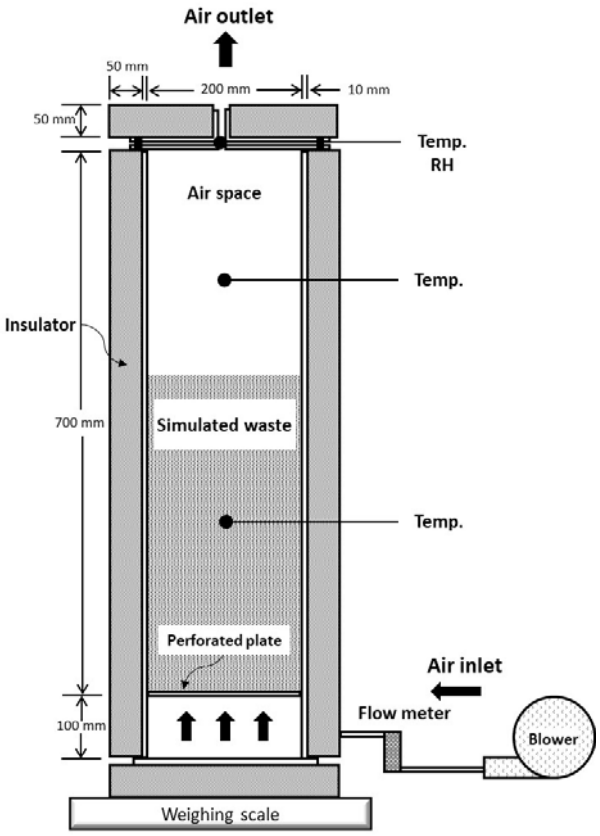

Figure 2-1 Schematic view of the reactor used in the bio-drying experiment

2.2.2 Measurement and analysis

The temperature and humidity of the inlet and outlet air were monitored by a humidity-temperature meter (TES-1365, TES, Taiwan). Three temperature sensors were installed (two inside the reactor and the one at the exhaust port in the lid) and connected to a thermometer (TES-1384, TES, Taiwan). The data logging interval was set to 4 min. Inlet and outlet gas were sampled every 12 h to quantify CO_2 concentrations by gas chromatography (GC-2014, Shimadzu, Japan). An in-line gas flow meter (RMA, Dwyer, United States) was used to monitor the AFR.

At the end of all experimental runs, simulated waste was taken from the reactor, and the final weight was measured. After weighing, the moisture content of the product was determined by oven drying (forced convection drying oven, Chang Shin scientific co., Korea) at 80 °C.

2.2.3 Experimental condition

In the experiment, commercial dog food (Prime Balance, Nutrena, Korea) was used to represent easily biodegradable matter in the simulated waste. Nakasaki et al. and Chang et al. reported that dry dog food can represent the easily biodegradable organic matter, and they demonstrated good reproducibility, which resulted in uniform properties at the beginning and end of the experiment [12, 13]. According to the nutrition level in the dog food used in this experiment, it consisted primarily of carbohydrates (70% d.w.), crude protein (14% d.w.), crude fat, crude fiber, and miscellaneous elements. Based on elemental compositions (C 44.7%, H 6.3%, N 2.4%, O 39.0%, ash 7.6% dry basis) determined by the authors, the chemical composition of the VS was estimated to be $C_{21}H_{36}O_{14}N$.

OC was controlled by changing the ratio of dog food to wood pellets and included 10%, 25%, 50%, 75%, and 100%, by mass. Although the dog food is not 100% biodegradable, its dry basis ratio is referred to as OC for the purpose of this study. The wood pellets were assumed to be non-degradable during the bio-drying process due to their relatively low biodegradability in the relatively short process time of the experiment [8]. As a simulated waste, 3.1 kg of the dog food and wood pellet mixture with the previously mentioned ratios was placed in the column reactor, and the initial moisture content (MC) was set at 40% by adding distilled water. Forty percent of the initial moisture content was determined after measuring the field capacity of the dog food. With over 50% of moisture content, the dog food easily becomes broken down. Return activated sludge, which was collected from an operating wastewater treatment facility, was injected to inoculate the simulated waste and was equal to 10% of the dog food mass on a dry basis.

Regarding aeration, it has been suggested that the recommended aeration rates depend on the substrate in the composting process [14]. The bio-drying process is a modified composting process but focused more on water removal. Therefore, a slightly higher range of AFR can be applied. In this study, the operation range applied in the past study, 0.4–1.1 L/min·kgVS, was used by referring to Adani et al. and Colomer-Mendoza et al. [1, 3]. When the initial OC was 100%, 0.4 L/min·kgVS was multiplied by 3.1 kg, resulting in a value of 1.2, which corresponded to approximately 1 L/min. Therefore, the AFRs selected for experimental analysis were set at 1, 2, and 3 L/min.

Table 2-1 summarizes the experimental conditions employed in this study [11]. All the experimental runs were identified by the initial OC and AFR, such as “10-1” (i.e., 10% OC and a flow rate of 1 L/min). The average relative humidity (RH) of the inlet air in each experiment depended on the season. The total days of operation, initial organic matter (dog food), and final organic matter and MC are also presented in Table 2-1. The equations presented in section 2.3 were used to estimate these final values.

Table 2-1 Different variables and initial conditions in the experiments

Experimental condition							
Runs	Initial				Initial	Final	
	OC	V	RH ± SD	Time	M_O	M_O	W
	%	L/min	%	days	kg	kg	kg
10-1	10	1	61.1 ± 4.7	19	0.314	0.000	1.842
25-1	25	1	23.8 ± 5.0	16	0.786	0.375	1.404
50-1	50	1	23.8 ± 5.5	16	1.571	0.879	1.420
75-1	75	1	15.0 ± 7.2	32	2.357	1.475	0.919
100-1	100	1	33.9 ± 6.1	26	3.143	2.181	1.070
10-2	10	2	59.4 ± 3.2	12	0.314	0.053	1.603
25-2	25	2	15.4 ± 5.3	10	0.786	0.484	1.090
50-2	50	2	23.3 ± 5.1	14	1.571	1.094	0.817
75-2	75	2	10.1 ± 1.7	14	2.357	1.815	0.719
100-2	100	2	36.3 ± 6.8	16	3.143	2.639	0.629
10-3	10	3	59.4 ± 3.2	11	0.314	0.062	1.303
25-3	25	3	16.9 ± 5.4	7	0.786	0.612	0.996
50-3	50	3	14.0 ± 4.7	8	1.571	1.318	0.884
75-3	75	3	9.9 ± 1.9	10	2.357	2.003	0.579
100-3	100	3	33.6 ± 6.7	13	3.143	2.644	0.350

2.3 Model

2.3.1 Model equations

The moisture balance in the reactor can be described by Eqs. (2-1) and (2-2) which show two types of water removal rate in kg/h.

$$\Delta w_{nom} = (V_{out} \times X_{out} \times 10^{-3}) - (V_{in} \times X_{in} \times 10^{-3}) \quad (2\text{-}1)$$

$$\Delta w_{act} = \Delta w_{nom} - \Delta w_{gen} \quad (2\text{-}2)$$

where V is AFR in m^3/h, and X represents the water vapor content per unit air volume, in g/m^3. Eq. (2-1) is the nominal water removal rate (Δw_{nom}), determined by the difference between moisture measured at the inlet and outlet of the airflow on a per hour basis, but the metabolic water generation

(Δw_{gen}) is not considered. Therefore, the actual water removal rate, Δw_{act}, was calculated using Eq. (2-2).

Table 2-2 summarizes other equations used in the model, and the nomenclature is provided at the end of this chapter [11]. The outlet AFR (V_{out}) was calculated by considering the change in air density of the inlet airflow (V_{in}) (Eq. (2-3)), where T_{in} and T_{out} are temperature of inlet and outlet air in ℃. X, which denotes the water vapor per unit air volume, was calculated using Eq. (2-4) as a function of water vapor pressure (pv). The maximum value of water vapor pressure that can be reached at any temperature is defined as the saturated water vapor pressure (pvs). The ratio between pv and pvs is the RH.

For biodegradation, it was assumed that the organics were fully degraded which can thus be expressed by Eq. (2-7). CO_2 generation rate ($\triangle C_{gen}$) was estimated by the difference between the CO_2 concentrations in the air at the inlet and outlet (Eq. (2-8)). Degraded organics and generated metabolic water per unit time can be calculated using Eqs. (2-9) and (2-10), which are based on Eq. (2-8).

The mass of organics (M_O) and moisture (W) at a particular time or its change during a particular period of time can be estimated by the integration of each rate ($\triangle M_O$, $\triangle w$). MC can be calculated by the ratio between water mass to total waste mass at a specific time, and OC was estimated by the ratio of M_O to total dry mass.

The rate of heat generation, ΔQ_{gen}, was calculated using Eq. (2-11) by multiplying the reaction heat of the degraded organics. Spoehr and Milner suggested the empirical method for calculating the heat of combustion for any type of organic matter is expressed by Eq. (2-12),

$$Q = \left(127 \times \frac{\{100 \times (2.66 \times C\% + 7.94 \times H\% - O\%)\}}{398.9} + 400\right) \times \frac{4.184\ kJ}{1\ kcal} \qquad (2\text{-}12)$$

where Q is the heat of combustion for degraded organics in kJ/kg, and C%, H%, and O% are the weight percentages of carbon, hydrogen, and oxygen, respectively, on an ash-free basis [15]. For the dog food used in this study, its heat of combustion was estimated to be 20406 kJ/kg. Heat transfer in the inlet and outlet airflow (ΔQ_{in} and ΔQ_{out}) is calculated using the sum of dry air and water vapor enthalpy by applying Eq. (2-13).

Table 2-2 Equations used for mass and heat balance

Contents	Equation	
Airflow rate of outlet air (m^3/h)	$V_{out} = \frac{(273.15 + T_{out})}{(273.15 + T_{in})} \times V_{in}$	(2-3)
Water vapor per unit air volume (g/m^3)	$X = \frac{217 \times pv}{273.15 + T}$	(2-4)
Water vapor pressure (Pa)	$pv = RH \times pvs$	(2-5)
Saturated water vapor pressure (Pa)	$pvs = 6.1078 \times 10^{\frac{7.5 \times T}{T + 237.3}}$	(2-6)
Organic degradation	$C_{21}H_{36}O_{14}N + 22.3\ O_2 \rightarrow 21\ CO_2 + 16.3\ H_2O + NH_3 + Heat$	(2-7)
Generated CO_2 (kmol/h)	$\Delta C_{gen} = [(V \times CO_2)_{out} - (V \times CO_2)_{in}] \times \frac{1}{100} \times \frac{1\ kmol\ CO_2}{22.4\ m^3}$	(2-8)
Degraded organics (kg/h)	$\Delta M_O = \frac{1}{21} \times \Delta C_{gen} \times \frac{533.2\ kg}{1\ kmol}$	(2-9)
Metabolic water (kg/h)	$\Delta w_{gen} = \frac{16.3}{21} \times \Delta C_{gen} \times \frac{18\ kg}{1\ kmol}$	(2-10)
Heat generation (kJ/h)	$\Delta Q_{gen} = \Delta M_O \times 20406\ kJ/kg$	(2-11)
Heat transfer in air flow (kJ/h)	$\Delta Q = h_{dry} \times \rho_a \times V + h_{vapor} \times X \times 10^{-3} \times V$	(2-13)
Enthalpy of dry air (kJ/kg)	$h_{dry} = 1.006 \times T$	(2-14)
Enthalpy of water vapor (kJ/kg)	$h_{vapor} = 1.805 \times T + 2501$	(2-15)
Density of dry air (kg/m^3)	$\rho_a = 1.293 \times \frac{273.15}{273.15 + T}$	(2-16)

2.3.2 Example of model output

As an example of model output, Fig. 2-2 shows the time profile for the run 50-3 (i.e., 50% of initial OC and a 3 L/min inlet AFR) [11]. The average inlet RH was 14.0% (see Table 2-1). Values in Fig. 2-2a were measured, and the others were calculated using the equations in Table 2-2. During the initial period when biodegradation had not yet begun, which is referred to as "w/o BIO" in the figure, T_{in} and T_{out} were held constant, and the slight decrease of T_S (temperature inside reactor) was due to heat loss associated with evaporation.

After one day, CO_2 concentrations began to increase, which is indicative of a biodegradation process at work. The integrated area under the CO_2 curve presents the extent of organic degradation. During the biodegradation period, referred to as "w/ BIO," nominal water removal rate (Δw_{nom}) increased as T_{out} increased. This is one of the fundamental features of bio-drying, though actual water removal rate (Δw_{act}) was decreased by metabolic water generation rate (Δw_{gen}).

Microbial biodegradation of organic matter gradually decreased after it peaked at its maximum. Either remaining OC or MC could have affected microbial activity, which is discussed in detail later. Fig. 2-2c shows the heat balance. The difference between ΔQ_{gen} and ΔQ_{out} was indicative of the heat used for evaporation or loss from the reactor.

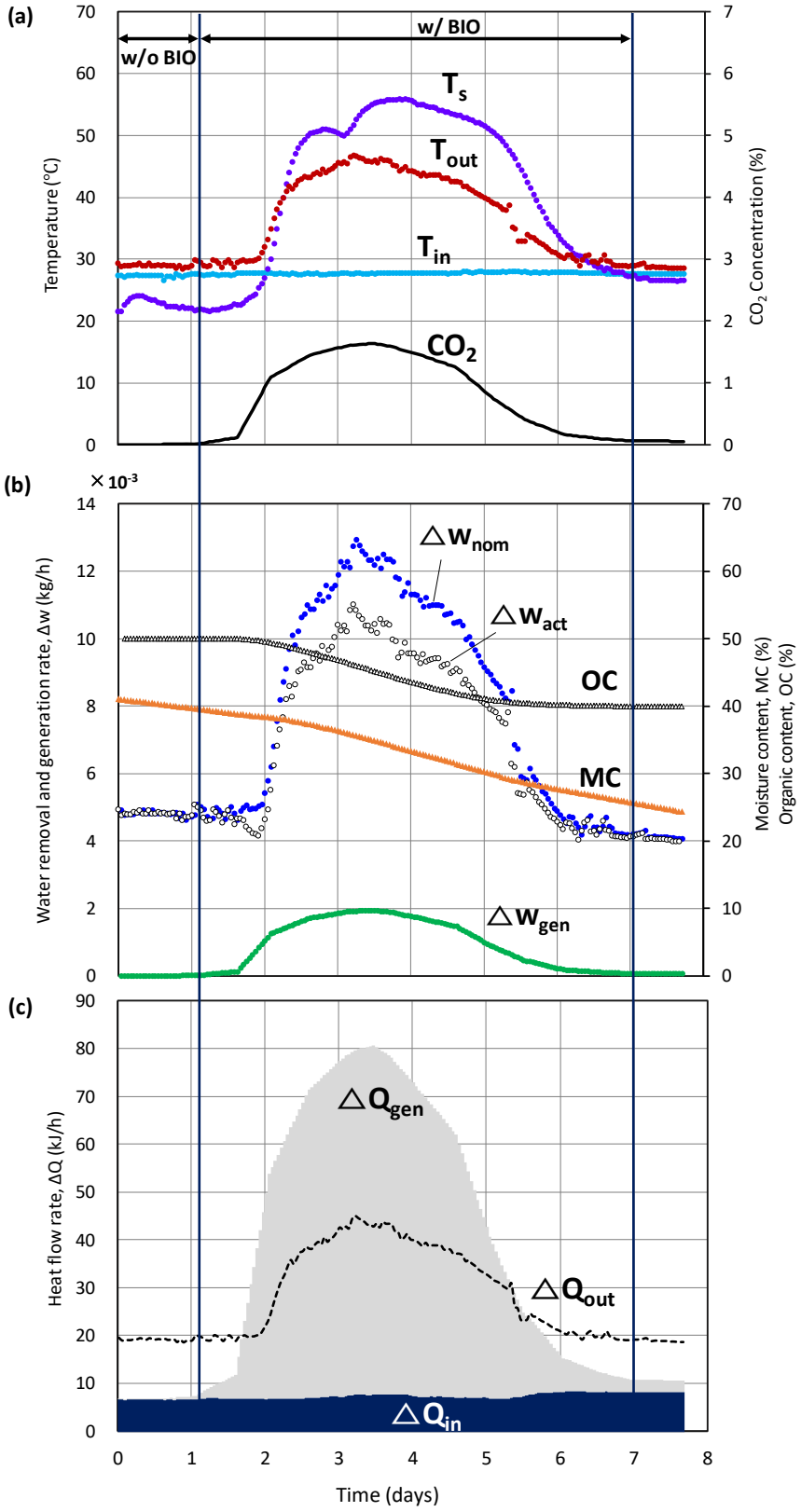

Figure 2-2 Experimental data and model output of run "50-3"

(a) Temperature and CO_2 concentration profiles (Measured), (b) Rate of water mass changes in balance (Estimated), (c) Heat profiles (Estimated)

2.3.3 Reliability of model

The mass of removed water (W_{act}) calculated by the model (integration of $\triangle w_{act}$) was compared with that of the measured in experiments during entire experimental period, as shown in Fig. 2-3, where each label indicates the initial OC [11]. The magnitude of error is generally within 20%. Therefore, the model estimated the bio-drying phenomena reasonably well.

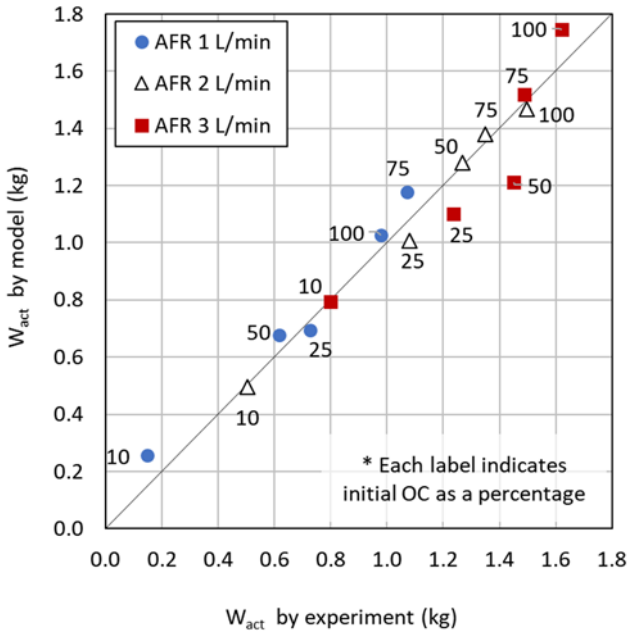

Figure 2-3 Comparison of actual removed water mass (W_{act}) between experiment and model during entire experimental period

2.4 Discussion

2.4.1 Drying mechanism in the bio-drying process

Fig. 2-4 shows drying mechanism and changes of pvs (saturated water vapor pressure) and X_{sat} in the bio-drying process. As shown in Fig. 2-4a, drying is a process of moisture transfer from the surface of waste to air. Evaporation is driven by the differences of pvs on the waste surface and water vapor pressure (pv) of the air. Since the RH of the outlet air was always 100% in all experimental runs, pv (water vapor pressure) at inlet temperature increases to pvs at outlet temperature. The difference between those pvs and pv i.e. pvs-pv, is the driving force of evaporation. As the temperature increased, the pvs in the air increased so as water vapor per unit air volume (X), thus more water can be evaporated.

The change of pv in the air from the inlet to outlet is schematically shown by the broken arrow in Fig. 2-4b. In w/o BIO period, before biological decomposition occurred, there were no increases in

temperature due to the absence of heat associated with biodegradation. Consequently, pv in the air increased only up to the pvs at the same temperature when it was introduced into the reactor. However, once biodegradation proceeded under w/ BIO period, the heat generation increased the waste temperature. Simultaneously, the initial driving force of evaporation increased dramatically due to a high pvs, which was indicative of an increase in the water content in the outlet air, X_{out}.

Water removal rate is increased with biodegradation as shown in Fig. 2-4b, and the airflow carried saturated vapor out of the reactor. In w/o BIO period, only the influence of AFR can be discussed, and the relationship of 1-(RH/100) = (Δw_{act} = Δw_{nom} in this case) for different AFR can be considered as shown in Fig. 2-5 [11]. A regression line for AFR = 1 L/min was first determined by assuming the removal rate was zero at a RH of inlet air = 100%, whereby the lines for AFR = 2 L/min and 3 L/min are simply multiplied by 2 and 3, respectively.

The lower the RH of the inlet air, which resulted from the large amount of water removal associated with the increasing gap between the pvs and the pv. The water removal rate is proportionate to AFR. Since outlet air was always saturated, AFR has simply the replacement effect of saturated air in the reactor.

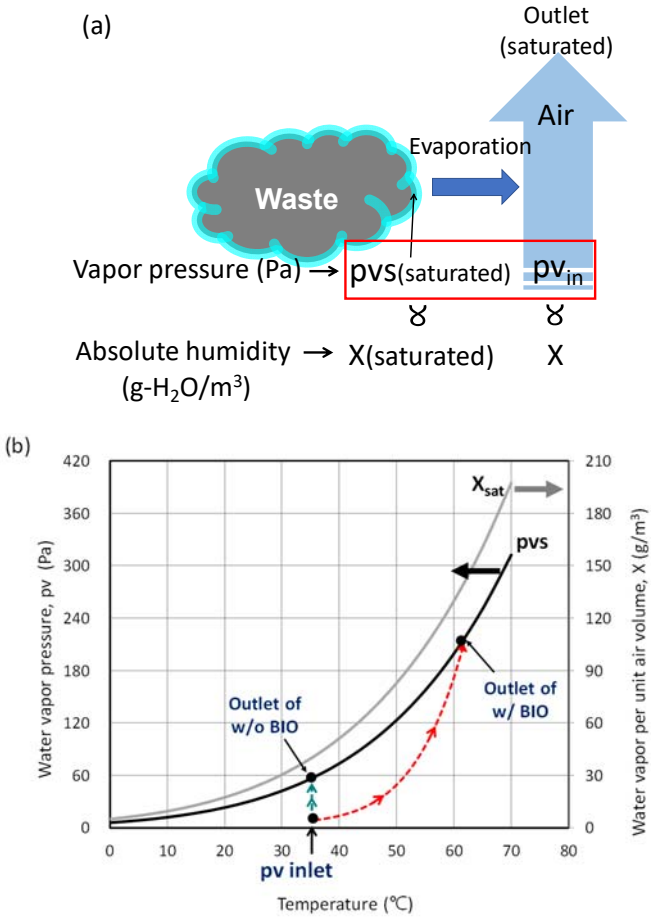

Figure 2-4 Schematic diagram of mechanism and driving force of drying in bio-drying process

(a) drying mechanism, (b) temperature dependence of pvs and X_{sat} and increase of water vapor pressure (pv)

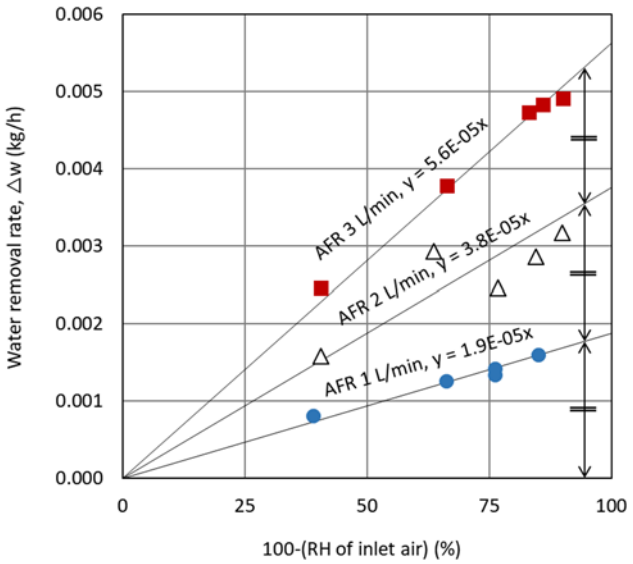

Figure 2-5 Relations between water removal rate and RH of inlet air under different AFR during w/o BIO period

2.4.2 Biodegradation of organic matter and limiting factors

Different initial conditions of the OC and AFR induced different biodegradation characteristics. To observe the extent of biodegradation, the CO_2 generation rate ($\triangle C_{gen}$) and MC profiles are shown in Fig. 2-6 [11]. The $\triangle C_{gen}$, expressed in kmol/h, is calculated using the AFR and CO_2 concentrations in the outlet air (Eq. (2-8)). The integration of each curve is proportional to the amount of degraded OC. The numbers in brackets indicate the initial and final OC, which are defined by the ratio of organics to total dry solids.

CO_2 generation rate curves of all runs were bell-shaped and had longer tails at lower AFRs and higher OC values. In runs with the AFR set at 3 L/min (Fig. 2-6c), biodegradation did not continue very long compared to the runs with lower AFRs because microbial activity was limited by low levels of MC, even though sufficient OC was still available (i.e., 19%, 42%, and 84% corresponding to initial OC values of 25%, 50%, and 100%, respectively). The low MC was caused by high AFR values that rapidly carried out all vaporized water.

By contrast, in runs using an AFR of 1 L/min, biodegradation continued for a longer period of time until the OC decreased to 12% and 28%, corresponding to initial OC values of 25% and 50%, respectively. During the experiment, MC was maintained around 40% due to the low AFR. In this case, biodegradation was terminated due to the low concentrations of organics, not by moisture.

In run 100-1, biological degradation ceased in spite of 69% of the organics remaining because the feed material was composed only of dog food. Without bulking material (wood pellets), the dog food stuck together, and the biodegradation was limited due to a reduction in the contact area associated with short-circuiting of the airflow around larger masses of dog food.

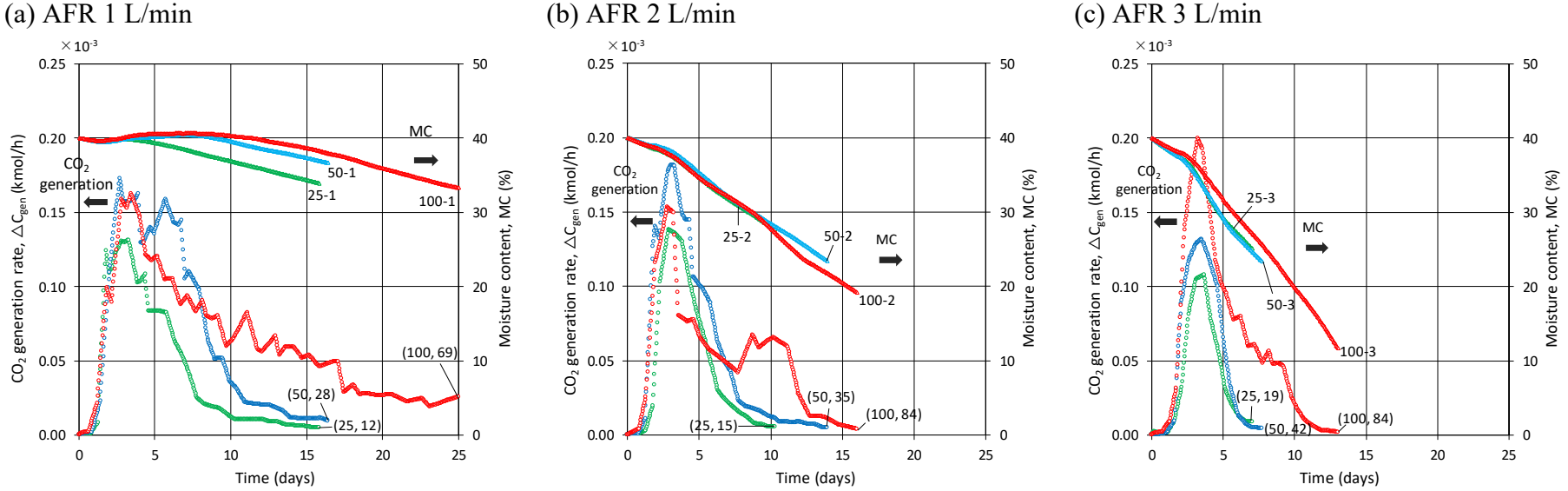

Figure 2-6 CO_2 generation rate and moisture content profiles during entire experimental period

2.4.3 Effects of air flow and biodegradation

Fig. 2-7 depicts a conceptual diagram of the water removal rate in the bio-drying process [11]. Metabolic water generation rate ($\triangle w_{gen}$) is depicted as a negative value to indicate water addition in bio-drying process, and the water removal rate during the w/o BIO period is denoted as $\triangle w_{air}$. From this figure, the following three water removal rates during the w/ BIO period can be defined.

Effect of airflow: $\triangle w_{air}$ (constant from w/o BIO)

Effect of temperature increase (nominal): $\triangle w_{nom}$-$\triangle w_{air}$

Effect of temperature increase (actual): $\triangle w_{nom}$ - $\triangle w_{air}$ - $\triangle w_{gen}$

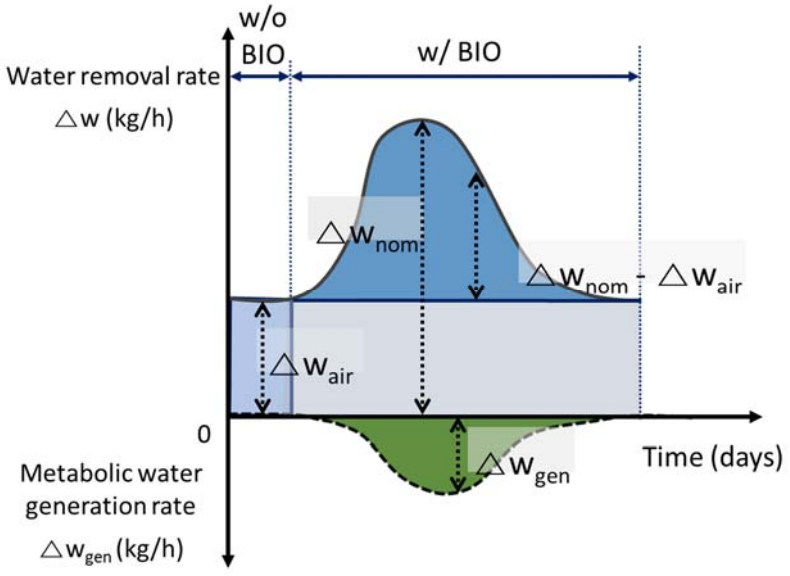

Figure 2-7 Conceptual diagram of water removal rate in the bio-drying process

Given that the time profile was different among experiments (refer to Fig. 2-6), a comparison of the water removal rate and maximum temperature of the simulated waste at the peak point of CO_2 concentration for all the runs is shown in Fig. 2-8 [11].

Except for the runs with 10% of the initial amount of OC, where less heat generation occurred due to the small amount of organic matter, the maximum temperature of the outlet air ranged between 45 ℃ and 50 ℃. The metabolic water generation rate, $\triangle w_{gen}$, remained virtually constant regardless of AFR and initial OC. A constant $\triangle w_{gen}$ indicates that biodegradation rate at peak time did not depend on the experimental conditions in this study.

Compared with the Fig. 2-8a and Fig. 2-8b, the nominal effect of temperature increase ($\triangle w_{nom}$-$\triangle w_{air}$) on water removal remarkably increased as the AFR increased, but so did $\triangle w_{air}$. Airflow replace the saturated vapor as mentioned in previous section, so replaced volume of air is proportionately

increased with AFR in unit time. To exclude the increased effect of replaced air, each water removal rate was divided by the AFR, $(\triangle w_{nom}-\triangle w_{air}) / V$ and $\triangle w_{air} / V$, as shown by the broken line in Fig. 2-8b and 8c, and these were similar to the result when the AFR was 1 L/min. Therefore, the effect of airflow was higher than the temperature increase.

As a result, the actual water removal rate, which was determined by the difference between $(\triangle w_{nom}-\triangle w_{air})$ and $\triangle w_{gen}$ curves also increased with AFR because $\triangle w_{gen}$ remained virtually constant regardless of the AFR.

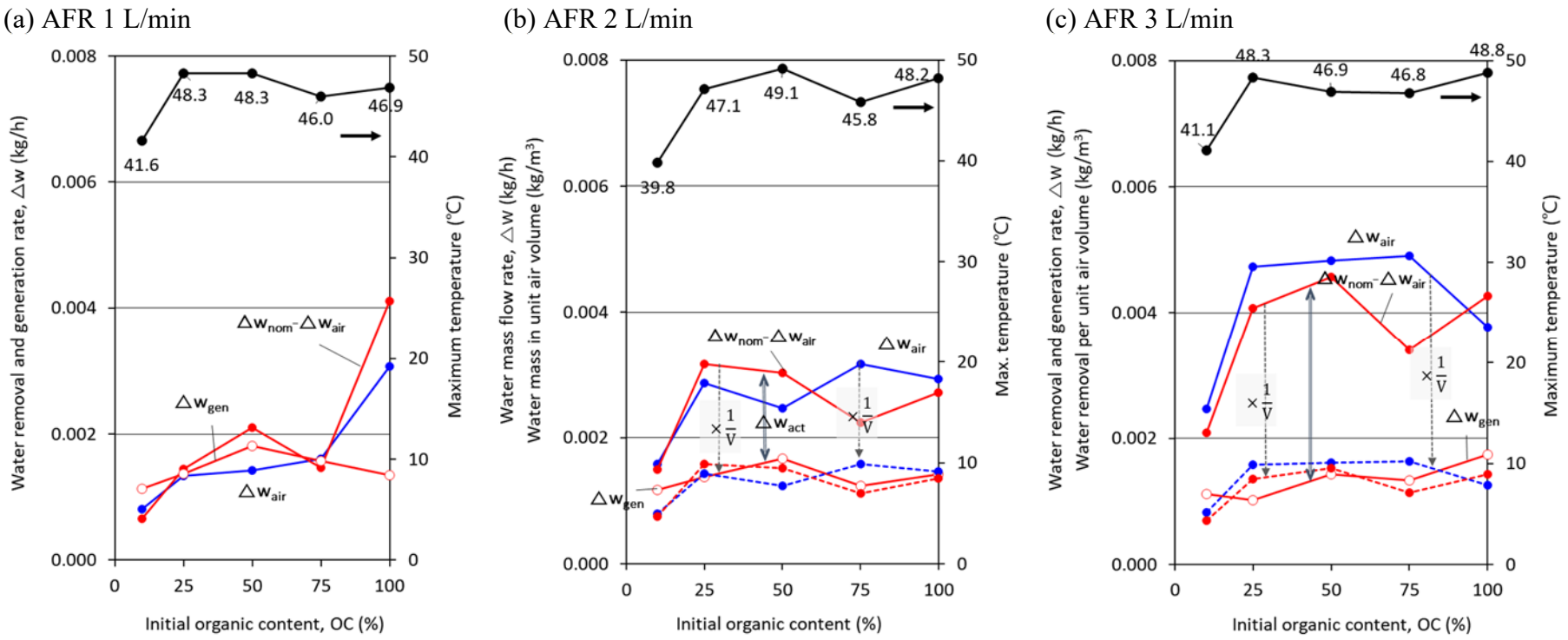

Figure 2-8 Water removal rate defined in Fig. 2-7 at the peak point of CO_2 concentration

2.4.4 Total water removal by effect of AFR and temperature increase

The previous section discussed the water removal rate at the peak point of CO_2 concentration. However, the efficiency of drying should be evaluated by the total amount of removed water throughout the experiment period.

As shown in Fig. 2-9 for the integrated amount of water removal during the w/ BIO period, the amount of nominal removed water mass, W_{nom}, increased as the initial OC increased [11]. This was caused by the difference in the duration of aerobic biodegradation. In other words, as shown in Fig. 2-6a, when the initial OC is high, the aerobic reaction continued for a longer period of time. Therefore, the amount of moisture removal increased with a higher water vapor pressure (pvs) and with a longer duration of saturated vapor replaced by airflow.

There was little difference by AFR in W_{nom} (Fig. 2-9), because the shorter duration of the aerobic reaction associated with high AFR was made up or vice versa (see Fig. 2-6). The duration of active biodegradation is shown in the bracket. On the other hand, W_{act} significantly decreased in lower AFR runs because of the considerable amount of metabolic water generation by long biodegradation. Meanwhile, aerobic biodegradation was terminated due to low MC (see Fig. 2-6c) which resulted from the significant replacement of moisture by a high AFR.

Finally, the effect of temperature increase compared with the effect of AFR on water removal is presented in Fig. 2-10. ($W_{nom}-W_{air}$) refers to the water mass removed by increases in temperature and ($W_{nom}-W_{air}-W_{gen}$) shows the ultimate amount of water removed, including the negative effect of added metabolic water. All points were plotted against W_{air}, which is the water removal solely associated with aeration. OC values of 10%, 50%, and 100% are plotted for comparison among all runs, and each OC is represented with different marks.

In each AFR condition, the higher the initial OC, both W_{air} and ($W_{nom}-W_{air}$) increased due to the longer period of elapsed time, which maximizes the effect of increases in temperature. However, when metabolic water is taken into account, the actual water removal ($W_{nom}-W_{air}-W_{gen}$) by biodegradation decreased at lower AFR values, which was especially true in runs 10-1 and 50-1 that showed negative values or values close to zero due to the reduced replacement effect. In case 100-1, agglomerated feed materials interrupted the air passage, and this resulted in less biodegradation as well as less metabolic water generation. When comparing the x- and y-axis values of ($W_{nom}-W_{air}-W_{gen}$), of which sum are equal to the actual water removal, the effects of airflow associated with air replacement was always greater on water removal than effect of temperature increase associated with biodegradation.

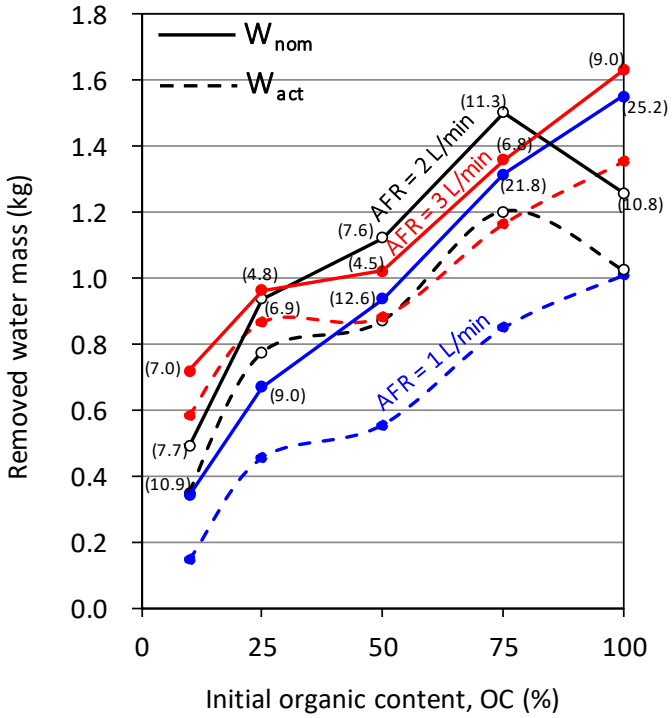

Figure 2-9 Comparison of nominal removed water mass (W_{nom}) and actual removed water mass (W_{act}) during w/ BIO period

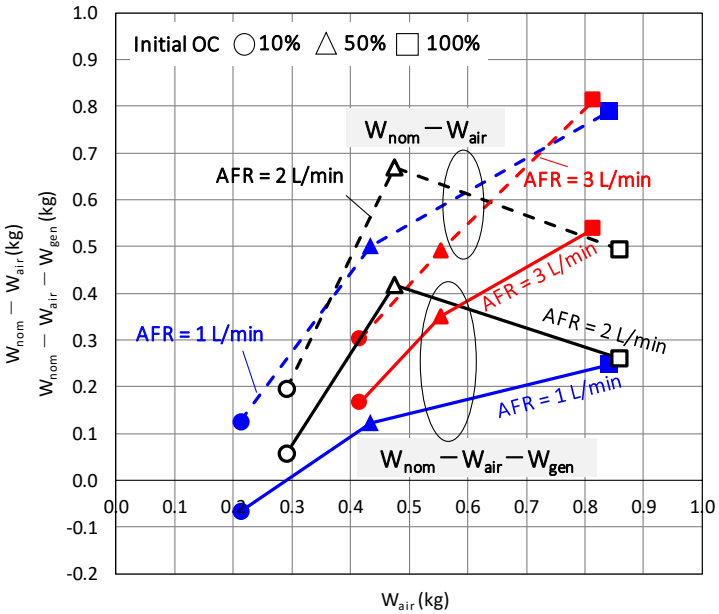

Figure 2-10 Effect of temperature increase (W_{nom}-W_{air}, W_{nom}-W_{air}-W_{gen}) on water removal compared with the effect of airflow (W_{air})

2.5 Conclusion

Fig. 2-11 summarizes the overall water removal mechanism in the bio-drying process under different initial conditions, including variations in OC (organic content), AFR (airflow rate), and RH (relative humidity) of the inlet air. Evaporation is driven by the difference between the pvs (saturated water vapor pressure) of the waste surface and the pv (water vapor pressure) in the passing air, and this driving force increased either due to temperature increases associated with biodegradation or the dryness of introducing air. However, high OC was a negative contribution with respect to water removal due to the generation of metabolic water. On the other hand, saturated vapor in the reactor was carried out by airflow, so high AFR enhanced the water removal rate. But excessive AFR would terminate biodegradation due to the reduction in MC even though organics remained. Water removal associated with air replacement was generally greater than that associated with temperature increases caused by biodegradation.

In the bio-drying process, all the parameters are interdependent, and there are several feedback loops as previously mentioned. The findings of this study can be used for the design and operation of a full-scale system.

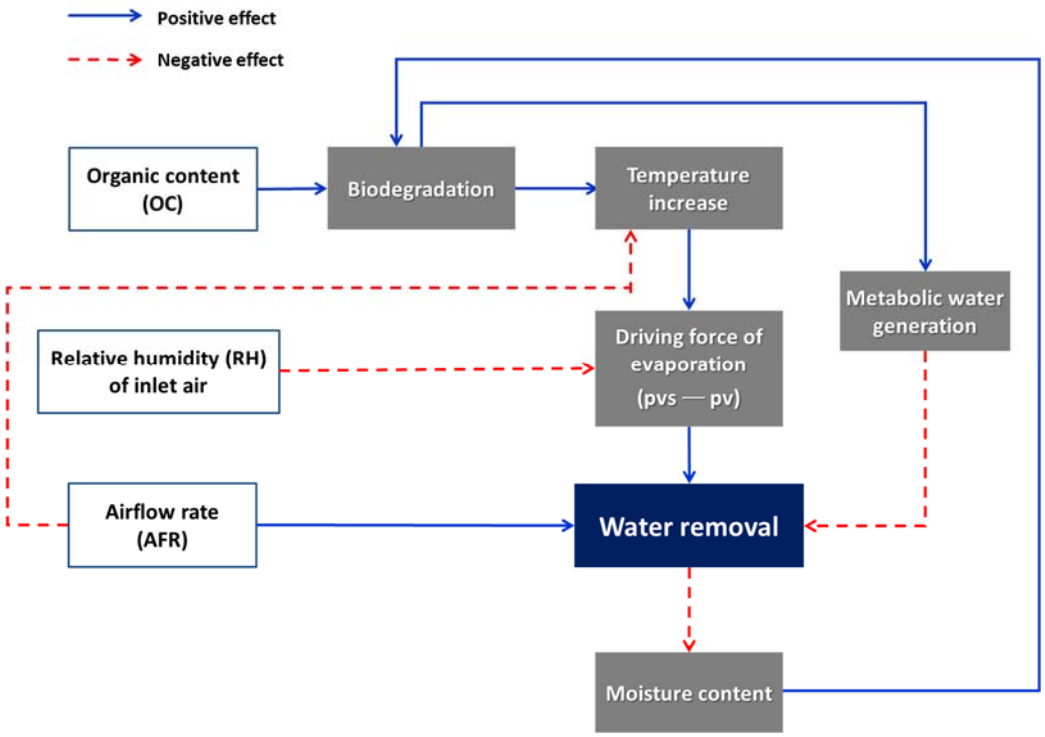

Figure 2-11 Overall water removal mechanism in the bio-drying process

Nomenclature			
Symbol		Unit	Definition
State variables	t	days	Time
	T	℃	Temperature
	V	m^3/h	Airflow rate
	CO_2	%	CO_2 concentration
	X	g/m^3	Water vapor per unit air volume
	RH	%	Relative humidity
	ρ_a	kg/m^3	Density of dry air
	pv	Pa	Water vapor pressure
	pvs	Pa	Saturated water vapor pressure
Decomposition	M_O	kg	Organic mass
	ΔM_O	kg/h	Organic degradation rate
	ΔC_{gen}	kmol/h	CO_2 generation rate
	OC	%	Organic content
Moisture	W	kg	Water mass
	Δw	kg/h	Water removal rate
	Δw_{gen}	kg/h	Metabolic water generation rate
	MC	%	Moisture content
Heat	ΔQ	kJ/h	Heat flow rate
	ΔQ_{gen}	kJ/h	Metabolic heat generation rate
	Q	kJ/kg	Heat of combustion for degraded organics
	h_{dry}	kJ/kg	Enthalpy of dry air
	h_{vapor}	kJ/kg	Enthalpy of water vapor

Subscript	Definition
in	Inlet
out	Outlet
s	Waste
nom	Nominal
act	Actual
air	Removed by airflow

References

1. Colomer-Mendoza FJ, Herrera-Prats L, Robles-Martínez F, et al (2013) Effect of airflow on biodrying of gardening wastes in reactors. J Environ Sci 25:865–872. https://doi.org/10.1016/S1001-0742(12)60123-5
2. Huiliñir C, Villegas M (2015) Simultaneous effect of initial moisture content and airflow rate on biodrying of sewage sludge. Water Res 82:118–28. https://doi.org/10.1016/j.watres.2015.04.046
3. Adani F, Baido D, Calcaterra E, Genevini P (2002) The influence of biomass temperature on biostabilization-biodrying of municipal solid waste. Bioresour Technol 83:173–179. https://doi.org/10.1016/S0960-8524(01)00231-0
4. Navaee-Ardeh S, Bertrand F, Stuart PR (2010) Key variables analysis of a novel continuous biodrying process for drying mixed sludge. Bioresour Technol 101:3379–3387. https://doi.org/10.1016/j.biortech.2009.12.037
5. Yang B, Zhang L, Lee Y, Jahng D (2013) Novel bioevaporation process for the zero-discharge treatment of highly concentratedorganic wastewater. Water Res 47:5678–5689. https://doi.org/10.1016/j.watres.2013.06.044
6. Song X, Ma J, Gao J, et al (2017) Optimization of bio-drying of kitchen waste: inoculation, initial moisture content and bulking agents. J Mater Cycles Waste Manag 19:496–504. https://doi.org/10.1007/s10163-015-0450-3
7. Yang B, Zhang L, Jahng D (2014) Importance of Initial Moisture Content and Bulking Agent for Biodrying Sewage Sludge. Dry Technol 32:135–144. https://doi.org/10.1080/07373937.2013.795586
8. Zhao L, Gu WM, He PJ, Shao LM (2011) Biodegradation potential of bulking agents used in sludge bio-drying and their contribution to bio-generated heat. Water Res 45:2322–2330. https://doi.org/10.1016/j.watres.2011.01.014
9. Cai L, Gao D, Chen T Bin, et al (2012) Moisture variation associated with water input and evaporation during sewage sludge bio-drying. Bioresour Technol 117:13–19. https://doi.org/10.1016/j.biortech.2012.03.092
10. Zhao L, Gu WM, He PJ, Shao LM (2010) Effect of air-flow rate and turning frequency on bio-drying of dewatered sludge. Water Res 44:6144–6152. https://doi.org/10.1016/j.watres.2010.07.002
11. Ham GY, Lee DH, Matsuto T, et al (2020) Simultaneous effects of airflow and temperature increase on water removal in bio-drying. J Mater Cycles Waste Manag. https://doi.org/10.1007/s10163-020-01000-x

12. Chang JI, Tsai JJ, Wu KH (2005) Mathematical model for carbon dioxide evolution from the thermophilic composting of synthetic food wastes made of dog food. Waste Manag 25:1037–1045. https://doi.org/10.1016/j.wasman.2005.01.018
13. Nakasaki K, Nag K, Karita S (2005) Microbial succession associated with organic matter decomposition during thermophilic composting of organic waste. Waste Manag Res 23:48–56. https://doi.org/10.1177/0734242X05049771
14. Ahn HK, Richard TL, Choi HL (2007) Mass and thermal balance during composting of a poultry manure-Wood shavings mixture at different aeration rates. Process Biochem 42:215–223. https://doi.org/10.1016/j.procbio.2006.08.005
15. Spoehr HA, Milner H (1949) The chemical composition of Chorella; effect of environmental conditions. Plant Physiol 120–149. https://doi.org/10.1104/pp.24.1.120

CHAPTER 3

Material and moisture balance in a full-scale bio-drying MBT system for solid fuel production

3.1 Introduction

Most of full-scale Bio-drying MBT systems in operation employ enclosed static-type reactors. Depending on waste input, waste loading methods, and management of exhaust gas, either biocell (100 to 1000m^3 volume, waste loading by wheel loader or conveyor belt) or biocontainer (20 to 40m^3 volume, waste loading from top of the reactor) type is decided [1–3].

Researches of full-scale bio-drying MBT system with enclosed, static-type reactors have carried out many researchers. Tambone et al. investigated the fuel quality and biogas generation potential of biodried outputs from a windrow pile system by analyzing the heating value, respiration index, and biochemical methane potential (BMP) test [4]. Dębicka et al. analyzed the heating value and respiration index of a biocell that has a 150 m^3 to determine the moisture reduction and fuel qualities [5]. Evangelou et al. monitored the composting process of a 360 m^3 biocell-type bio-drying MBT system for 1.5 years to evaluate organic stabilization and the qualities of the resulting fuel by measuring the dynamic respiration index and heating values [6]. Dziedzic et al. studied a 36 m^3 biocontainer to investigate the fuel qualities and biogas generation potential of biodried outputs [7].

Unlike the above MSW-treatment facilities, Winkler et al. studied a 1900 m^3 biocell-type reactor used to treat sewage sludge [8]. In this system, air was recirculated and biodried sludge was returned as a bulking agent and an inoculum. They evaluated the water removal of sewage sludge and estimated the evaporation during the bio-drying process by using the operation data.

In this study, an operating 900 m^3 biocell-type bio-drying reactor employing material and air recirculation was investigated. The produced fuel is recovered after 17 days of the bio-drying process, at which point wood and fine residue are returned to the next reactor. Air in the reactor is recirculated to the same reactor by changing the fresh air intake ratio.

Unlike prior studies, this work focuses on the material balance and model estimation of water removal in the system. The material balance of changes during the bio-drying process and during the separation of biodried materials is estimated by analyzing samples in terms of proximate analysis, total organic carbon (TOC) content, and BMP. To identify the simultaneous effects of AFR and temperature increase on water removal in full-scale, which was discussed in the Chapter 2, daily water removal rate is estimated by using the monitored operation data and moisture removal model.

3.2 Materials and methods

3.2.1 Investigation of bio-drying MBT system

Mitoyo city in Kagawa prefecture treated their mixed MSW mostly by incineration in association with next Kanonji city. However, incineration facility had shut down in 2013 with the decision of operating company, so a countermeasure for MSW treatment was required. In this context, Biomass Resource Center Mitoyo have commenced its operation since April 1st in 2017 to treat MSW as first full-scale bio-drying MBT system in Japan and produces raw material of refuse-derived paper and plastics densified fuel (RPF) after its feasibility had confirmed through demonstration project [9].

A process flow diagram of the investigated bio-drying MBT system is shown in Fig. 3-1 [10]. Six biocell reactors (BR) are installed and operated in turn. Approximately 260 tons of input mixture is processed in one BR. Each BR has a capacity of 900 m^3 consists of 6-m wide, 5-m high, and 30-m long. After 17 days of bio-drying operation, biodried output is transferred to a ballistic separator to sort out three different materials: raw materials of RPF, wood residue and fine residue. Wood and fine residues are then transferred to next BR as bulking agent and inoculation after being mixed with shredded MSW by a rotary shear shredder, and new wood occasionally. Input mixtures are transferred by a wheel loader to the BR. Water (11.5 to 20.7 m^3) is added to the waste during the first stage of the bio-drying process to promote the biodegradation with mixing generated leachate. Separated raw RPF materials are subjected to NIR (Near-infrared) separator to remove PVC and any inert materials. RPF materials are baled and carried out to adjacent fuel production facility.

As shown in Fig. 3-2, ballistic separator is tilted 20 degrees and has paddles oscillating by circular movement. Heavy materials (wood residue) goes down by bouncing and discharged at the lower end. Light materials (RPF materials) are lifted upward by the air currents and discharged at the higher end. Fine residue falls down passing the round-shaped screen sized 40 mm in diameter. Rotary shear shredder consists of two parallel counterrotating shaft with a series of disc mounted perpendicular that serve as substitute of a cutter. Ferrous materials are removed from wood and fine residues by magnetic separator equipped in conveyor belts.

Actual images of each process are shown in Fig. 3-3.

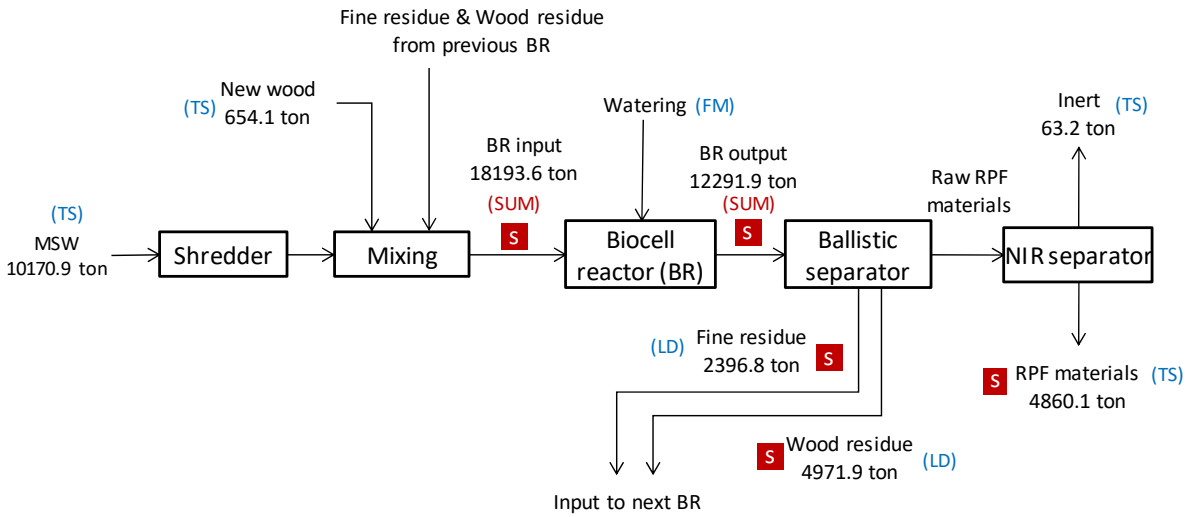

Figure 3-1 Process flow and annual mass in the facility and sampling location of the investigated bio-drying MBT system

(S mark, collected waste samples; TS, truck scale; FM, flow meter; LD, weighing scale on the wheel loader; SUM, Mass sum of each waste stream)

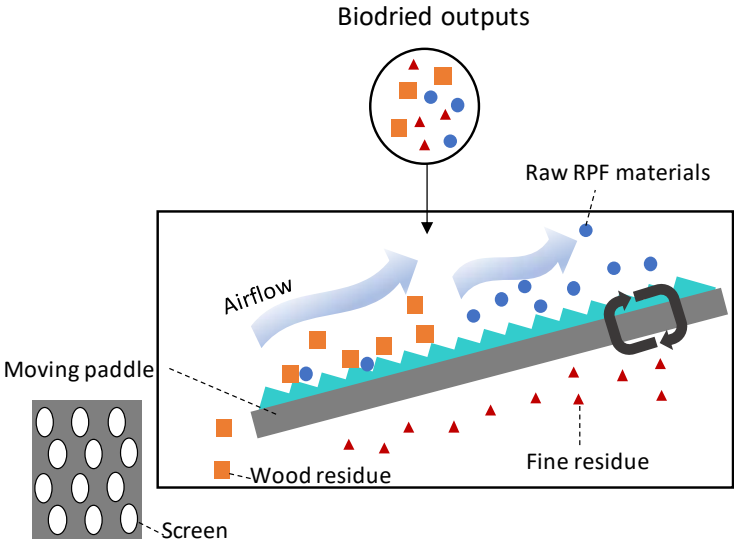

Figure 3-2 Separating principles of the ballistic separator

Figure 3-3 Images of process flow in Biomass Resource Center Mitoyo referred from the pamphlet

3.2.2 Waste sample collection

In October 2018, a total of 30 kg of waste samples were collected from five different locations in the facility (Table 3-1), indicated with an S in Fig. 3-1.

All samples except for the BR input was taken from one of the BRs after 17 days of operation. BR output, wood residue, and fine residue samples were taken from each pile, and RPF materials sample was taken from bailed products. The BR input sample was collected from next BR that was in the filling stage before the process initiation. Residues contained in BR input sample were the outputs of previous BR. MSW and wood were not sampled because MSW was mixed with return residues just after shredding, and wood was hard to collect representative sample due to large size.

The tonnage shown in Fig. 3-1 indicates the total amount from April 2017 to March 2018. Waste mass was measured either by truck scale (TS) or weighing scale on the wheel loader (LD). Water added to the BR was measured through a flowmeter (FM). The input and output mass of each BR were estimated from the summation of each waste stream.

The images of the locations on the sampling day are shown in Fig. 3-4.

Table 3-1 Amount of collected waste samples

Locations	BR input	BR output	Wood residue	Fine residue	RPF materials
Weight (g)	8057.8	5428.8	8560.8	3555.6	4806.1


BR input


BR output


Wood residue


Wood residue


Fire residue


RPF materials

Figure 3-4 Five different locations for waste sample collection

3.2.3 Laboratory analyses and procedures

Fig. 3-5 shows the procedures of waste sample analysis. To determine moisture content, the collected samples were dried in a drying oven (hot-air circular drying machine, Toyo) at 50 °C until the changes of sample weight showed below 1% variance. Samples were manually turned two times a day. Moisture content was determined by the difference of sample weight before and after the drying. Dried samples were hand-sorted into six components: plastics, paper, textiles, wood, incombustibles, and mixed material. Mixed material was then sieved with a 4.0 mm screen, at which point the oversized fraction was sorted into its components and undersized fraction was categorized as mixed fine.

For further analysis, samples were ground by cutting mill (MRK-Retsch ultra cutting mill, Germany). As this mill could not grind textiles, they were cut into small pieces using scissors and then

ground with a freeze grinder (AS One Freeze grinder, TPH-02, Monotaro, Japan). All samples were analyzed for combustible and TOC content. A BMP test was conducted to determine biogas generation as an index of biodegradable organics.

To measure the combustible contents, 5 g of each dried sample were placed in a crucible and ignited using a muffle furnace (Box furnace, KBF-894N1, Koyo, Japan) at 800 °C for 2 hours. The TOC content was determined by the difference between the total carbon (TC) and inorganic carbon (IC) of 30 mg dried samples using a TOC-TN analyzer (TOC-V CPH/CPN, connected with TOC-V SSM-5000A Shimadzu Corporation, Japan). Pure glucose ($C_6H_{12}O_6$) and sodium carbonate (Na_2CO_3) were used as a standard carbon source for the TC and IC analysis, respectively.

The BMP was experimentally analyzed as done by Hansen et al. and Pantini et al. [11, 12]. Here, one gram of the sample was mixed with 40 mL of distilled water and 20 mL of inoculum in a 135 mL vial. The samples were then purged with nitrogen to remove traces of oxygen and sealed with a butyl rubber stopper and aluminum crimps. The test materials were incubated at 55 °C for 28 days; paper and textiles were incubated for 35 days due to prolonged biodegradation. The inoculum used was taken from the liquid sludge of an AD process at Fuji Clean Center in Kagawa, Japan.

Generated biogas was extracted by inserting a 50 or 100 mL syringe until the piston movement stopped, at which point the gas volume generated was measured. Then, 0.1 mL of gas was withdrawn using a 0.5 mL gas syringe; the gas composition was determined by gas chromatography (GC-TCD, type 164, HITACHI, Japan). Gas was extracted every day during the initial stage and every 2–3 days afterwards. Gas generation was adjusted by subtracting the amount found in a blank containing only water and sludge. After 28 or 35 days (depending on the material) of testing, the gas composition of the air phase of the vial was also measured.

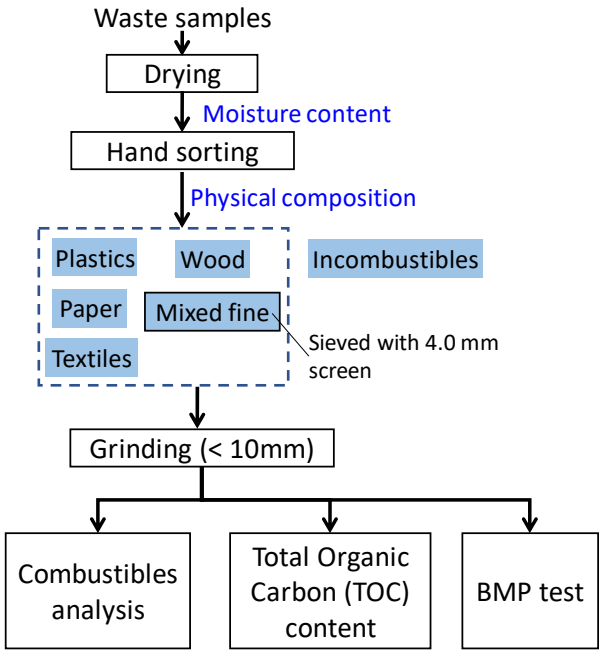

Figure 3-5 Procedures of waste sample analysis

3.3 Material balance by waste component

3.3.1 Physical composition

The physical composition of the five samples taken from the facility is shown on a wet basis in Fig. 3-6 [10]. From the input to the output of the BR, the moisture content decreased from 40% to 28% and rest were shown around 20% or less. In the wood and fine residue, a considerable amount of wood and mixed fine component was contained. Since MSW and wood were not available for sampling as mentioned in above, the composition of MSW and new wood was assumed based on the literature values. The data of MSW was referred to the report of incineration facility that operated previously in Mitoyo city [13]. High moisture content of MSW is caused by 61% of food waste. Large sized hard wood is introduced to keep porosity [14].

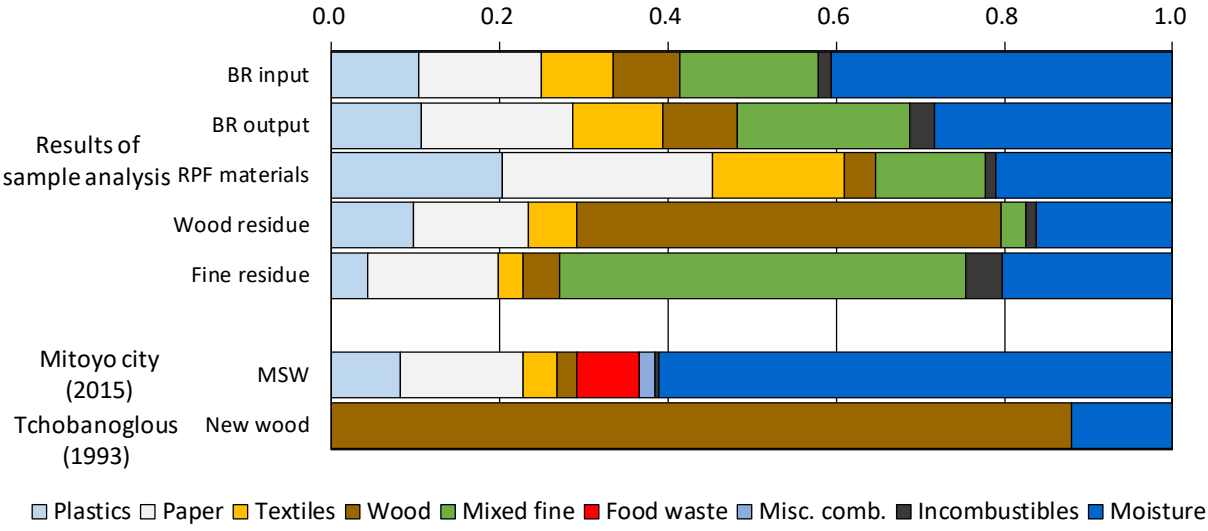

Figure 3-6 Physical composition of waste on a wet basis

(Misc. comb: Miscellaneous combustibles)

3.3.2 Combustible and biodegradable contents

The determined TOC content, combustible content, and gasified carbon in biogas through BMP test are compared in Fig. 3-7 and Fig. 3-8 [10], where each component is plotted using same symbols, but BR input samples are differentiated by no colored mark, as they contained fresh MSW. The striped mark in each component indicates the characteristics of MSW and new wood as reference [14, 15]. Food wastes that only exist in MSW were marked by star mark.

In Fig. 3-7, the TOC/combustibles is carbon content that indicates the characteristics of the combustible fraction, where a low combustibility was caused by contaminated inorganic materials. The broken lines in Fig. 3-7 represent the characteristics of polyethylene and cellulose [14]. The

TOC/combustibles of plastics is similar to polyethylene. The TOC/combustibles of textiles that is slightly higher than cellulose suggests that they are composed of synthetic and natural fibers. The TOC/combustibles of the mixed fine component was similar to that of the textiles, suggesting that it contained high-carbon-content organics, such as humic substances. Referred characteristics of MSW and new wood are similar to the sample analysis results.

The gasified carbon by anaerobic digestion, or gasified carbon in the biogas, determined by the BMP test and TOC content of waste components are compared in Fig. 3-8. The ratio is carbon balance between gasified carbon and TOC content. The slope is considered to be close to degradation rate and it is 60% for paper, 5%–10% for wood and plastics, and 30% for textiles and mixed fine components. The generated gas from plastics was caused by attached organic material. The determined biogas generation of textiles is reasonable, considering they likely consisted of synthetic and natural fibers. The low ratio of gasified carbon to TOC in the mixed fine components is reasonable, as they consist of stabilized and/or hardly biodegradable organics output from the BR.

Comparing each component in Fig. 3-7 and Fig. 3-8, no significant differences were seen among the samples, even between the input to and output of the BR. This is likely because the partial reduction of organic matters after the 17-day bio-drying process is only the decrease of the amount and its characteristics including BMP test was not changed.

Raw data of sample analysis result are in appendix (Fig. A3-1, A3-2, A3-3).

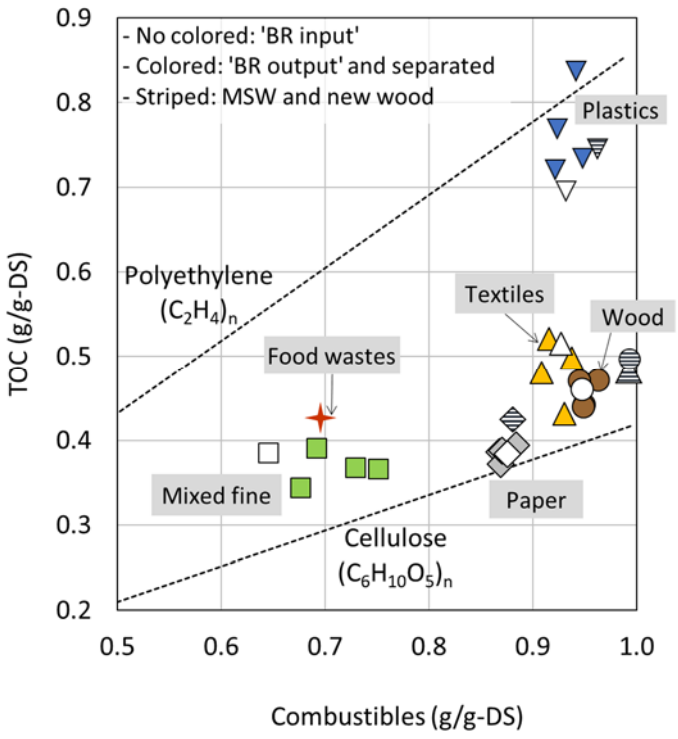

Figure 3-7 Carbon content of waste samples by ratio of TOC content and combustibles

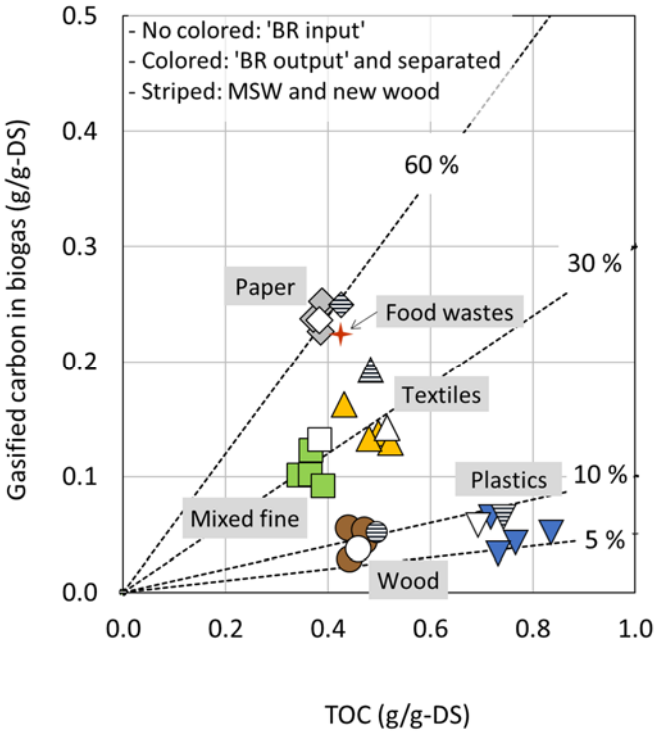

Figure 3-8 Carbon balance between gasified carbon content in biogas and TOC content

No colored marks indicate 'BR input' samples which includes fresh MSW; Colored marks indicate 'BR output' and other separated waste stream; Striped marks indicate referred characteristics of MSW and new wood (DS: Dry solids)

3.3.3 Component mass fraction by waste stream

Fig. 3-9 was obtained by multiplying the mass in Fig. 3-1 with the physical composition in Fig. 3-6 for each waste stream in dry basis excluding moisture [10]. As shown by the arrows on the top of the figure, the sum of RPF materials, wood residue and fine residue were output from the BR, and the input to the BR consisted of wood residue, fine residue, MSW, and new wood. Results of sample analysis for BR input and BR output were not used in the calculation as it was considered less creditable than the summation of other samples in terms of the homogeneity.

Fig. 3-9a was normalized by the total dry mass of the input. In this figure, 76% of wood originates from the return residue, whereas 17% is provided from new wood. For the RPF materials, i.e., plastics and paper, 60% was introduced through the MSW stream, whereas 40% was from returned residue.

Fig. 3-9b–c were calculated similarly for gasified carbon in biogas and combustibles by multiplying their characteristics (Fig. 3-7 and Fig. 3-8) with the dry mass of each component in Fig. 3-9a. The mass fraction of combustibles in Fig. 3-9c looks similar to the dry solids in Fig. 3-9a.

(a) Dry solids

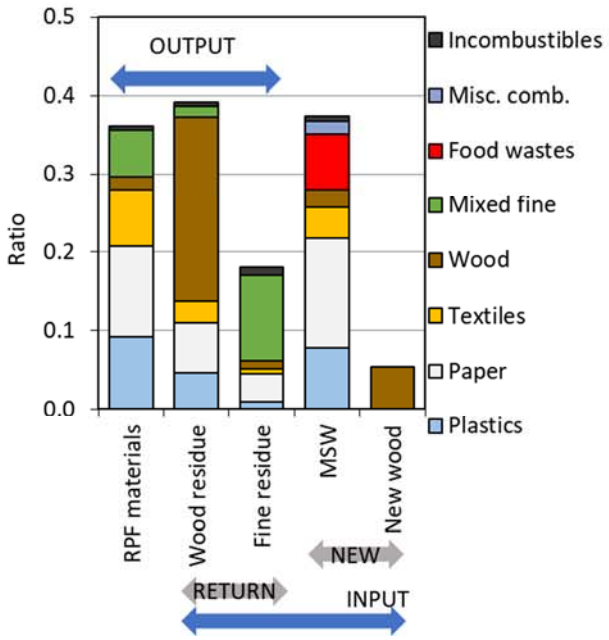

(b) Gasified carbon in biogas

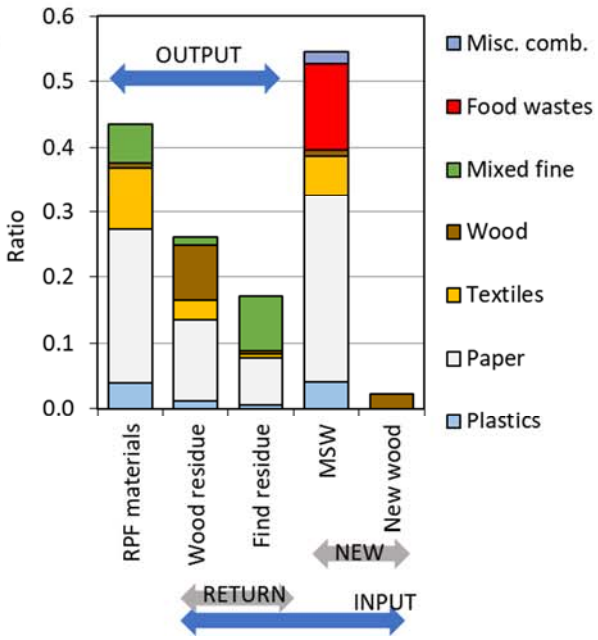

(c) Combustibles

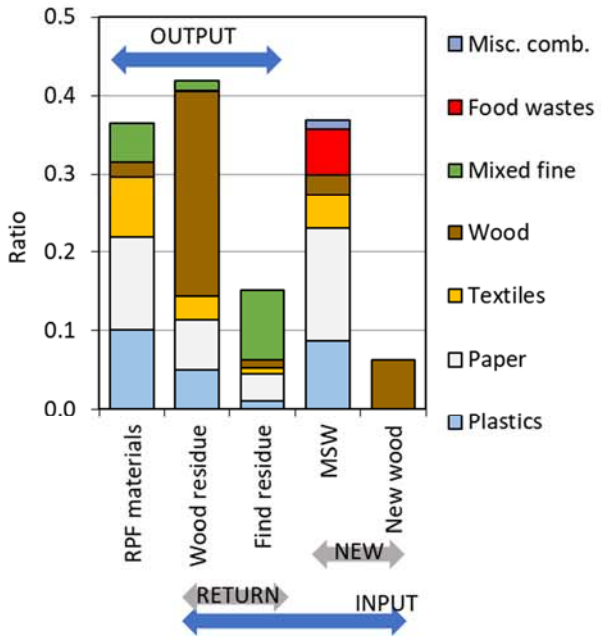

Figure 3-9 Mass fraction of dry solids, gasified carbon in biogas, and combustibles of each waste stream component on a dry basis

Values are normalized by the total dry mass of the INPUT (Misc. comb.: Miscellaneous combustibles)

3.3.4 Separation efficiency of output from BR

The separation ratio of the output from the BR into the three streams for total dry mass and each waste component was calculated from the data in Fig. 3-9 and is shown in Table 3-2 [10].

Of the fuel materials, only 62% of plastics and 54% of paper was recovered as a fuel and the rest were returned to the next BR. Sixty percent of recovery rate can be considered to be low, but it is not considering the fact that the returned residue will be subjected to bio-drying process again and the materials will be recovered eventually. To investigate the cause of unrecovered fuel materials (plastics and paper), the size distribution for RPF materials and wood residue was measured and is shown in Fig. 3-10 and Fig. 3-11. In case of plastics, the unrecovered ratio was approximately 40% and was considered as the performance of wind separation. The size of recovered plastic particles ranged from 5 cm to 65 cm. The recovery rate of plastic particles to RPF materials under 15 cm in size was only 28%. However, the paper components were mostly smaller than 20 cm and had a recovery rate to RPF of 54%.

Wood and the mixed fine component were separated into return stream more effectively; 90% of the wood and 60% of the mixed fine components were returned to the mixing process before being introduced to the next BR.

Table 3-2 Separation ratio of the output streams on a dry basis

		RPF materials	Wood residue	Fine residue
Total dry mass		0.39	0.42	0.19
Material	Plastics	0.62	0.31	0.07
	Paper	0.54	0.30	0.16
	Textiles	0.68	0.25	0.06
	Wood	0.06	0.90	0.04
	Mixed fine	0.33	0.08	0.60

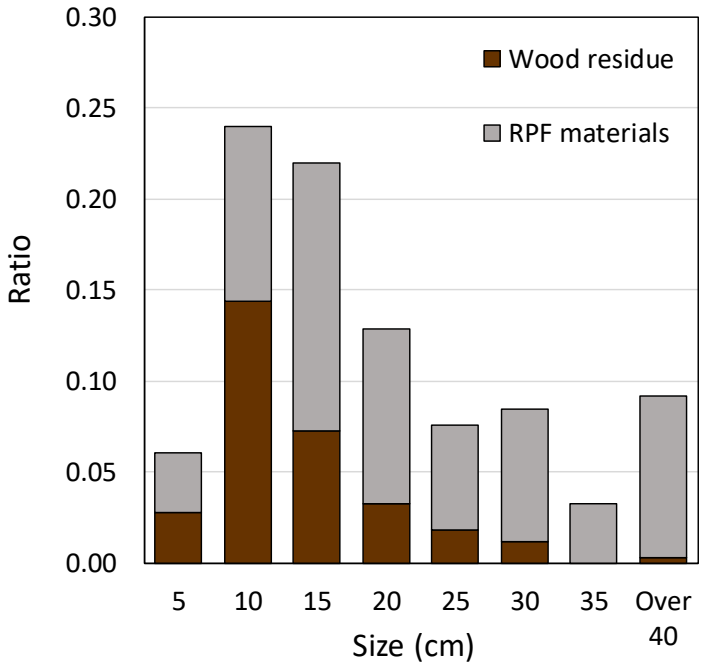

Figure 3-10 Size distribution of plastics in wood residue and RPF materials

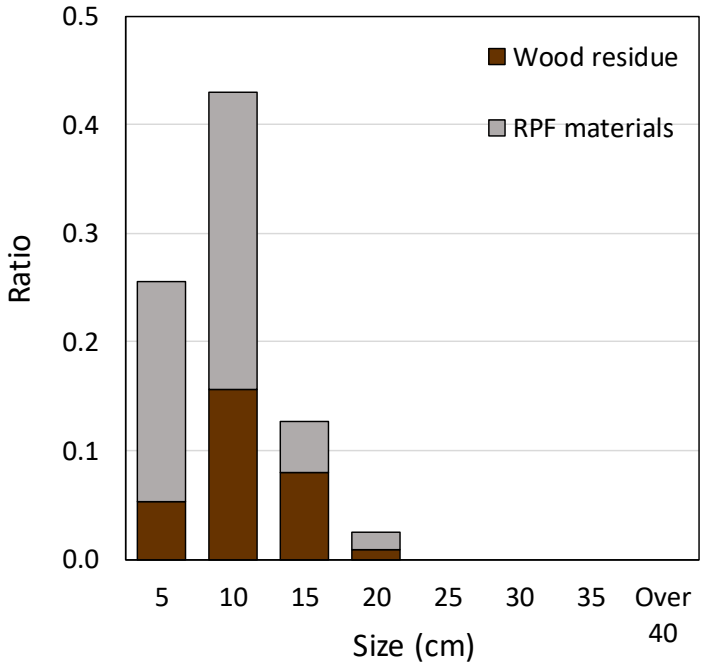

Figure 3-11 Size distribution of papers in wood residue and RPF materials

3.3.5 Mass balances before and after the bio-drying process

The difference in dry mass of each component between the input and output of the bio-drying process is shown in Fig. 3-12a, where the mass fraction of each component was calculated by summing up for INPUT and OUTPUT in Fig. 3-9a, and they are depicted by bar graph and dot, respectively. The food waste included in the MSW was added to the mixed fine component in the process input stream. Fig. 3-12b and 12c, for gasified carbon in biogas and combustibles, were calculated from Fig. 3-9b and 9c in the same manner [10].

The small reduction of paper shown in Fig. 3-12a is reasonable, as paper does not fully degrade even during the 6 to 8 weeks of the composting process [16]. As wood is a hardly biodegradable organic, the decrease of wood may have been caused by a reduction in particle size, allowing the fine particles to be transferred to the mixed fine component. The reduction in Fig. 3-12b can be explained by the transfer of wood, and the loss of organic matters can be another reason. Also, no changes of combustibles of mixed fine in Fig. 3-12c is also proved by same reason.

The gasified carbon in biogas was reduced by 13% between the input and output of the bio-drying process (Fig. 3-12b). Among the waste components in the input, food waste in the MSW and the mixed fine component could be biodegraded in 17 days of the bio-drying process, and their fractions were 13% and 9% of the input, respectively. A decrease from 21% to 13% can be considered reasonable for biodegradation.

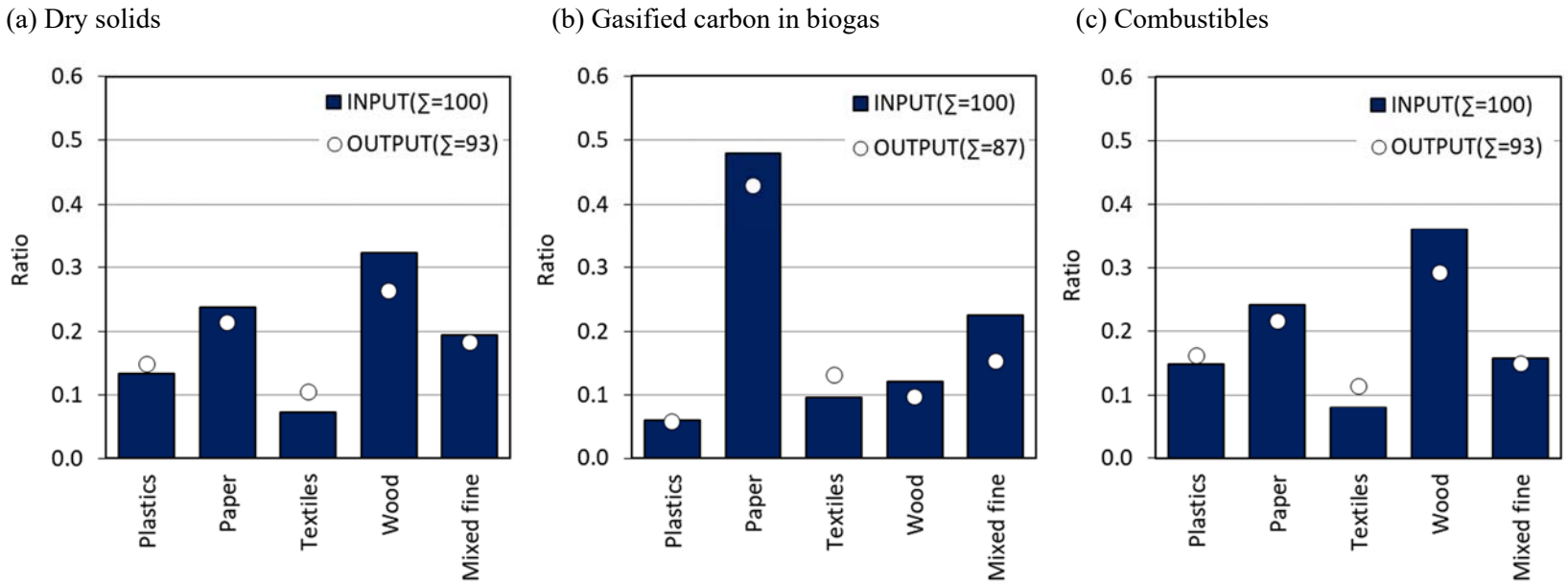

Figure 3-12 Mass balance of dry solids, gasified carbon in biogas, and combustibles before and after the bio-drying process on a dry basis

3.4 Moisture balance during bio-drying process

3.4.1 Working of bio-drying process

To promote aerobic degradation and removal of evaporated water at the same time, aeration is important in a bio-drying process. Fig. 3-13 shows schematic diagram of biocell reactor and airflow [10]. Mixture of fresh air and recirculating air from the same BR is used for aeration of the waste by electrically driven fan and dampers operation. Exhaust air is sent to a biofilter to control odor emission. During the operation, various parameters (blue-colored) have monitored and logged in real-time which have shown in Fig. 3-14.

Depending on the waste temperature (Fig. 3-14a) which is an indication of biodegradation, flow rate of aeration and mixing ratio of fresh air are changed which are monitored by fan speed (q_A) in Fig. 3-14b and fresh air damper opening in Fig. 3-14c, respectively. The higher the fan speed and the damper openness, high flow rate of aeration with more fresh air is provided to the reactor. This will lower the waste temperature and based on this change, next operation of fan and damper is adjusted.

Besides the parameters related to aeration, pressure inside the reactor is monitored, which have maintained under a slightly negative to prevent any gas emission or odor from biocell reactor (Fig. 3-14d).

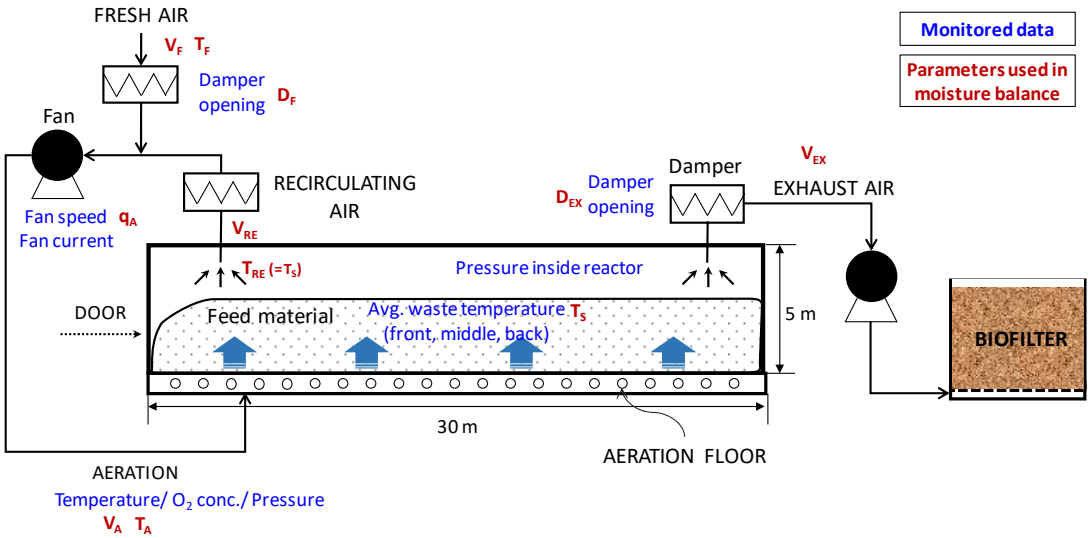

Figure 3-13 Schematic diagram of airflow in the biocell reactor and parameters used in estimation of water removal

(Symbols: V, airflow rate; T, temperature; D, degree of openness in damper; q, fan speed in percentage unit / Subscript: F, fresh air; A, aeration; S, solid waste; EX, exhaust air; RE, recirculating air)

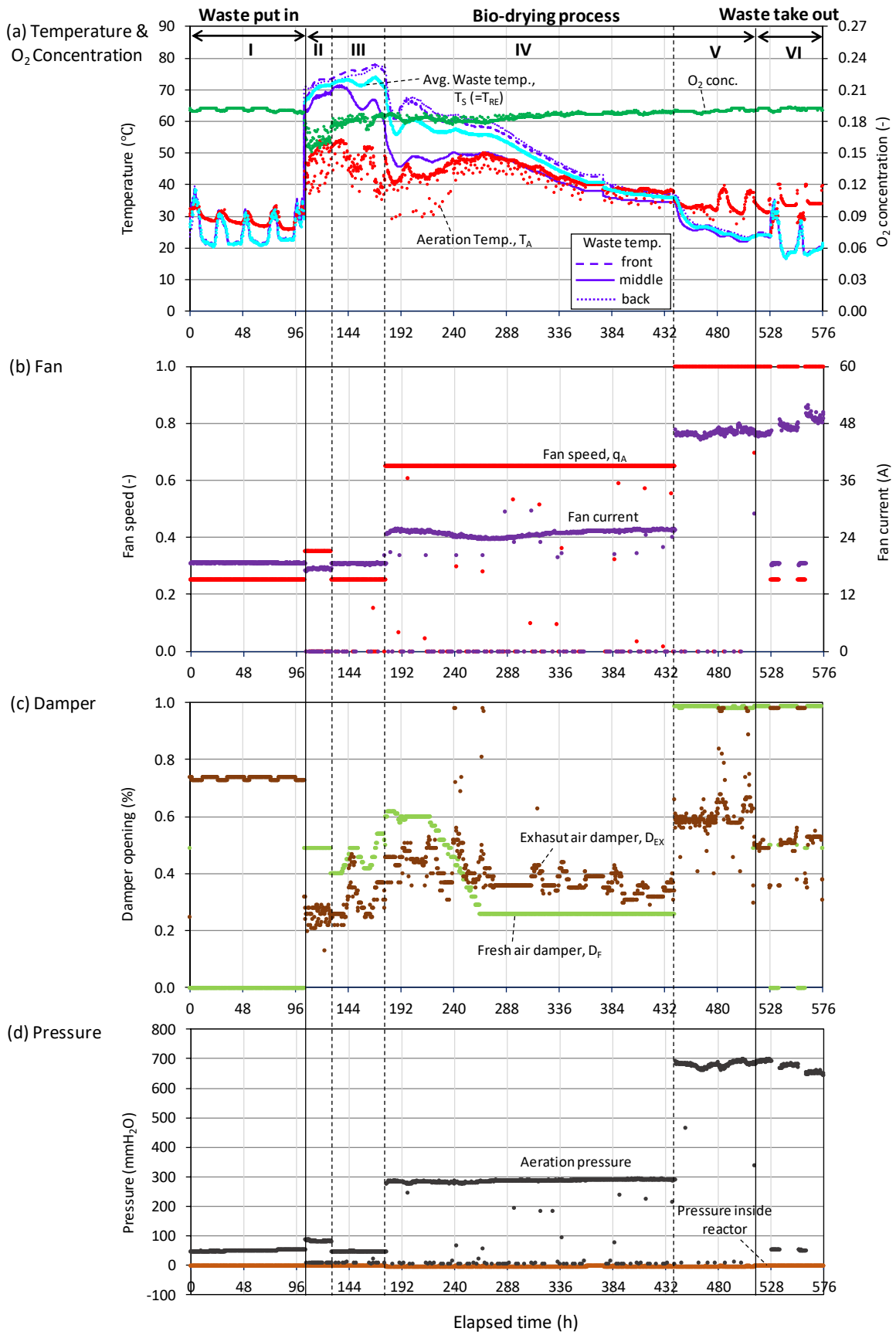

Figure 3-14 Profiles of monitored parameters of biocell reactor (BR2) during bio-drying process (9/11/2018 – 10/5/2018)

3.4.2 Estimation of airflow rate and water removal

To estimate the water removed during bio-drying, the evaporated water mass was then calculated [10]. As shown in Fig. 3-13, the four unknown airflow rates were V_A, V_F, V_{RE}, and V_{EX}, where subscripts A, F, RE, and EX refer to aeration, fresh air, recirculating air, and exhaust air, respectively. A mixture of fresh air and recirculating air from the BR is aerated to the same BR. The mass and heat balances before and after the mixing of air can be written as Eq. (3-1) and (3-2), respectively.

$$V_A = V_F + V_{RE} \tag{3-1}$$

$$V_A T_A = V_F T_F + V_{RE} T_{RE} \tag{3-2}$$

The ratio of fresh air to total aeration λ_F can be defined as Eq. (3-3). The recirculating airflow rate can be then determined as Eq. (3-4). Equation (3-5), derived from Eq. (3-2) by substituting V_F and V_{RE} with Eq. (3-3) and (3-4), respectively, can then be used to calculate λ_F. In Eq. (3-5), T_{RE} was presumed to be equal with waste temperature (T_S). The exhaust airflow rate, V_{EX}, was determined to equal V_F by assuming steady state. The value of T_F was assumed as 22.8 °C with 57.9% relative humidity (RH) based on meteorological data [17].

$$\lambda_F = \frac{V_F}{V_A} \tag{3-3}$$

$$V_{RE} = (1 - \lambda_F) \times V_A \tag{3-4}$$

$$T_A = \lambda_F \times T_F + (1 - \lambda_F) \times T_{RE} \tag{3-5}$$

The flow rate of aeration, V_A can then be calculated by Eq. (3-6) where 16000 is the specified airflow rate of the fan in m^3/h, and q_A is the fan speed as a percentage.

$$V_A = 16000 \times q_A \tag{3-6}$$

The water removal rate in the BR can then be calculated as the difference between the water inlet through fresh air from water outlet, shown in Eq. (3-7), where X represents the water vapor per unit volume of air in g/m^3, which is a function of pv, water vapor pressure (Pa) and temperature (T) (Eqs. (3-8)–(3-10)).

As shown in Eq. (3-7), water removal rate in kg/h is mostly governed by airflow rate V_{EX} and X_{EX}. X_{EX} increases exponentially with temperature by Eqs. (3-8)-(3-10). So, airflow rate and temperature are two major factors for moisture removal.

Exhaust air was assumed to always be saturated and its temperature (T_{EX}) was equal to the waste temperature (T_S).

$$\text{Water removal rate} = (V_{EX} \times X_{EX} - V_F \times X_F) \times 10^{-3} \quad (3\text{-}7)$$

$$X = \frac{217 \times pv}{273.15 + T} \quad (3\text{-}8)$$

$$pv = RH \times pvs \quad (3\text{-}9)$$

$$\text{When saturated: } pvs = 6.1078 \times 10^{\frac{7.5 \times T}{T + 237.3}} \quad (3\text{-}10)$$

3.4.3 Different operation phase during the bio-drying process

The profiles of airflow rate and temperature are shown in Fig. 3-15. T_S is measured average waste temperature of three sections of waste piles inside the reactor and T_A is measured temperature of aeration as shown in Fig. 3-14c. V_A is the flow rate of aeration, calculated by Eq. (3-6) using fan speed (q_A) shown in Fig. 3-14a. V_F is the flow rate of fresh air, calculated by Eq. (3-3) and Eq. (3-5).

The process is subjected to six consecutive operation phases.

- Phase I (Waste put in): BR input was fed into the reactor. Waste temperature fluctuated according to loading work of the input. T_A also fluctuated by the change of T_{RE}, which is equal to T_S because no fresh air was provided.
- Phase II (Warm-up): After putting waste in, the reactor had closed and bio-drying process was initiated. Flow rate of aeration, V_A was increased to warm-up the waste. Fresh air was also added.
- Phase III (Sanitization): Maintain waste temperature over 60 ℃ for 48 hours for sanitization.
- Phase IV (Stabilization): Because waste temperature was decreasing along with biodegradation progress, the ratio of fresh air was decreased to maintain the waste temperature.
- Phase V (Cooling and drying): Flow rate of aeration was set at maximum level to cool down as well as to remove moisture. Only fresh air was provided (λ_F =1).
- Phase VI (Waste take out): The reactor was opened and waste was taken out.

Fig. 3-16 shows another example of operation profile of bio-drying process in different biocell reactor.

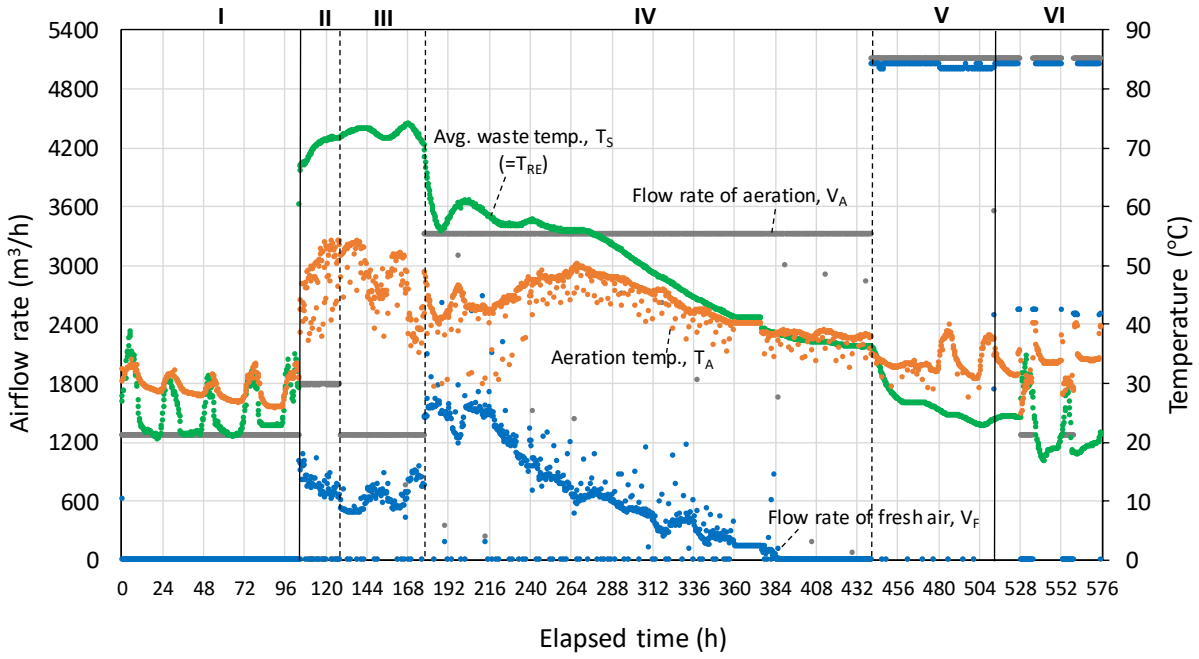

Figure 3-15 Profiles of operation variables of biocell reactor (BR-2) from 9/11/201/ to 10/5/2018

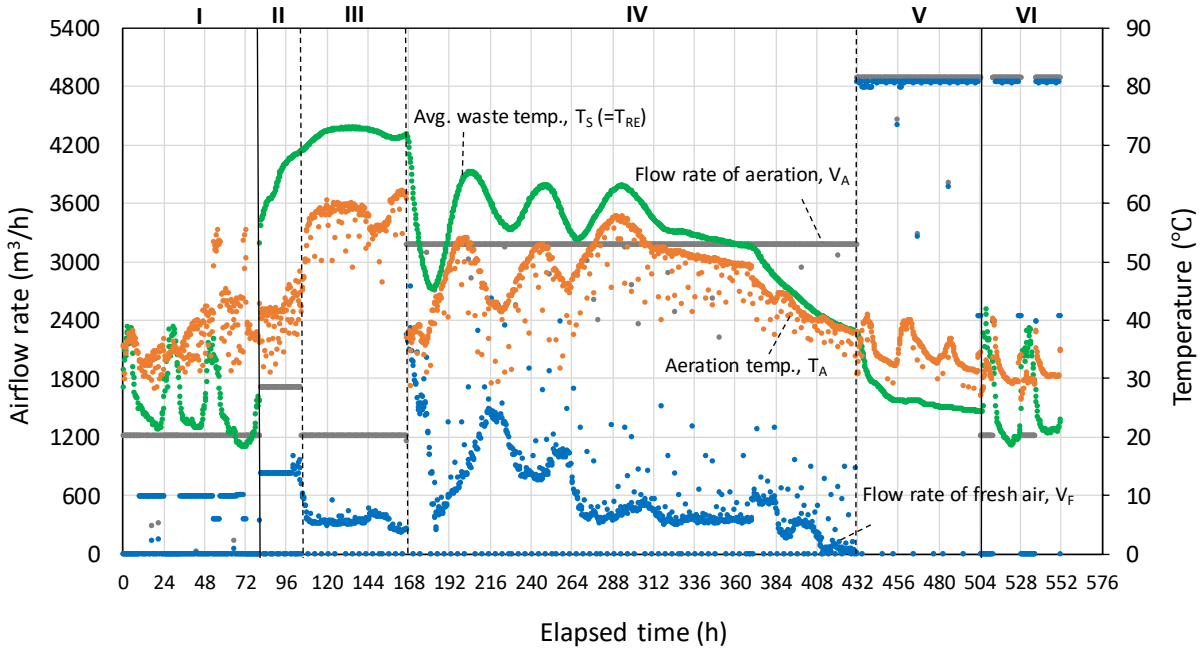

Figure 3-16 Profiles of operation variables of biocell reactor (BR-3) from 9/17/2018 to 10/10/2018

3.4.4 Daily water removal rate

The daily water removal rate as calculated by Eq. (3-7) is shown in Fig. 3-17b with operation profiles (Fig. 3-15) [10]. The numbers on the figure indicate the portion of water removed at each phase

over the total water removal. Considering that the reactor was not closed during phase I and VI, only water removal rate during the bio-drying process (II~V) is calculated.

Half of the water removal occurred during phase IV (Stabilization), which had the longest elapsed time, and the moisture removal rate declined with the decrease of temperature. Phase II (Warm-up) and III (Sanitization) showed relatively higher removal rate despite their of short duration and low airflow rate, as the saturated moisture content in air is 198 g/m^3 high at 70 °C while 104 g/m^3 at 55 °C. In phase V (Cooling and drying), the water removal rate was lowered due to the decrease in temperature, but the maximum flow rate of fresh air for 3 days enhanced moisture removal.

The estimated total water removed, as shown in Fig. 3-17, was 86.6 tons. Based on the material flow in Fig. 3-1 and the measured moisture content in Fig. 3-6, the amount of water removed was 55.5 tons, from 105.3 ton to 49.8 ton for 260 tons of wet waste per BR. The difference may have been caused by metabolic water generation or sampling error.

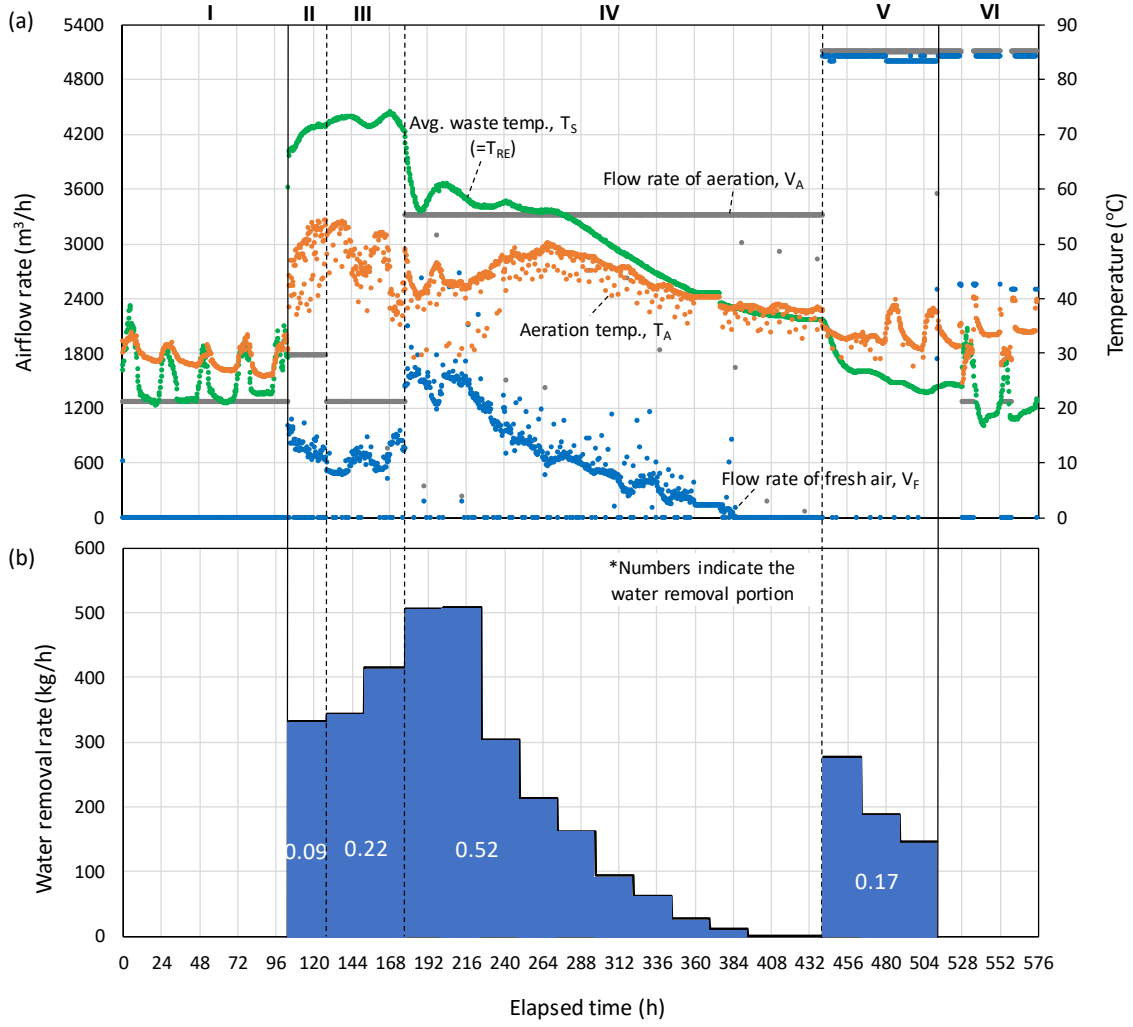

Figure 3-17 Profiles of operation variables and daily water removal rate under different operation phase during the bio-drying process (BR-2)

(a) Profiles of operation variables (from Fig. 3-15), (b) daily water removal rate

3.5 Conclusion

In this study, a full-scale biocell type bio-drying MBT system was investigated. Mass balance of each waste component was estimated by using composition analysis, characterization of waste samples, and waste tonnage data. During separation of biodried outputs, 62% of plastics and 54% of paper were recovered as raw material for RPF. The ratios are not low because unrecovered plastics and paper were returned to next biocell reactor. Due to low biodegradation of plastics and paper for 17-days of bio-drying, almost 100% of the RPF materials could be recovered. Wood was decreased by reduction in particle size during the bio-drying process, 90% of wood was returned to next BR. Mixed fine seems barely reduced, but reduced wood particle moved to mixed fine and filled up the loss caused by organic degradation and 60% of mixed fine was returned to next BR.

Water removal phenomena was simulated by the model of daily water removal based on the operation data. The process was subjected to four distinct operation phases and was operated according to the waste temperature. The main phase of water removal was expected to be occurred in stabilization phase (IV) for 11 days. However, half of water removal was occurred at initial two phases and phase V for only 6 days in total and this is caused by high waste temperature for sanitization (phases II and III) and high airflow rate for cooling phase. Phase IV was long, but decreasing temperature resulted in low water evaporation. As concluded in Chapter 2, effect of airflow promotes moisture removal, but also high temperature also contributed high moisture removal though considerable metabolic water generation could be accompanied.

The findings of this study which are separation efficiency of biodried outputs and effects of temperature and airflow rate on drying efficiency, can give some contribution on improving the full-scale bio-drying MBT system.

References

1. Chiumenti A, Chiumenti R, Diaz L, et al (2005) Modern Composting Technologies. the JG Press Inc.
2. Juniper Consultancy Services Ltd (2005) Mechanical-Biological Treatment: A Guide for Decision Makers, Processes, Policies and Markets
3. Velis CA, Longhurst PJ, Drew GH, et al (2009) Biodrying for mechanical-biological treatment of wastes: A review of process science and engineering. Bioresour Technol 100:2747–2761. https://doi.org/10.1016/j.biortech.2008.12.026
4. Tambone F, Scaglia B, Scotti S, Adani F (2011) Effects of biodrying process on municipal solid waste properties. Bioresour Technol 102:7443–7450. https://doi.org/10.1016/j.biortech.2011.05.010
5. Dębicka M, Żygadło M, Latosińska J (2017) The effectiveness of biodrying waste treatment in full scale reactor. Open Chem 15:67–74. https://doi.org/10.1515/chem-2017-0009
6. Evangelou A, Gerassimidou S, Mavrakis N, Komilis D (2016) Monitoring the performances of a real scale municipal solid waste composting and a biodrying facility using respiration activity indices. Environ Monit Assess 188:. https://doi.org/10.1007/s10661-016-5303-6
7. Dziedzic K, Łapczynska-Kordon B, Malinowski M, et al (2015) Impact of aerobic biostabilisation and biodrying process of municipal solid waste on minimisation of waste deposited in landfills. Chem Process Eng - Inz Chem i Proces 36:381–394. https://doi.org/10.1515/cpe-2015-027
8. Winkler MKH, Bennenbroek MH, Horstink FH, et al (2013) The biodrying concept: An innovative technology creating energy from sewage sludge. Bioresour Technol 147:124–129. https://doi.org/10.1016/j.biortech.2013.07.138
9. Mitoyo city (2013) Biomass Industrial City Plan (in Japanese). Mitoyo city, Kagawa, Japan
10. Ham GY, Matsuto T, Tojo Y, Matsuo T (2020) Material and moisture balance in a full-scale bio-drying MBT system for solid recovered fuel production. J Mater Cycles Waste Manag 22:167–175. https://doi.org/10.1007/s10163-019-00925-2
11. Hansen TL, Schmidt JE, Angelidaki I, et al (2004) Method for determination of methane potentials of solid organic waste. Waste Manag 24:393–400. https://doi.org/10.1016/J.WASMAN.2003.09.009
12. Pantini S, Verginelli I, Lombardi F, et al (2015) Assessment of biogas production from MBT waste under different operating conditions. Waste Manag 43:37–49. https://doi.org/10.1016/J.WASMAN.2015.06.019
13. Mitoyo city (2015) Solid Waste Management Master Plan for Mitoyo city (in Japanese). Mitoyo city, Kagawa, Japan

14. Tchobanoglous G, Theisen H, Vigil SA (1993) Integrated solid waste management : engineering principles and management issues. McGraw-Hill
15. Bae SJ (2005) Estimation of ultimate methane yields from municipal solid waste components using BMP test. University of Seoul, Korea
16. Alvarez JVL, Larrucea MA, Bermúdez PA, Chicote BL (2009) Biodegradation of paper waste under controlled composting conditions. Waste Manag 29:1514–1519. https://doi.org/10.1016/J.WASMAN.2008.11.025
17. Japan Meteorological Agency (2019) Past weather by city. https://www.data.jma.go.jp/risk/obsdl/index.php#!table

CHAPTER 4

Comparison of bio-drying MBT with other energy recovery system as MSW management

4.1 Introduction

As discussed in previous chapters, a bio-drying MBT system can treat MSW and recover solid fuel by enhancing mechanical separation rate after the biological drying. It has been attracted more attention as the demand for energy recovery from MSW had been increasing. Another system of energy recovery from mixed MSW is the integration of AD and incineration processes. This is a type of MBT where the organic fraction and combustibles are mechanically separated and sent to AD and incinerator, respectively. In the AD process, organic matter is decomposed to produce biogas, but the undecomposed residue is returned to the incinerator. All fractions of the mixed MSW are used for energy recovery in an integrated system. This integrated system can deal with the drawbacks of individual treatment of waste separated at source. Treatment efficiency depends heavily on citizens participation and increased collection and treated costs required for waste components.

Many studies have evaluated the bio-drying MBT system and combined system in terms of energy efficiency, environmental impacts such as potential for global warming and acidification, and economic feasibility. Psaltis and Komilis [1] evaluated the application of bio-drying process as a pretreatment for a mixed MSW incinerator by comparing its energy, environmental impacts, and direct costs associated with mass-burn incineration. Fei et al. [2] compared the components of MBT system including the bio-drying and AD processing of moisture in mixed MSW with landfill and incineration (with energy recovery) from the energy, environmental, and economic perspectives. Cimpan and Wenzel [3] compared four MBT systems with different biological processes such as composting, bio-drying, AD, and mechanical separation (without biological processing) with the mass-burn incineration of mixed MSW from the energy perspective. On the other hand, Inoue and Matsuto [4] compared a combined system consisting of incineration and dry AD processes with direct incineration from the viewpoint of energy efficiency. Takata et al. [5] evaluated a combined system in terms of GHG emissions, but their study essentially focused on the operation of AD process without the incineration process. The best energy recovery system recommended in the above studies depends largely on system boundaries, local conditions, assumed operating parameters and efficiency.

In this context, this chapter is dedicated for a comparison of a bio-drying MBT system and a combined system for the treatment of MSW from the viewpoint of energy balance and CO_2 emissions under the same boundary conditions. In additional, the other two popular energy recovery systems, including incineration and RDF production systems were also compared. Incineration is one of the most

popular technologies for energy recovery. In Japan, about 760 MSW incinerators are in operation for energy recovery [6]. The RDF production systems recover solid fuels by using fuel oil. As of 2017, a total of 48 facilities are in operation, producing RDF and RPF as alternative fuels for heat and power generation [7]. Therefore, incineration with energy recovery, combined system, bio-drying MBT system, and RDF production system are called S1 to S4 in sequence.

The actual situation in Asahikawa City, Hokkaido was considered in order to compare all four systems as possible waste management options in the future. To compare the four systems, life cycle energy and CO_2 emissions for operation were estimated based on utility consumption such as electricity, fuel, and chemicals. Finally, a sensitivity analysis was performed to realize the impact of parameter variations on energy balance.

4.2 Compared systems

4.2.1 Generation and characteristics of waste and life cycle unit

The amount of solid waste generated in Asahikawa City in 2017 is shown in Table 4-1 [8]. Approximately 100,000 tons of waste were generated from the household and business sectors, of which 78,000 tons of combustible waste were incinerated. This combustible waste was the input waste into four systems. Table 4-2 shows the physical composition and characteristics of combustible waste. Combustible waste consists of six waste components, the physical composition (C) of which is a measured value, and 90% is organic matter including paper, garden waste, and food waste on a wet basis. The moisture content (M), ash content (A), and higher heating value (H_D) of each waste component are typical of general MSW [4, 9]. In S2 and S3, the residue characteristics (i=4) are given by the weighted average of garden (k=4) and food (k=5) wastes. The moisture content is on a wet basis, and ash and higher heating values are on a dry basis.

To compare the energy balance, unit of consumptions including utilities and energy and of electricity recovery should be unified. Table 4-3 shows the life cycle energy and CO_2 emission for different items. The top three items are the direct energy consumption of electricity, heavy oil, and diesel oil. The lower half of the table corresponds to the indirect consumption and emissions of the used materials and landfills. For example, the life cycle energy (ε^1) and CO_2 emission (θ^1) units of electricity are MJ/kWh and kg-C/kWh, respectively. Multiplying these units by the annual electricity consumption gives the energy consumption and CO_2 emissions for the entire life cycle. In terms of generated electricity, one can save and avoid life cycle energy and CO_2 emissions. ε^9 and θ^9 are energy consumption and CO_2 emissions during landfill operation when one ton of waste is disposed of [9–11].

Table 4-1 Waste generation and disposal in Asahikawa city in 2017

Source	Generation (t-waste)	Disposal (t-waste)	
		Combustible waste (Incineration)	Incombustible waste (Landfill)
Household	69877	43143	9747
Business	36366	33283	2572
Reference [8]			

Table 4-2 Physical composition and characteristics of Combustible waste

Component	k	i*	Physical composition[a] (-) wet, C^k, C^i		Moisture content[b] (-), M^k, M^i		Ash content[b] (g/g-dry), A^k, A^i		Higher heating value[a] (MJ/t-dry), H_D^k, H_D^i	
plastics	1	1	0.032		0.05		0.06		36000	
paper	2	2	0.325		0.27		0.07		16000	
textiles	3	3	0.059		0.20		0.03		18100	
garden waste	4	4	0.153	0.580	0.40	0.73	0.03	0.08	17900	17653
food waste	5		0.427		0.85		0.15		17300	
Incombustibles	6	5	0.004		0.01		1.00		0	

a-Reference [4]
b-Reference [9]
*For S2 and S3, superscript i is used.

Table 4-3 Life cycle energy and CO_2 emission per utility consumption

Classification	m	Items (*)	Energy MJ/*, ε^m	CO_2 emission kg-C/*, θ^m	Reference
Energy	1	Electricity (kWh)	9.4	0.13	[9]
	2	Energy content of heavy oil (L)	38.9	0.71	[9]
	3	Energy content of diesel oil (L)	38.5	0.74	[9]
Chemicals and others	4	Water (tap water) (m^3)	13.4	0.18	[9]
	5	Slaked lime (Alkali chemicals) (t)	2218	299	[9]
	6	Cement (t)	3799	225	[9]
	7	Coagulant for WWT (t)	9745	136	[9]
	8	Wood (t)	1.7	24.53	[10]
	9	Landfill (t)	631	8.78	[11]

4.2.2 Incineration with energy recovery (S1)

Fig. 4-1 shows the process and material flow of incineration with energy recovery (S1). Combustible waste is burned in the incinerators and electricity is generated by steam turbines. The generated fly ash is solidified by cement and disposed of together with the bottom ash at the designated landfill site. Alkali chemicals are used for flue gas treatment.

Table 4-4 shows the parameters for utilities and operation of S1. Based on the data from the incineration facility [9], the incineration residue was composed of 10% fly ash and 90% bottom ash. The amount of incineration residue will be calculated from ash contents of combustible waste later in section 4.3. Most S1 values refer to a questionnaire survey of incineration facilities in Japan [12]. The power generation efficiency (η_1) is set at 19% so that it can be applied to high-rate power generation [13]. From hence, gray-colored area is a boundary of energy balance in all system and number in subscript of various symbols indicate each system as 1 for S1.

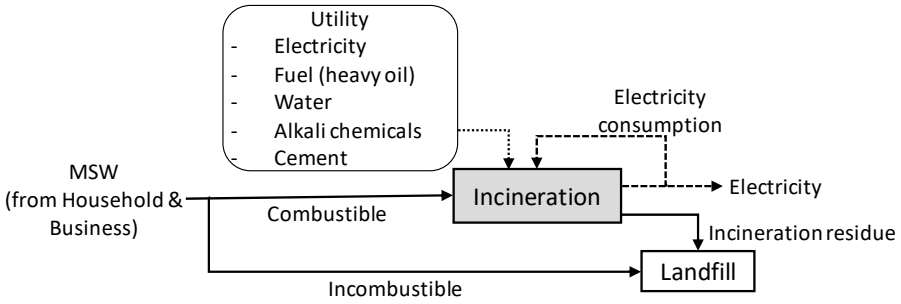

Figure 4-1 Process flow of S1 with material flow and utilities

Table 4-4 Operation and utility parameters of S1

Classification	Parameters	Value	Reference
Mass balance	Bottom ash generation (t/t-ash), P_{BA}	0.9	[9]
	Fly ash generation (t/t-ash), P_{FA}	0.1	[9]
Utility consumption	Electricity (kWh/t-waste), u_{E1}	178.4	[12]
	Fuel (heavy oil) (L/t-waste), u_{O1}	2.13	[12]
	Water (m^3/t-waste), u_{W1}	0.6	[9]
	Alkali chemical (t/t-waste), u_{AC1}	0.00584	[12]
	Cement for fly ash solidification (t/t-fly ash), u_{S1}	0.13	[12]
Operation	Power generation efficiency, incineration (-), η_1	0.19	[13]

4.2.3 Combined system (Anaerobic digestion + Incineration) (S2)

Fig. 4-2 shows the process and material flow of the combined system, which consists of the dry-AD process and incineration with energy recovery. Combustible waste is mechanically separated from the waste stream. The waste suitable for the AD process is digested and produces biogas which is sent to a biogas engine for power generation. The digestate from the AD reactor is dewatered and the solid

digestate is sent to an incinerator where it is combusted with waste mechanically separated as unsuitable for the AD process. Liquid digestate is subjected to wastewater treatment (WWT) process and undergoes coagulation. Some treated water is recirculated to the AD process to adjust the TS content of the AD input to 0.2. The fly ash generated by the incineration process is solidified by cement and is landfilled together with the bottom ash.

The mechanical separation rate for the AD process (R_2^i) is shown in Table 4-5. All the values of waste components (plastics, paper, etc.) were measured (excluding moisture) on a dry basis using the samples collected from a currently operating combined system [14]. Residues represent the sum of garden and food wastes in the combustible waste input. As shown in the Table 4-5, 96% of residues and 55% of paper are properly separated in the AD process with about 30% plastics and textiles.

Total organic carbon (TOC) content (g-TOC/g-TS) and biochemical methane potential (BMP) were obtained by analyzing waste samples collected from an operating combined system [14]. The degradation rate (D^i) of each component was determined by Eq.(4-1). Here, the degraded carbon was estimated from gas generation rate (L/g-TS) using the BMP test. Since some carbon is stored in microorganisms, the estimate was less than the actual degraded mass. Paper and residues are considered organic materials with a degradation rate of about 50%. Although plastic is a biologically non-degradable materials, it showed some degradability due to attached organic matter. The methane gas generation potential (B^i) was estimated by multiplying the CH_4 concentration (-) by the gas generation rate (L/g-TS) (Eq. (4-2)).

Degradation rate (-)

$$D^i = \frac{Gas\ generation^i \times 12/22.4}{TOC\ content^i} \quad (4\text{-}1)$$

Methane gas generation potential (m^3-CH_4/t-TS)

$$B^i = Gas\ generation^i \times CH_4\ Concentration^i \times 1000 \quad (4\text{-}2)$$

Table 4-7 shows the parameters for utility consumption and operation of dry AD process. Electricity consumption refers to the AD process in an operating combined system, which covers the consumptions for mechanical separation and the WWT process. Coagulant consumption per wastewater volume refers to the an operating WWT facility. The power generation efficiency (η_2) of a biogas engine is assumed to be 30% [4, 9, 15, 16]. The incineration process in a combined system is assumed to be the same as S1 (Table 4-4).

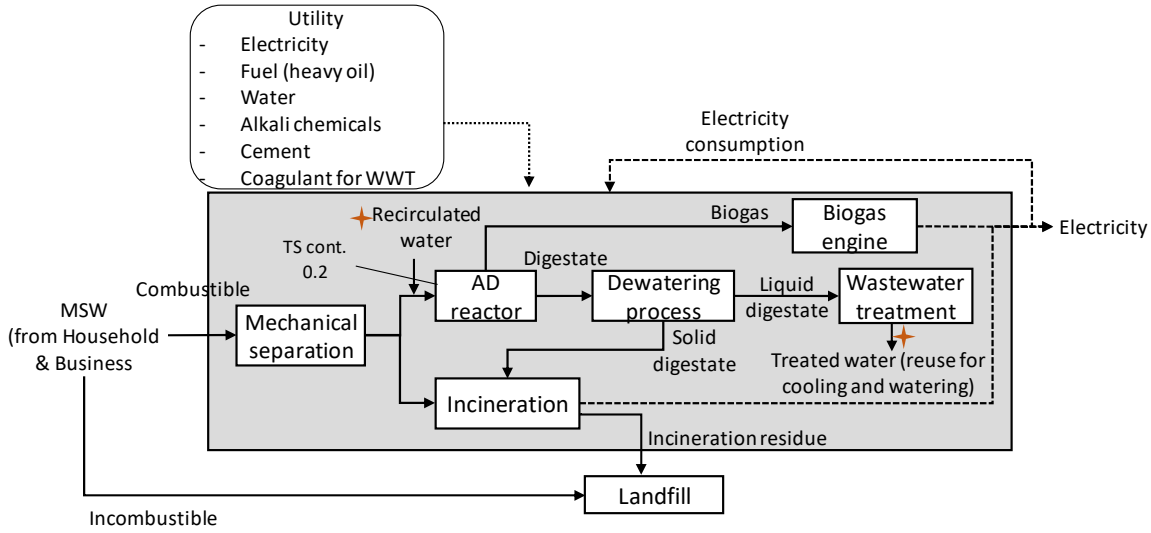

Figure 4-2 Process flow of S2 with material flow and utilities

Table 4-5 Separation rate to AD process by mechanical separation

Component, i		Separation rate to AD (-), R_2^i	Note
1	plastics	0.33	Dry basis
2	paper	0.55	
3	textile	0.26	
4	residue (garden waste +food waste)	0.96	
5	incombustibles	0.22	
m	moisture	0.76	Wet basis
Reference [14]			

Table 4-6 Measured BMP test result and performance of AD process

Component, i		TOC content[i] (Measured)[a] (g-TOC/g-TS)	BMP test result[a]		Performance of AD process Estimated from BMP test	
			Gas generation[i] (L/g-TS)	CH_4 concentration[i] (-)	Degradation rate (-), D^i	Biogas gen. potential (m^3-CH_4/t-TS), B^i
1	plastics	0.82	0.06	0.68	0.04	40
2	paper	0.47	0.49	0.52	0.56	253
3	textile	0.59	0.30	0.55	0.27	164
4	residue (garden waste + food waste)	0.48	0.48	0.55	0.53	266
5	incombustibles	0	0	0	0	0
a-Reference [14]						

Table 4-7 Parameters for utility and operation in dry-AD process

Classification	Parameters	Value	Reference
Utility consumption	Electricity (kWh/t-waste), u_{E2}	290	[4]
	Coagulant for WWT (t/m^3), u_{C2}	0.00015	[9]
Operation	Power generation efficiency, biogas engine (-), η_2	0.3	[4, 15, 16]

4.2.4 Bio-drying MBT system (S3)

Fig. 4-3 shows the process and material flow of S3, the bio-drying MBT system. Combustible waste is dried by an aerobic biological process (called bio-tunnel) for three weeks [17]. Wood is added to combustible waste before introducing the reactor to keep porosity. Then dried outputs are subjected to mechanical separation to recover the fuel materials. Since fine residue and bulky wood are returned to another bio-tunnel, only a small portion of inert residues (0.6% of input combustible waste) are generated. The recovered fuel materials are sent to a fuel production facility and pelletized with other raw materials to produce fuel and SRF. Then, it is combusted in a power plant to generate electricity.

Table 4-8 shows the dry mass of waste components at the input and output of the bio-drying MBT system calculated using the measured physical composition data of waste samples and annual waste tonnage data (see Fig. 3-1 and Fig. 3-5 in Chapter 3) [18, 19]. Mixed fines represent garden waste and food waste in the input combustible waste. When the output to input mass ratio was defined as recovery rate (R_3^i), the rate of plastics, textiles and incombustibles was over 100%. In this case, the recovery rate was assumed to be 100%. Rate of paper and mixed fine was resulted from biodegradation, while the loss of wood was due to abrasion by material recirculation for reusing within the system.

Table 4-9 shows the parameters associated to the utilities and operation for the bio-drying MBT system. The utility and operation of a bio-drying MBT system refers to a full-scale facility in operation [18]. Utility consumption in fuel production and power plant are not considered. The power generation efficiency (η_P) of a solid fuel power plant is assumed to be 31% [20, 21].

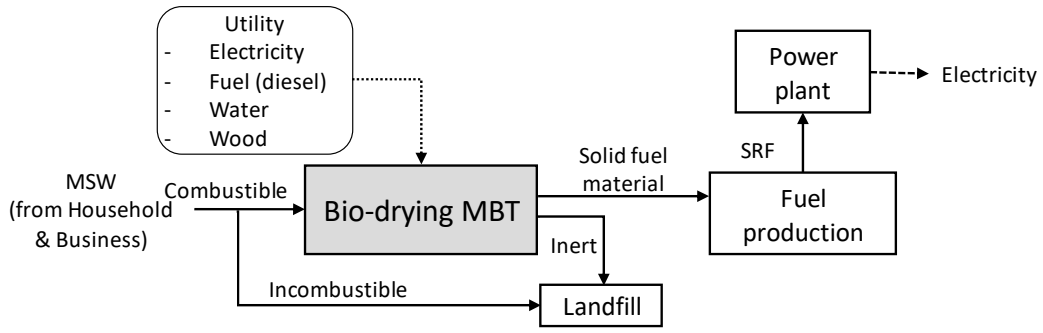

Figure 4-3 Process flow of S3 with material flow and utilities

Table 4-8 Annual mass changes of waste component and recovery rate on the dry basis

Component, i		Annual mass changes			Recovery rate (-)		
		Input (t)	Output (t)		Calculated		Modified, R_3^i
			Fuel	Rejects	Fuel	Rejects	
1	plastics	833.00	983.83		1.18		1.00
2	paper	1479.03	1216.95		0.82		0.82
3	textiles	409.09	764.22		1.87		1.00
4	mixed fine (garden waste + food waste)	1186.03	628.80		0.53		0.53
5	Incombustibles	59.50	63.06	63.19	1.06	1.06	1.00
6	wood	575.61	181.07		0.31		0.31

Reference [18, 19]
Operation data of Biomass Resource Center Mitoyo from 2017 April to 2018 March

Table 4-9 Operation and utility parameters of S3

Classification	Parameters	Value	Reference
Utility consumption	Electricity (kWh/t-waste), u_{E3}	97.30	[18]
	Fuel (diesel) (L/t-waste), u_{O3}	1.30	[18]
	Water (m^3/t-waste), u_{W3}	0.067	[18]
	Wood (t/t-waste), u_{WD}	0.064	[18]
Operation	Power generation efficiency, power plant (-), η_P	0.31	[20, 21]

4.2.5 RDF production system (S4)

Fig. 4-4 shows the process and material flow of RDF production system (S4). Combustible waste is first mechanically separated to remove the rejects such as metals and glass, which are carried to the landfill. Then, the separated fuel materials are dried using fuel oil to reduce their moisture content and convert them to RDF after pelletizing. RDF is sent to a power plant and combusted to generate electricity.

Table 4-10 shows the separation rates by waste component on the wet basis (R_4^k). Garden waste and food waste are difficult to separate, so they were classified as residues in S2 and mixed fines in S3. Therefore, the superscript k value was used for S4. Rates were estimated using the rejects rate of waste at a commercial RDF facility consisting of a manual sorter and a wind separator. With the exception of 50% incombustibles, most combustibles were converted to RDF.

Table 4-11 shows the parameters related to utility and operation for RDF production system. The electricity consumption refers to an RDF production facility in operation [22]. Utility consumption of power plant are not considered. The power generation efficiency (η_P) of a solid fuel power plant is assumed to be 31% [20, 21].

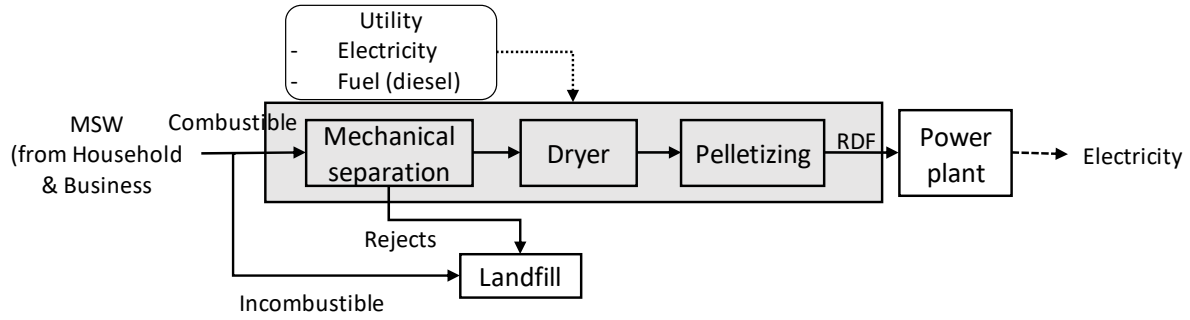

Figure 4-4 Process flow of S4 with material flow and utilities

Table 4-10 Separation rate on the wet basis in RDF production system

Component, k		Separation rate, R_4^k
1	plastics	0.99
2	paper	0.99
3	textiles	0.99
4	garden waste	0.99
5	food waste	1.00
6	Incombustibles	0.50
Reference [9]		

Table 4-11 Operation and utility parameters of S4

Classification	Parameters	Value	Reference
Utility consumption	Electricity (kWh/t-waste), u_{E4}	288.5	[22]
Operation	Power generation efficiency, power plant (-), η_P	0.31	[20, 21]

4.3 Model calculation

4.3.1 Incineration with energy recovery (S1)

As shown in Fig. 4-5, combustible waste is burned all at once. The moisture content of mixed waste is calculated using Eq. (4-3), where M^k and C^k are the moisture content and wet-weight ratio of each component in Table 4-2, respectively. The incineration residue (Q_{Ash1}) is calculated using Eq. (4-4), where Q is the wet mass of incinerated combustible waste in Table 4-1, equal to 78,000 t/y and A^k is the ash content on a dry basis, as shown in Table 4-2. The fly ash generation (Q_{FA1}) used for calculating chemicals is estimated using the fly ash ratios (P_{FA}) as shown in Table 4-4. Q_{Ash1} represents landfilling with incombustible waste separated at the source, as shown in Fig. 4-5.

Power generation from the incineration facility (E_{R1}) is calculated using Eq. (4-7), where H_D^k is the higher heating value of the waste component in Table 4-2 and 2500 is the latent heat of water in MJ/t. In the incineration process, η_1 is the power generation efficiency (Table 4-4). One kilowatt hour is 3.6

MJ. Utility consumption can be calculated using the utility consumption (u) parameters in Table 4-4. In Eq. (4-9), ε^2 is the energy content of heavy oil shown in Table 4-3.

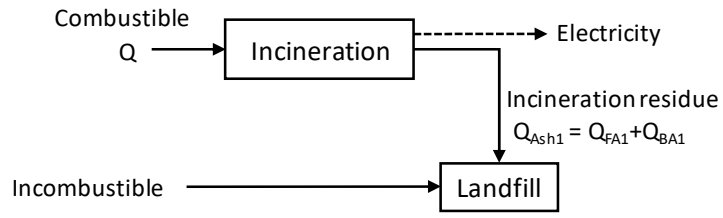

Figure 4-5 Mass flow in S1

Moisture content of combustible waste (-)

$$M = \sum M^k C^k \quad (4\text{-}3)$$

Incineration residue (t-dry/y)

$$Q_{Ash1} = \sum QC^k(1 - M^k)A^k \quad (4\text{-}4)$$

Fly ash (t-dry/y)

$$Q_{FA1} = Q_{Ash1} P_{FA} \quad (4\text{-}5)$$

Landfill (t/y)

$$U_{LF1} = 12319 + Q_{Ash1} \quad (4\text{-}6)$$

Power generation from S1 (kWh/y)

$$E_{R1} = \left(\sum QC^k(1 - M^k){H_D}^k - 2500 \cdot QM\right)\eta_1/3.6 \quad (4\text{-}7)$$

Utility consumption in S1

Electricity (kWh/y): $U_{E1} = Q \cdot u_{E1}$ (4-8)

Fuel oil (L/y): $U_{O1} = Q \cdot u_{O1}/\varepsilon^2$ (4-9)

Water (m^3/y): $U_{W1} = Q \cdot u_{W1}$ (4-10)

Alkali chemical (t/y): $U_{AC1} = Q \cdot u_{AC1}$ (4-11)

Cement (t/y): $U_{S1} = Q_{FA1} \cdot u_{S1}$ (4-12)

4.3.2 Combined system (Anaerobic digestion + Incineration) (S2)

Mechanical separation

Fig. 4-6 shows the mass balance of the combined system. Combustible waste is separated into AD and incineration processes according to the separation rate of each component (R_2^i) in Table 4-5. The dry solids and moisture sent to AD and incineration processes can be calculated using Eqs. (4-13) to (4-16). Here, C^i and M^i are from Table 4-2.

From hence, symbol Q with superscript W indicates water mass. q^i indicates dry solids mass by waste component and its integration is shown with Q with specific subscript, e.g. Q_{AD} is total dry mass of waste separated to AD process.

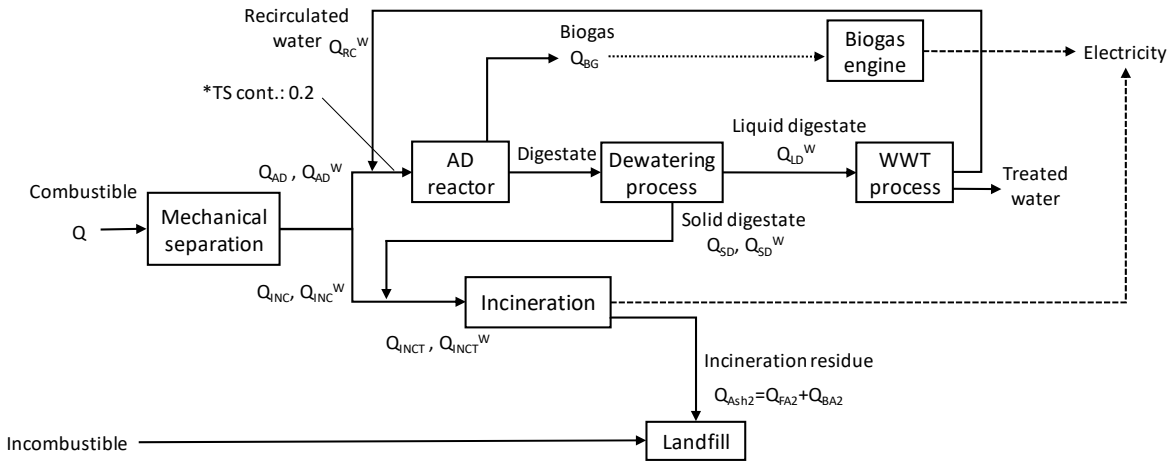

Figure 4-6 Mass flow in S2

Mechanically separated to AD process (t/y)

$$\text{Dry solids: } Q_{AD} = \sum q_{AD}{}^{i} = \sum QC^{i}(1 - M^{i})R_2{}^{i} \quad (4\text{-}13)$$

$$\text{Moisture: } Q_{AD}{}^{W} = QMR_2{}^{m} \quad (4\text{-}14)$$

Mechanically separated to incineration process (t/y)

$$\text{Dry solids: } Q_{INC} = \sum q_{INC}{}^{i} = \sum QC^{i}(1 - M^{i})(1 - R_2{}^{i}) \quad (4\text{-}15)$$

$$\text{Moisture: } Q_{INC}{}^{W} = QM(1 - R_2{}^{m}) \quad (4\text{-}16)$$

Biodegradation during AD process

In the AD reactor, the organic matter is degraded and converted into biogas. Eq. (4-17) shows the degraded organics, where $q_{AD}{}^{i}$ corresponds to the dry solids from the separated waste, which is sent to the AD process based on components (Eq. (4-13)), and D^{i} is the biodegradation rate in Table 4-6. The mass of undegraded organics (Eq. (4-18)) converts to solid digestate (Q_{SD}) after the dewatering process. The produced methane gas is determined by Eq. (4-19), where B^{i} corresponds to the methane gas generation potential of waste component during the AD process on a dry basis in Table 4-6.

Degraded organics during AD process (t-dry/y)

$$\sum q_{AD}{}^{i} D^{i} \quad (4\text{-}17)$$

Undegraded organics (solid digestate) (t-dry/y)

$$Q_{SD} = \sum q_{SD}{}^{i} = \sum q_{AD}{}^{i}(1 - D^{i}) \quad (4\text{-}18)$$

Methane gas generation (m^3-CH_4/y)

$$Q_{BG} = \sum q_{AD}{}^{i} B^{i} \quad (4\text{-}19)$$

Moisture balance around AD process

The Eq. (4-20) is used to calculate the moisture balance between input and output of the AD process. Some treated water is recirculated to the AD process, so the total moisture input of AD equals to sum of $Q_{AD}{}^{W}$ (Eq. (4-14)) and recirculated water ($Q_{RC}{}^{W}$). The moisture output from the AD process is separated into liquid and solid digestate, $Q_{LD}{}^{W}$ and $Q_{SD}{}^{W}$. Since TS content of AD input should be 0.2, the recirculating water ($Q_{RC}{}^{W}$) can be estimated using Eq. (4-21). By assuming the ratio of moisture removal from digestate to be 0.8 in dewatering process, the liquid digestate ($Q_{LD}{}^{W}$) can be determined using Eq. (4-22). Finally, the moisture of solid digestate, $Q_{SD}{}^{W}$ is obtained from the Eq. (4-20).

Moisture balance between input and output of AD process

$$Q_{AD}{}^{W} + Q_{RC}{}^{W} = Q_{SD}{}^{W} + Q_{LD}{}^{W} \quad (4\text{-}20)$$

TS content of AD input (-)

$$Q_{AD}/\left(Q_{AD} + Q_{AD}{}^{W} + Q_{RC}{}^{W}\right) = 0.2 \quad (4\text{-}21)$$

Ratio of moisture to liquid digestate (-)

$$Q_{LD}{}^{W}/(Q_{AD}{}^{W} + Q_{RC}{}^{W}) = 0.8 \quad (4\text{-}22)$$

Incineration and ash generation

The dry solids and moisture of the incineration process can be calculated using the Eqs. (4-23) and (4-24), which is the sum of the waste sorted out by mechanical separation and the returning solid digestate. Since the total ash content in the AD process is finally transferred to incineration, the amounts of incineration residues and fly ash are calculated using Eqs. (4-25)-(4-26). Incineration residue is landfilled with source separated incombustible waste (Eq. (4-27)).

Total waste input to incineration process (t/y)

Dry solids: $Q_{INCT} = \sum q_{INCT}{}^{i} = \sum(q_{INC}{}^{i} + q_{SD}{}^{i})$ (4-23)

Moisture: $Q_{INCT}{}^{W} = Q_{INC}{}^{W} + Q_{SD}{}^{W}$ (4-24)

Incineration residue (t-dry/y)

$$Q_{Ash2} = \sum QC^{i}(1 - M^{i})A^{i} \quad (4\text{-}25)$$

Fly ash (t-dry/y)

$$Q_{FA2} = Q_{Ash2}P_{FA} \quad (4\text{-}26)$$

Landfill (t/y)

$$U_{LF2} = 12319 + Q_{Ash2} \quad (4\text{-}27)$$

Power generation and utility consumption

In the combined system, energy is recovered from both incineration (E_{R2_INC}) and AD processes (E_{R2_AD}). $q_{INCT}{}^{i}$ is the dry mass of each component (Eq. (4-23) and $H_{D}{}^{i}$ is taken from Table 4-2. In the Eq. (4-29), Q_{BG} is the methane gas produced from the AD process, and the lower heating value (LHV)

of the methane gas is 35.9 MJ/m^3. η_1 and η_2 correspond to the power generation efficiency of incineration and gas engine shown in Table 4-4 and Table 4-7, respectively.

Utility consumption can be calculated by using each parameter i.e. u_{E1}, u_{O1}, u_{W1}, u_{AC1}, u_{S1} from Table 4-4 and u_{E2}, u_{C2} from Table 4-7 (Eq. (4-30) – (4-35)). In Eq. (4-30), ε^2 is the energy content of heavy oil, shown in Table 4-3.

Power generation from S2 (kWh/y)

Incineration: $E_{R2\_INC} = \{\sum {q_{INCT}}^i {H_D}^i - 2500 \cdot {Q_{INCT}}^W\}\eta_1/3.6$ (4-28)

AD: $E_{R2\_AD} = Q_{BG} \cdot 35.9 \cdot \eta_2/3.6$ (4-29)

Utility consumption in S2

Electricity (kWh/y): $U_{E2} = (Q_{INCT} + {Q_{INCT}}^W)u_{E1} + (Q_{AD} + {Q_{AD}}^W)u_{E2}$ (4-30)

Fuel oil (L/y): $U_{O2} = (Q_{INCT} + {Q_{INCT}}^W)u_{O1}/\varepsilon^2$ (4-31)

Water (m^3/y): $U_{W2} = (Q_{INCT} + {Q_{INCT}}^W)u_{W1}$ (4-32)

Alkali chemical (t/y): $U_{AC2} = (Q_{INCT} + {Q_{INCT}}^W)u_{AC1}$ (4-33)

Cement (t/y): $U_{S2} = Q_{FA2} \cdot u_{S1}$ (4-34)

Coagulant (t/y): $U_{C2} = {Q_{LD}}^W \cdot u_{C2}$ (4-35)

4.3.3 Bio-drying MBT system (S3)

Fig. 4-7 shows the mass balance of the bio-drying MBT system. The dry solids (Q_{BD}) and moisture content (Q_{BD}^W) of bio-drying input are the sum of the combustible waste and wood (Eqs. (4-36) and (4-37)). Here, C^i and M^i are taken from Table 4-2. The wood input ratio to combustible waste is indicated by u_{WD}, and 0.12 is the moisture content of the wood [23]. The Eq. (4-38) calculates the dry solids (Q_{F3}) of the recovered fuel materials, as determined by the recovery rate of the waste component on a dry basis, R_3^i, as shown in Table 4-8. In the Eq. (4-39), the water removal rate observed in the bio-drying process equals 0.69 [19]. Mass of the inert materials (Q_{IT}) generated from the system can be calculated using Eq. (4-40), where 0.006 indicates the inert generation rate per input waste. Eq. (4-41) shows the mass of landfilled waste generated from S3, where 12319 is the mass of source separated incombustibles shown in Table 4-1.

The energy recovered from the bio-drying MBT system can be calculated using the Eq. (4-42), the higher heating value of wood is 17,888 MJ/t [23]. η_P corresponds to the power generation efficiency of power plant [20, 21]. Utility consumptions are calculated using Eqs. (4-43) to (4-46).

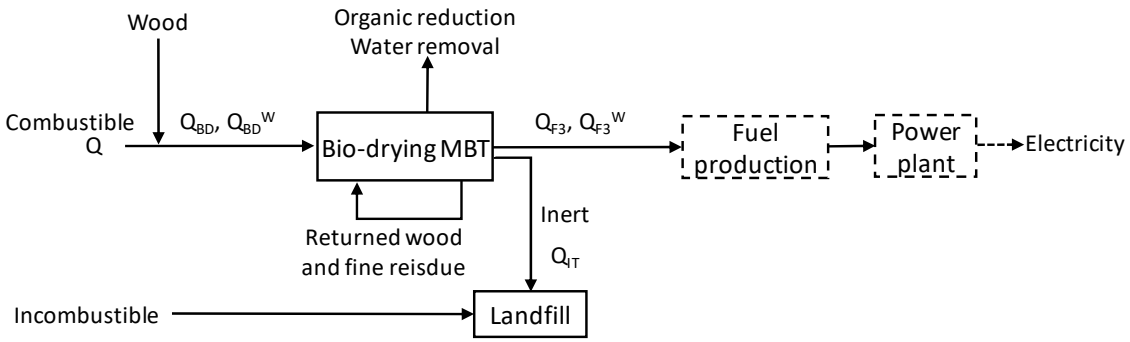

Figure 4-7 Mass flow in S3

Input to bio-drying process (t/y)

$$\text{Dry solids: } Q_{BD} = \sum {q_{BD}}^{i} = \sum QC^{i}(1 - M^{i}) + Qu_{WD}(1 - 0.12) \quad (4\text{-}36)$$

$$\text{Moisture: } {Q_{BD}}^{W} = \sum QC^{i}M^{i} + Qu_{WD} \cdot 0.12 \quad (4\text{-}37)$$

Output from bio-drying process (t/y)

$$\text{Dry solids: } Q_{F3} = \sum {q_{F3}}^{i} = \sum {q_{BD}}^{i} \times {R_3}^{i} \quad (4\text{-}38)$$

$$\text{Moisture: } {Q_{F3}}^{W} = {Q_{BD}}^{W}(1 - 0.69) \quad (4\text{-}39)$$

Inert generation from bio-drying MBT system (t-dry/y)

$$Q_{IT} = Q \cdot 0.006 \quad (4\text{-}40)$$

Landfill (t/y)

$$U_{LF3} = 12319 + Q_{IT} \quad (4\text{-}41)$$

Power generation from S3 (kWh/y)

$$E_{R3} = \left\{\left(\sum {q_{F3}}^{i} {H_D}^{i} + {q_{F3}}^{6} \cdot 17888\right) - 2500 \cdot {Q_{F3}}^{W}\right\}\eta_P/3.6 \quad (4\text{-}42)$$

Utility consumption in S3

$$\text{Electricity (kWh/y): } U_{E3} = Q \cdot u_{E3} \quad (4\text{-}43)$$

$$\text{Fuel oil (L/y): } U_{O3} = Q \cdot u_{O3} \quad (4\text{-}44)$$

$$\text{Water (m}^3\text{/y): } U_{W3} = Q \cdot u_{W3} \quad (4\text{-}45)$$

$$\text{Wood (t/y): } U_{WD} = Q \cdot u_{WD} \quad (4\text{-}46)$$

4.3.4 RDF production system (S4)

Fig. 4-8 shows the mass balance of the RDF production system. The dry solids and moisture balance after the mechanical separation are calculated using the Eqs. (4-47) to (4-50), where C^k and M^k are taken from Table 4-2. As shown in Table 4-10, $R_4{}^k$ is the separation rate of each waste component on a wet basis. The mass of dry solids is constant before and after the drying process, i.e., $Q_{F4} = Q_{RDF}$. The moisture content after drying ($Q_{RDF}{}^W$) is calculated using the Eq. (4-51), where 0.13 is the moisture content set for RDF. The rejects are landfilled with source separated incombustible waste (Eq. (4-52)).

The energy recovered from the RDF combustion is calculated using the Eq. (4-53), where η_P is the power generation efficiency of power plant [20, 21]. The electricity consumption can be calculated using the Eq. (4-54). The fuel oil consumption in S4 is calculated using the Eq. (4-55), where the first and second terms indicate the latent heat consumption and sensible heat loss. The heat capacity of dry solids and water are 1.38 and 4.2 MJ/t·℃, respectively. The energy efficiency in the dryer, defined by the ratio between energy required for water removal and the provided energy, is supposed 0.3 and ε^3 indicates the energy content of diesel oil shown in Table 4-3. Using the Eq. (4-56), fuel oil consumption (U_{O4}) can be calculated.

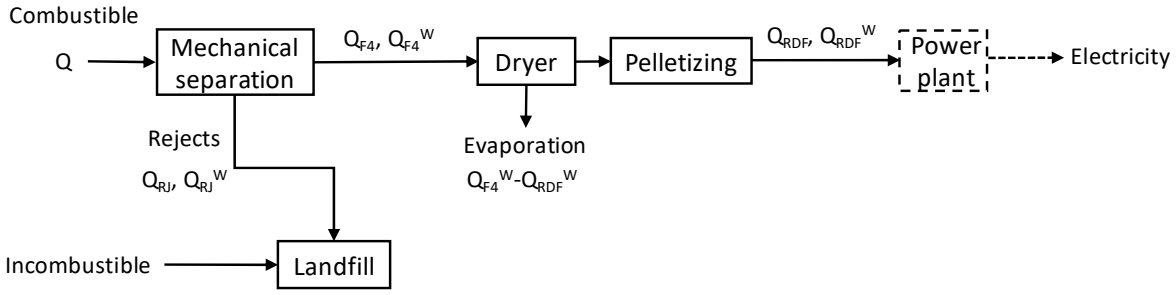

Figure 4-8 Mass flow in S4

Mechanically separated fuel materials (t/y)

$$\text{Dry solids: } Q_{F4} = \sum q_{F4}{}^k = \sum QC^k R_4{}^k (1 - M^k) \quad (4\text{-}47)$$

$$\text{Moisture: } Q_{F4}{}^W = \sum QC^k R_4{}^k M^k \quad (4\text{-}48)$$

Mechanically separated rejects (t/y)

$$\text{Dry solids: } Q_{RJ} = \sum QC^k \left(1 - R_4{}^k\right)(1 - M^k) \quad (4\text{-}49)$$

$$\text{Moisture: } Q_{RJ}{}^W = \sum QC^k \left(1 - R_4{}^k\right) M^k \quad (4\text{-}50)$$

Moisture in RDF after drying (t/y)

$$Q_{RDF}{}^W = Q_{F4} \cdot 0.13/(1 - 0.13) \quad (4\text{-}51)$$

Landfill (t/y)

$$U_{LF4} = 12319 + (Q_{RJ} + Q_{RJ}{}^W) \quad (4\text{-}52)$$

Power generation from S4 (kWh/y)

$$E_{R4} = \left\{\sum q_{RDF}{}^k H_D{}^k - 2500 \cdot Q_{RDF}{}^W\right\}\eta_P/3.6 \quad (4\text{-}53)$$

Electricity consumption (kWh/y)

$$U_{E4} = Q \cdot u_{E4} \quad (4\text{-}54)$$

Energy required for water removal (MJ/y)

$$L_O = \left(Q_F{}^W - Q_{RDF}{}^W\right) \cdot 2500 + (Q_F \cdot 1.38 + Q_{RDF}{}^W \cdot 4.20)(100 - 20) \quad (4\text{-}55)$$

Energy efficiency of dryer (-)

$$0.3 = L_O / U_{O4} \varepsilon^3 \quad (4\text{-}56)$$

4.3.5 Life cycle energy and CO_2 emission

Life cycle energy consumption and CO_2 emission for the four systems are calculated by multiplying the units (ε^m, θ^m) in Table 4-3 by the relevant utility consumptions. Regarding the power recovery, the energy consumption and CO_2 emissions in the life cycle are avoided. The Eq. (4-71) and (4-72) are the energy consumption and CO_2 emission, when one ton of waste is landfilled.

Table 4-12 Calculation of life cycle energy and CO_2

	Life cycle energy (MJ/y)		Life cycle CO_2 (kg-C/y)	
Electricity	$U_E \cdot \varepsilon^1$	(4-57)	$U_E \cdot \theta^1$	(4-58)
Fuel oil (heavy oil)	$U_O \cdot \varepsilon^2$	(4-59)	$U_E \cdot \theta^2$	(4-60)
Water	$U_W \cdot \varepsilon^4$	(4-61)	$U_W \cdot \theta^4$	(4-62)
Alkali chemicals	$U_{AC} \cdot \varepsilon^5$	(4-63)	$U_{AC} \cdot \theta^5$	(4-64)
Cement	$U_S \cdot \varepsilon^6$	(4-65)	$U_S \cdot \theta^6$	(4-66)
Coagulant	$U_C \cdot \varepsilon^7$	(4-67)	$U_C \cdot \theta^7$	(4-68)
Wood	$U_{WD} \cdot \varepsilon^8$	(4-69)	$U_{WD} \cdot \theta^8$	(4-70)
Landfill	$U_{LF} \cdot \varepsilon^9$	(4-71)	$U_{LF} \cdot \theta^9$	(4-72)

4.4 Results and discussion

4.4.1 Flow of mass and energy content

Fig. 4-9 shows the mass balance of dry solids and moisture in S2. About 65% of the dry combustible waste was dedicated to the AD process and the remaining (35%) was delivered to the incineration process after mechanical separation. About 50% of the dry solids were degraded by the AD process. The biodegradability of 50-60% sounds reasonable for both residues and paper. The balance of moisture is shown in the next to dry solids figure. By mechanical separation, 75 percent of the moisture was transferred to the AD process and mixed with the water recirculated from the WWT process, maintaining the TS content of the AD input at 0.2. Dewatering rate was assumed to be 80%, while 84% of the treated water was returned to the AD process. In mass balance of S3 (Fig. 4-10), the degradation rate of TS including size reduction of wood was 28%, while 69% of the moisture was removed by the bio-drying process. On the other hand, most of the dry solids were preserved throughout the S4 process, which had an evaporation rate of 87%.

Table 4-13 summarizes the total energy flows for the four systems where LHV is shown in brackets. The power recovery rate was calculated according to the assumed efficiency. In S1, all combustible waste was utilized for power generation. In S2, the dry mass was separated into the incineration and AD processes, and energy is recovered from both. In S3, the addition of wood increased the energy content of the input waste of the bio-drying process. Although LHV increased by decreasing moisture content, organic degradation lowered the total energy content of the fuel materials. The energy content of fuel materials in S4 was higher than that of S3 because all dry solids were preserved. Further details on power generation are provided in the next section. The energy contents, heating values, and moisture contents estimated for the four systems are shown in the Fig. A4-4 in appendices.

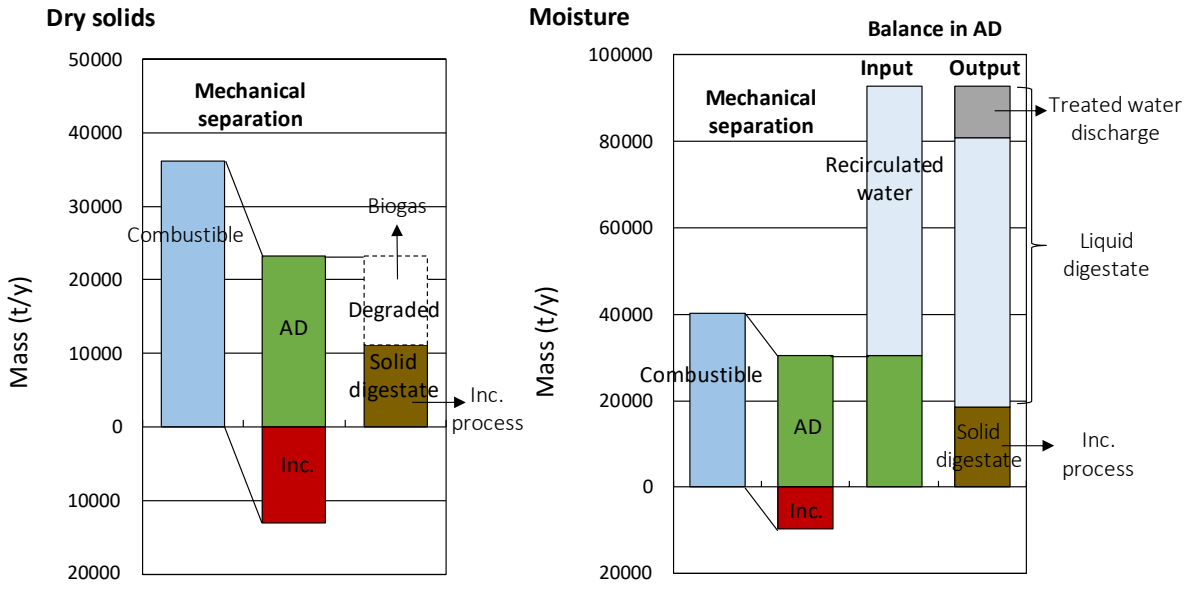

Figure 4-9 Dry solids and moisture balance of S2

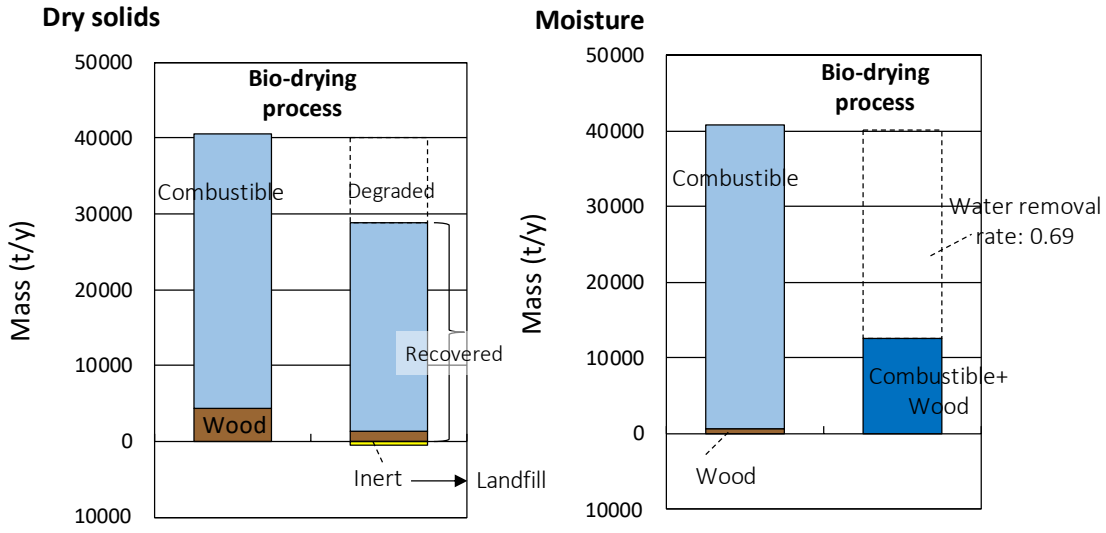

Figure 4-10 Dry solids and moisture balance of S3

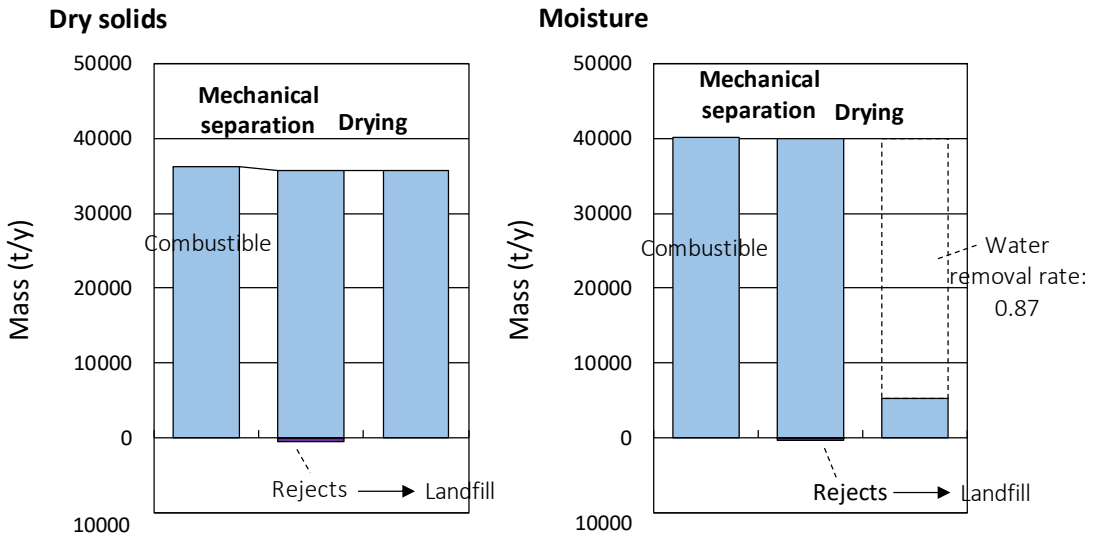

Figure 4-11 Dry solids and moisture balance of S4

Table 4-13 Total energy content of input and output waste and power recovery

		S1	S2		S3	S4
			Inc.	AD		
INPUT (GJ/y)	Combustibles	548285 (7174 MJ/t)	217910 (9564 MJ/t)	330376 (6159 MJ/t)	548285 (7174 MJ/t)	548285 (7174 MJ/t)
	Wood				75892 (15441 MJ/t)	
	Solid digestate		156758 (5265 MJ/t)			
OUTPUT (GJ/y)	Biogas			206669		
	Fuel materials				491387 (11858 MJ/t)	629327 (15313 MJ/t)
Power recovery (GWh/y)		28.9	19.8	17.2	41.6	53.3

4.4.2 Energy balance and CO_2 emission

Fig. 4-12 shows a comparison of the energy balance and CO_2 emissions of the four systems. The upper and lower bar graphs show energy recovery from power generation and energy consumption mainly from electricity and fuel. The remaining energy consumption is combined with 'others' in Fig. 4-12. The net amount is the sum of recovery and consumption, as shown by the dot symbol. In 4-12b, CO_2 emissions and avoided CO_2 emissions due to power recovery are shown in the lower and upper bars, respectively.

Comparing S2 with S1, S2 recovered more energy than S1 due to the additional energy recovery from the biogas engine with high power generation efficiency. However, high electricity consumption

in S2 reduced the net recovery in total. In S3, although the total energy content of the fuel materials decreased due to organic degradation, because of high power generation efficiency of the power plant, more electricity was generated than S1 and S2. In addition, power consumption was almost half that of S1, which significantly improved the net energy recovery from the system. S4 recovered the highest energy due to low moisture content of the fuel materials. However, significant fuel consumption for drying led to low net efficiency. Overall, S3 showed the highest energy efficiency and lowest CO_2 emission among various systems.

As shown in Fig. 4-12b, CO_2 emissions follow a similar trend to energy balance, indicating that electricity and fuel consumption were the main sources of emissions. Due to the low mass, there was no significant difference in life cycle energy and CO_2 emissions from landfills for the disposal of the materials produced by the four systems. Further details on energy balance and CO_2 emissions can be found in the Table A4-1 in Appendix.

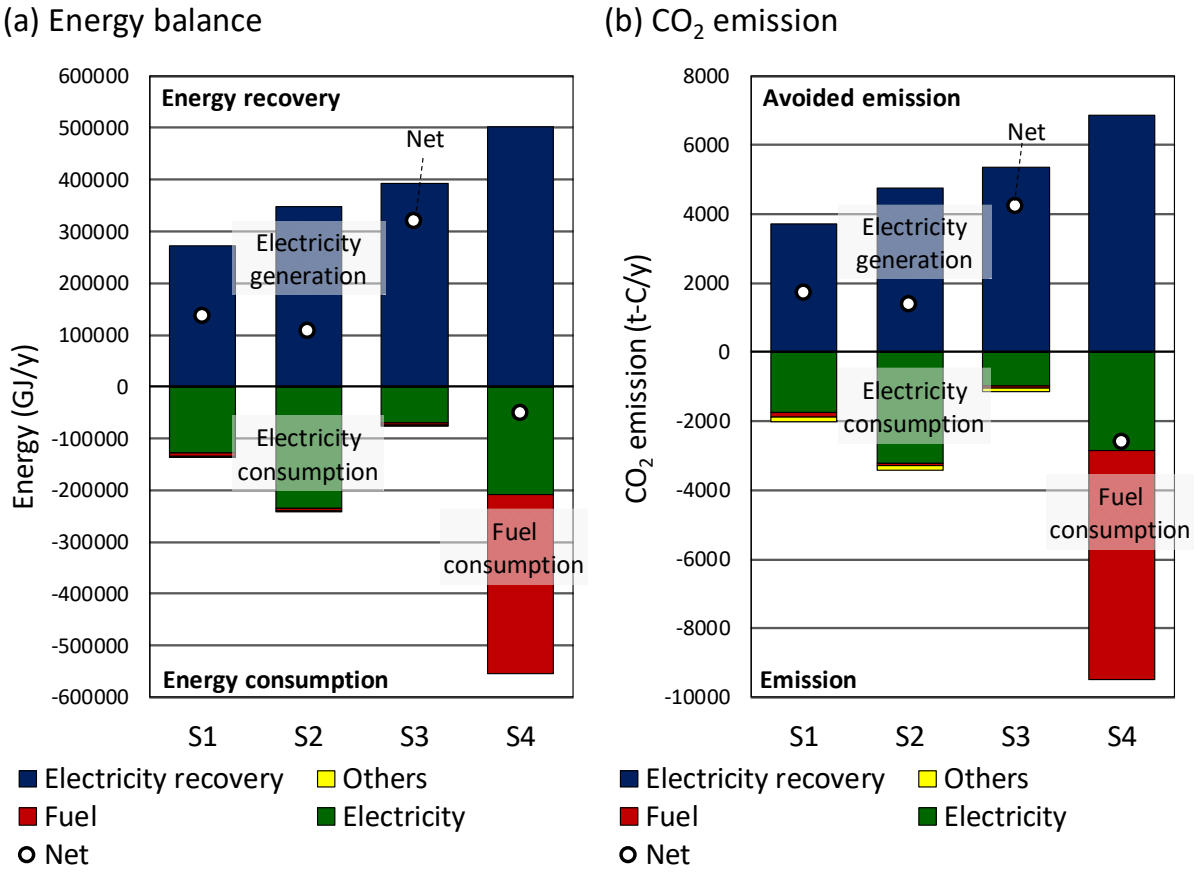

Figure 4-12 Result of energy balance and CO_2 emission

4.5 Sensitivity analysis

4.5.1 Parameters variation in each system

Since most parameters were obtained from the literature, sensitivity analysis of the key parameters was performed. Table 4-12 shows the possible ranges of parameters that shows reality based on the literature, in which "Max." means the value that increased the net energy recovery. The different between the set values ± 20%, and the parameters change with constant sensitivity.

Power consumption (u_E) and power generation efficiency (η) were different in all four systems. In S2, the mechanical separation rate to AD refers to investigated separation rate on a wet basis in commercial combined system [24]. Based on the gap between Max. and set, Min. value has determined. In case of residue, +20% value exceeds 100%, it has set to 100%. The good mechanical separation indicates the more paper and residue with less plastics are transferred to AD process. The AD performance, are determined by the same manner to S2-1 as the maximum values for possible ranges are referred from the manual for utilization of biomass report [25]. More organic degradation produces biogas for power generation. The dewatering performance are assumed to have 10%-point differences from set values. The high dewatering performance contributes to less water in solid digestate that returned to incineration process. The electricity consumption for AD process is set to ±10% variation due to lack of data. Ranges for power generation efficiency of biogas engine refers to the literature [4, 15, 16].

In S3, water removal rate, which affects the efficiency of mechanical separation and heating value of fuel materials varied based on previous studies reported to reach 82% [1, 26, 27]. In addition, the recovery rate of paper (R_3^2) and mixed fine (R_3^4) increased by decreasing the biodegradation rate. As defined in section 2.4, recovery rate is the ratio of output and input waste mass, biodegradation of organics (paper and mixed fine) influences on its output mass and recovery rate. Less paper would be recovered from the system when biodegradation rate of paper is high during bio-drying process. The electricity consumption is set to ±10% variation due to lack of data. The ranges for power generation efficiency of power plant in S3 and S4 refers to the literature for fuel combustion in power plant [20, 21]. In S4, the energy efficiency of the is ranged to 33% maximum, which has referred from 33.2% of energy efficiency in commercial RDF production system [9]. The moisture content of RDF is varied from 6 to 19% and having an effect on fuel consumption for drying and amount of energy recovery due to different LHV of RDF [9]. The ranges of electricity consumption are referred from the operating RDF production system data [22].

Table 4-14 Variation in parameters for sensitivity analysis

Scenario		Classification	Parameters	Possible ranges				Fixed sensitivity	
				Min.	Set	Max.	Reference	-20%	+20%
S1	1	Electricity consumption for operation	Electricity consumption (kWh/t-waste), u_{E1}	244	178	98	[12]	214	143
	2	Electricity power generation	Power gen. efficiency, incineration (-), η_1	0.17	0.19	0.21	[13]	0.15	0.23
S2	1	Mechanical separation	Separation rate to AD process (-, dry basis), R_2^i				[24]		
			plastics	0.46	0.33	0.20		0.39	0.26
			papers	0.46	0.55	0.65		0.44	0.66
			textiles	0.37	0.26	0.15		0.31	0.21
			residue	0.92	0.96	1.00		0.77	1.00
			moisture (wet)	0.68	0.76	0.83		0.61	0.91
	2	AD performance	Methane gas gen. potential (Nm^3/t-dry), B^i				[25]		
			paper	189	253	317		202	304
			residue	125	266	407		213	319
			Degradation rate (-), D^i				[25]		
			paper	0.49	0.56	0.63		0.45	0.67
			residue	0.33	0.53	0.74		0.43	0.64
	3	Dewatering performance	Moisture removal from digestate	0.70	0.80	0.90		0.64	0.96
	4	Electricity consumption for operation	Electricity consumption, Inc. (kWh/t-waste), u_{E1}	244	178	98	[12]	214	143
			Electricity consumption, AD (kWh/t-waste), u_{E2}	319	290	261	[4]	348	232
	5	Electricity power generation	Power gen. efficiency, Inc. (-), η_1	0.17	0.19	0.21	[5]	0.15	0.23
			Power gen. efficiency, biogas engine (-), η_2	0.22	0.30	0.37	[4, 15, 16]	0.24	0.35
	The higher the values, the lower the energy efficiency of the system								

Table 4-14 Variation in parameters for sensitivity analysis (Continued)

Scenario		Classification	Parameters	Possible ranges				Fixed sensitivity	
				Min.	Set	Max.	Reference	-20%	+20%
S3	1	Moisture removal	Water removal rate (-)	0.67	0.69	0.82	[1, 26, 27]	0.55	0.83
	2	Fuel material recovery	(Fuel material) recovery rate (-, dry basis), R_3^i						
			papers	0.74	0.82	0.91		0.66	0.99
			mixed fine	0.48	0.53	0.58		0.42	0.64
	3	Electricity consumption for operation	Electricity consumption (kWh/t-waste), u_{E3}	107	97	88		117	78
	4	Electricity power generation	Power gen. efficiency, power plant (-), η_P	0.28	0.31	0.33	[20, 21]	0.25	0.37
S4	1	Moisture content of RDF	Moisture content of RDF	0.06	0.13	0.19	[9]	0.10	0.16
	2	Fuel consumption for drying	Energy efficiency of dryer (-)	0.27	0.30	0.33	[9]	0.24	0.36
	3	Electricity consumption for operation	Electricity consumption (kWh/t-waste), u_{E4}	304	289	149	[22]	346	231
	4	Electricity power generation	Power gen. efficiency, power plant (-), η_P	0.28	0.31	0.33	[20, 21]	0.25	0.37
	The higher the values, the lower the energy efficiency of the system								

4.5.2 Energy balance results

Fig. 4-13 shows the results of a sensitivity analysis showing changes in net energy recovery and energy balance between power generation and recovery. The baseline shows the value obtained from the set value. The parameters sensitivity is represented by the symbol ± 20%. The power generation efficiency of the entire system, dewatering performance of S2, the fuel consumption of S4, and the recovery rate of S3 were highly sensitivity parameters.

On the other hand, in the actual situation presented by Min. and Max. values (marked with triangle symbols), the AD performance in S2 and the electricity consumption of all systems (except for S3) were high. Improving these parameters was the most effective solution for high energy performance. Separation efficiency in S2, water removal rate in S3, and moisture content of fuel in S4 had little impacts on energy balance.

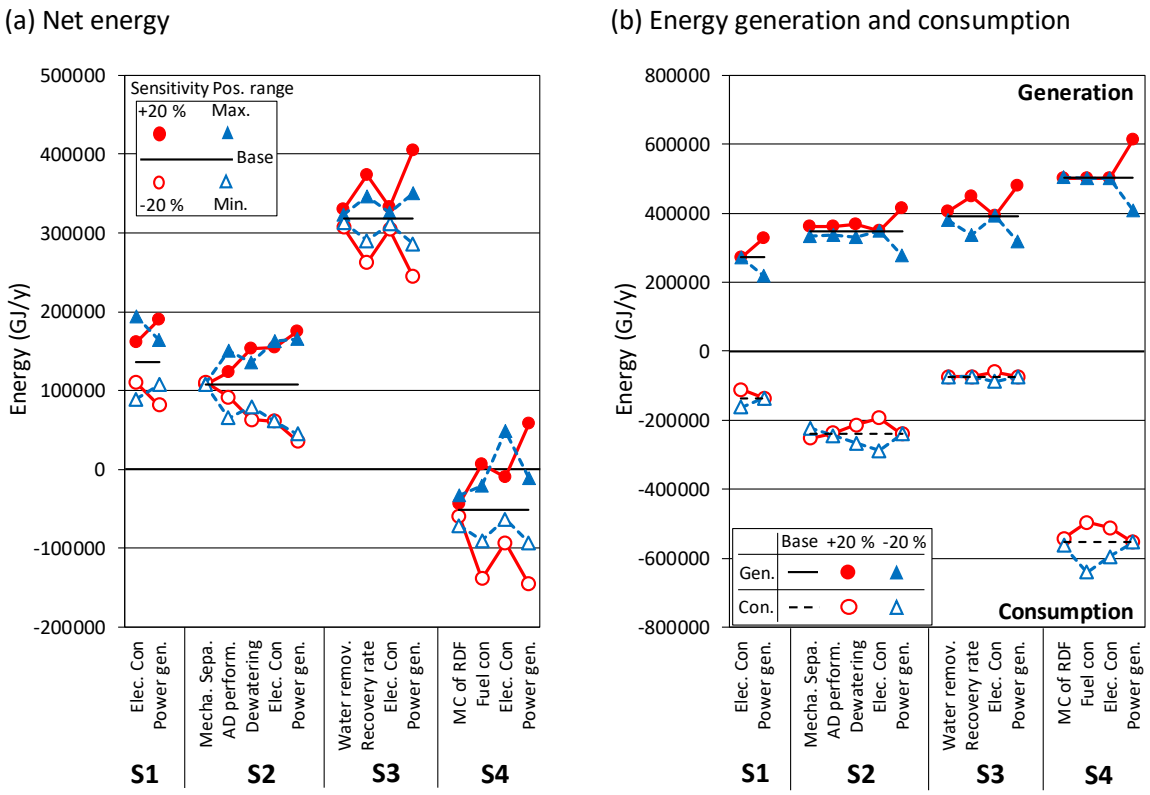

Figure 4-13 Changes of net energy and energy balance based on the ranges in Table 4-14

4.5.3 Energy efficiency under ideal conditions

Fig. 4-14 shows the best condition with all parameters in Table 4-14 improved to be “Max” and the worst condition with “Min” values for all parameters.

S2 showed the most noticeable improvement in energy balance and a higher energy recovery rate to be compatible with S3. Fig. 4-15 shows the gradual change in energy balance by adding the "Max" values in the order shown in Table 4-14. This showed changes in energy balance in cumulative Max. values. Sequentially, the AD performance and power generation efficiency were the most critical factors in energy balance by providing additional energy.

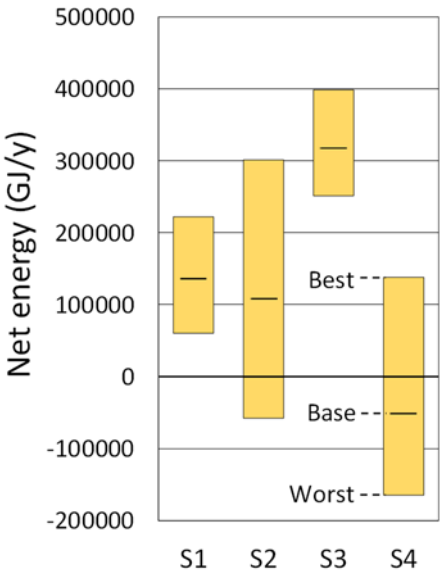

Figure 4-14 Net energy of best and worst case

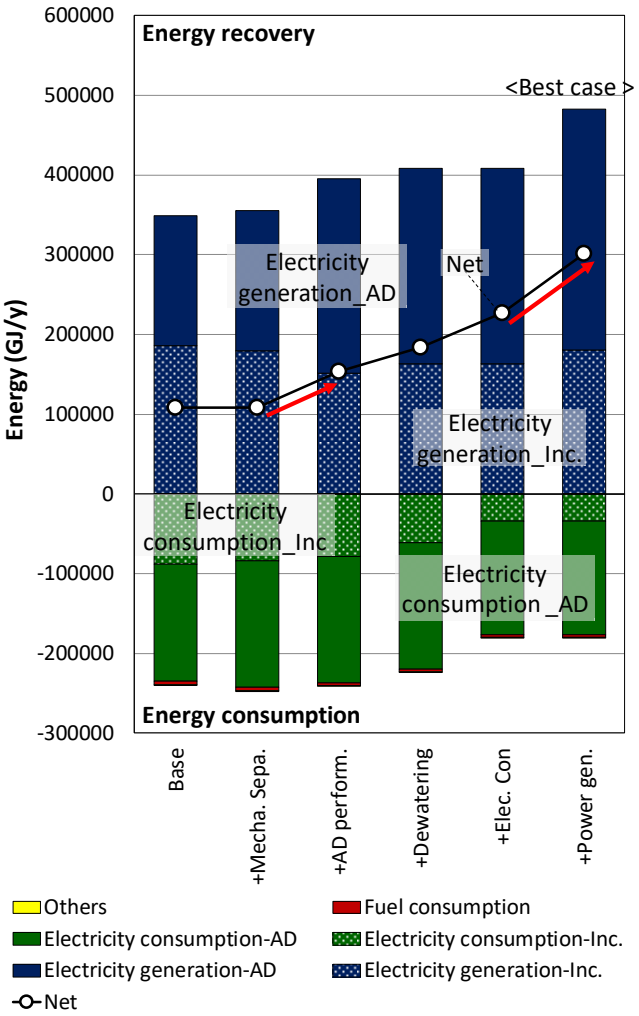

Figure 4-15 Changes of energy balance by applying Max. values of S2 parameters from Table 4-14 in sequence

4.6 Conclusion

In this chapter, four different systems that recover energy from MSW were evaluated and compared in terms of energy balance and CO_2 emissions. The bio-drying MBT system, which recovers solid fuel, combusted in the power plants showed the highest energy efficiency. The loss of organic matter during the bio-drying process reduced the energy input to the power plant. However, low electricity and fuel consumption enhanced the energy efficiency of the system. Meanwhile, the RDF production system recovered the highest energy, but a considerable fuel consumption resulted in the lowest energy efficiency. The combined system recovered electricity from the incinerator and biogas engine, but the high electricity consumption in the AD process made it less energy efficiency. CO_2 emissions followed the trend of energy balance, which was highly dependent on electricity consumption.

In this study, all basic parameters were obtained from a literature review and the authors conducted the study in a full-scale facility. Therefore, it was possible to improve energy recovery efficiency by modifying individual processes. According to sensitivity analysis, power generation efficiency and electricity consumption were the most influential parameters. The combined system showed low energy efficiency under a controlled set of parameters, but the efficiency was simultaneously compatible with the bio-drying system under ideal conditions of parameters.

Instead of burning waste directly in incineration, combustion of solid fuel made from mixed MSW by removing moisture and at the same time enable stabilizing of biodegradable fraction is advantageous on energy recovery. This conclusion is drawn from energy perspective, and further analysis including environmental impact and economic feasibility are needed.

References

1. Psaltis P, Komilis D (2019) Environmental and economic assessment of the use of biodrying before thermal treatment of municipal solid waste. Waste Manag 83:95–103. https://doi.org/10.1016/j.wasman.2018.11.007
2. Fei F, Wen Z, Huang S, De Clercq D (2018) Mechanical biological treatment of municipal solid waste: Energy efficiency, environmental impact and economic feasibility analysis. J Clean Prod 178:731–739. https://doi.org/10.1016/j.jclepro.2018.01.060
3. Cimpan C, Wenzel H (2013) Energy implications of mechanical and mechanical-biological treatment compared to direct waste-to-energy. Waste Manag 33:1648–1658. https://doi.org/10.1016/j.wasman.2013.03.026
4. Inoue T, Matsuto T (2014) Energy Appraisal of the Combined System with the Incinerator Using the Dry Type Methane Fermentation (in Japanese). Doboku Gakkai 70:32–41
5. Takata M, Fukushima K, Kawai M, et al (2013) The choice of biological waste treatment method for biological waste treatment methods for urban areas in Japan - An environmental perspective. Renew Sustain Energy Rev 23:557–567. https://doi.org/10.1016/j.rser.2013.02.043
6. Ministry of the environment Japan (2019) Survey on general waste management business in FY2017 (in Japanese)
7. Ministry of the environment Japan (2019) Waste Treatment in Japan in FY 2017 (in Japanese)
8. Asahikawa municipality (2018) Waste generation trend (in Japanese)
9. Matsuto T (2005) Analysis, Design and Evaluation of Solid Waste Treatment System-Materials flow and LCA program (in Japanese). Gihodoshuppan, Tokyo, Japan
10. Aomori Research Institution (2010) Explanation of wood pellet and extruder (in Japanese)
11. Osada M, Manako K, Hirai Y, Sakai S (2012) Life Cycle Assessment for Treatment and Recycling of Automobile Shredder Residue (ASR) (in Japanese). J Japan Soc Mater Cycles Waste Manag 23:264–278. https://doi.org/10.3985/jjsmcwm.1101201
12. Hokkaido University Laboratory of Solid Waste Disposal Engineering (2012) Analysis of Mass, Energy and Cost Balance of Continuous Incineration facility for MSW (in Japanese)
13. Ministry of the environment Japan (2018) Maintenance manual of high-efficient waste to energy facility (in Japanese)
14. Canabal EE (2018) Material and Energy balance in Combined system. Hokkaido University
15. Noike T, Yasui H, Matsumoto A, et al (2009) Methane fermentation (in Japanese). Gihodoshuppan, Tokyo, Japan
16. Takuma (2015) Corporate Profile & CSR Report 2015 (in Japanese)
17. Mitoyo city (2015) Solid Waste Management Master Plan for Mitoyo city (in Japanese). Mitoyo city, Kagawa, Japan

18. Biomass Resource Center Mitoyo (2018) Operation data in FY 2017 (in Japanese)
19. Ham GY, Matsuto T, Tojo Y, Matsuo T (2020) Material and moisture balance in a full-scale bio-drying MBT system for solid recovered fuel production. J Mater Cycles Waste Manag 22:167–175. https://doi.org/10.1007/s10163-019-00925-2
20. Surroop D, Mohee R (2011) Power generation from refuse derived fuel. In: 2011 2nd International Conference on Environmental Engineering and Application IPCBEE. LACSIT Press, Singapore, pp 242–246
21. National Institute of Environmental Studies (2009) Power generation from Solid waste (in Japanese). https://tenbou.nies.go.jp/science/description/detail.php?id=72. Accessed 30 Sep 2019
22. Yamanari M, Shimada S (2007) Life Cycle Assessment of RDF Power Generation in Northern Ishikawa Prefecture (in Japanese). J Japan Soc Waste Manag Expert 18:37–48. https://doi.org/10.3985/jswme.18.37
23. Tchobanoglous G, Theisen H, Vigil SA (1993) Integrated solid waste management : engineering principles and management issues. McGraw-Hill
24. Takaoka Y, Kawamura K, Kakuta Y (2014) Combined System Integrates Bio-gas Production Equipment and Waste Incineration in Nantan Area (in Japanese). Mater cycles waste Manag Res 25:36–42
25. Ministry of the environment Japan (2017) Manual for utilization of biomass (in Japanese)
26. Dziedzic K, Łapczynska-Kordon B, Malinowski M, et al (2015) Impact of aerobic biostabilisation and biodrying process of municipal solid waste on minimisation of waste deposited in landfills. Chem Process Eng - Inz Chem i Proces 36:381–394. https://doi.org/10.1515/cpe-2015-027
27. Adani F, Baido D, Calcaterra E, Genevini P (2002) The influence of biomass temperature on biostabilization – biodrying of municipal solid waste. Bioresour Technol 83:173–179

CHAPTER 5
Conclusions

5.1 Summary of this thesis

Chapter 1 describes the background of the MBT system and variation of the process flow under different operation aims. This thesis focused on understanding of bio-drying MBT system in terms of water removal, material and energy recovery efficiency.

Chapter 2 conducted a lab-scale experiment to investigate the simultaneous effects of airflow rate and organic contents on water removal. A 25L acrylic column reactor was filled with simulated waste, commercial dog food and wood pellet mixture. Temperature and humidity of the air inlet and outlet were continuously monitored, and CO_2 concentrations in outlet air were periodically analyzed to observe aerobic biodegradation as well as metabolic water generation. Based on the data, the different water removal contributions by airflow and biodegradation were compared. While the biodegradation of organics induced a significant amount of water removal due to increased temperature, high organic content has a negative contribution on water removal by generating metabolic water. Water removal by air replacement is generally greater than that associated with temperature increases caused by biodegradation. However, excessive airflow rate can terminate biodegradation by drastically lowered moisture content even though organics remained.

Chapter 3 investigated a full-scale biocell type bio-drying MBT system. In this system, shredded MSW is mixed with recirculated wood and fine residues, and biodried outputs are mechanically separated to recover solid fuel materials. Waste samples were collected from five locations and material flow by the waste component was estimated. During the separation of biodried outputs, 62% of plastics and 54% of paper were recovered as raw material for RDF. Considering that unrecovered plastics and paper were returned to next biocell reactor, this ratio is not low. Wood was decreased by reduction in particle size and 90% of biodried wood is returned to next biocell reactor. Changes of mixed fine caused by size reduced wood particle and the loss of organic matters and 60% of it were returned. Operation variables are aeration rate and mixing rate of fresh air according to the operational phase. Daily water removal during 17-days of bio-drying was simulated through the model by using the operation data. Among the six operation phases, the longest stabilization phase was expected to major water removal period, but half of the water removal occurred at initial two stages and phase of cooling and drying or only 6 days in total due to the high waste temperature for sanitization (initial two stages) and high airflow

rate for cooling, respectively. Decreasing waste temperature at the stabilization phase resulted in low water evaporation.

Chapter 4 evaluated four systems for recovering energy from MSW in terms of life cycle energy and CO_2 emissions. Two of these were a type of MBT system, including a combined system of AD and incineration after mechanical separation, and bio-drying followed by mechanical separation for recovery SRF. The other two systems were incineration with high rate power generation and RDF production system by a mechanical drying process. Systems were compared based on the data collected from Asahikawa city and assumed to recover energy as a form of electricity. Process flow and parameters for operation and utility consumption in the four systems were adopted from the literature. The bio-drying system showed the highest energy efficiency. It reduced the fuel materials' energy content due to organic loss, but improved energy efficiency by low electricity and fuel consumption. The RDF production system recovered the highest energy by huge evaporation, but considerable fuel consumption resulted in the lowest energy efficiency. The combined system showed a higher energy recovery than incineration, but AD was less energy efficient due to electricity consumption. Lifecycle CO_2 emissions are closely related to energy balance. Among the various parameters, power generation efficiency and electricity consumption were highly sensitive to energy balance. The combined system showed low energy efficiency under a controlled set of parameters, but the efficiency was simultaneously compatible with the bio-drying MBT system under ideal conditions of parameters.

5.2 Possible application of the bio-drying MBT system

Based on these findings, possible applications of bio-drying MBT system are suggested.

In Japan, package plastics, PET bottles, glass, paper and other recyclables are source separated by citizen's active participation and residual combustible fractions are mostly treated by incineration for a long time targeting reduce the volume and amount of the waste. However, source separation depends highly on citizen's participation which often caused low efficiency. Additionally, collected individual waste requires individual waste treatment depending on waste type and results a parallel treatment system such as kitchen waste for animal feed or composting and PET bottles or package waste would be recycled. Meanwhile, Japan society is confronting the decrease in population and this urges small- or medium-sized cities where treated waste mainly by simple incineration without energy recovery a countermeasure of it. In this context, bio-drying MBT system can be a countermeasure in above issues by treating mixed MSW with low cost and energy consumption. At the same time, it recovers SRF that can be utilized as a substitute fuel in boilers of cement, paper manufacturing, or RDF exclusive boilers.

On the other hand, bio-drying MBT system can be applied to Asian countries where treats mixed MSW mainly by open dumping or landfill without any form of pretreatment. As a result, long term

management of leachate and landfill gas is required and this brings enormous financial burden to operator. Moreover, emission of gases such as methane carbon dioxide nitrous oxide, contributes to global warming and climate change. By application of bio-drying MBT system, organic fractions in mixed MSW would be partially stabilized and also recyclables and energy can be recovered by followed mechanical separation. Especially, static type reactor, is advantageous on energy efficiency in terms of low energy consumption and this would be beneficial in the cost for operation and maintenance. Still, marketability of fuel and securing its demand are need to be considered in Asian countries.

APPENDICES

Appendix for Chapter 2

Appendix for Chapter 3

Appendix for Chapter 4

Appendix for Chapter 2

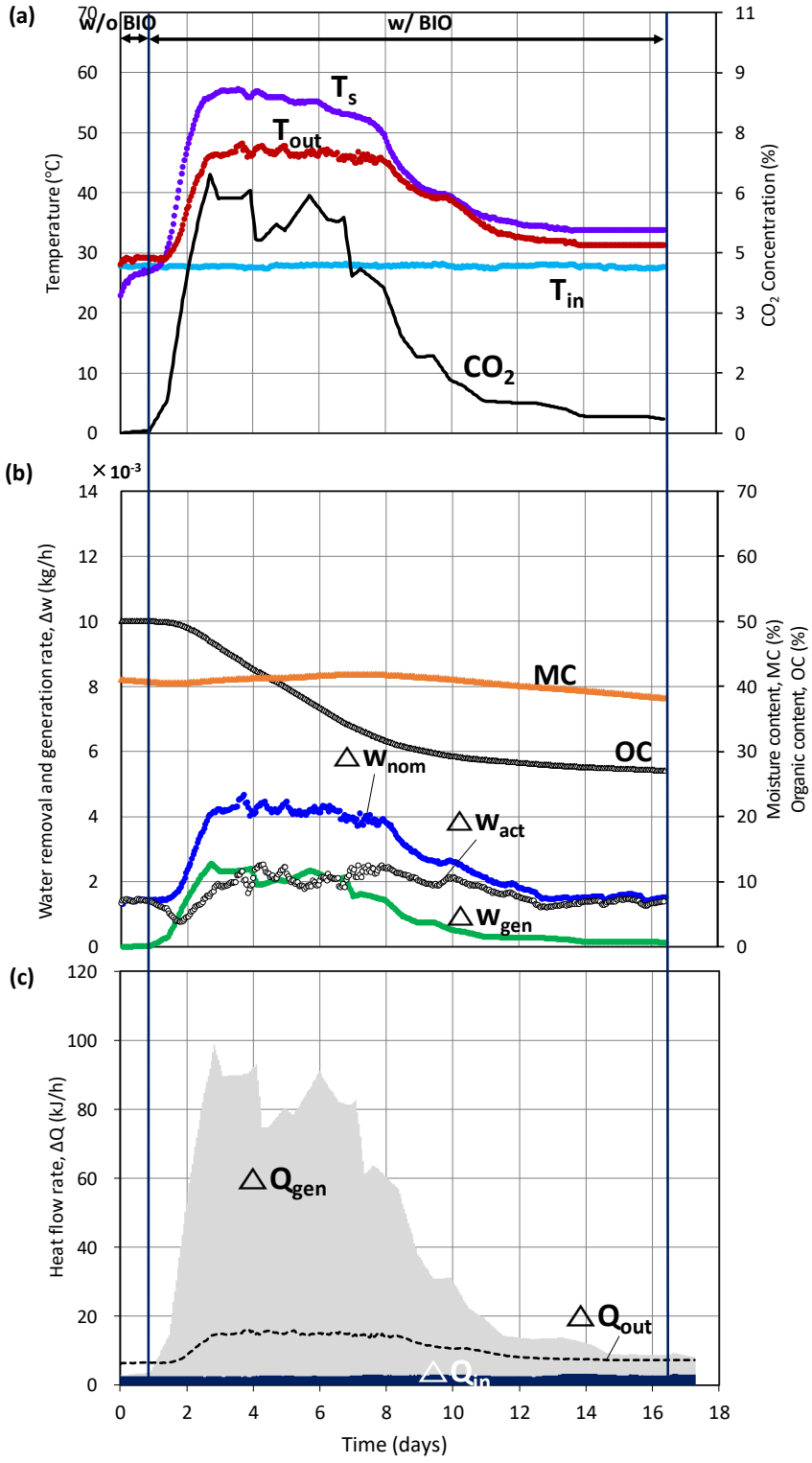

Figure A2-1 Experimental data and model output of run "50-1" (OC 50%, AFR 1 L/min)

(a) Temperature and CO2 concentration profiles (Measured) (b) Rate of water mass changes in balance (Estimated), (c) Heat profiles (Estimated)

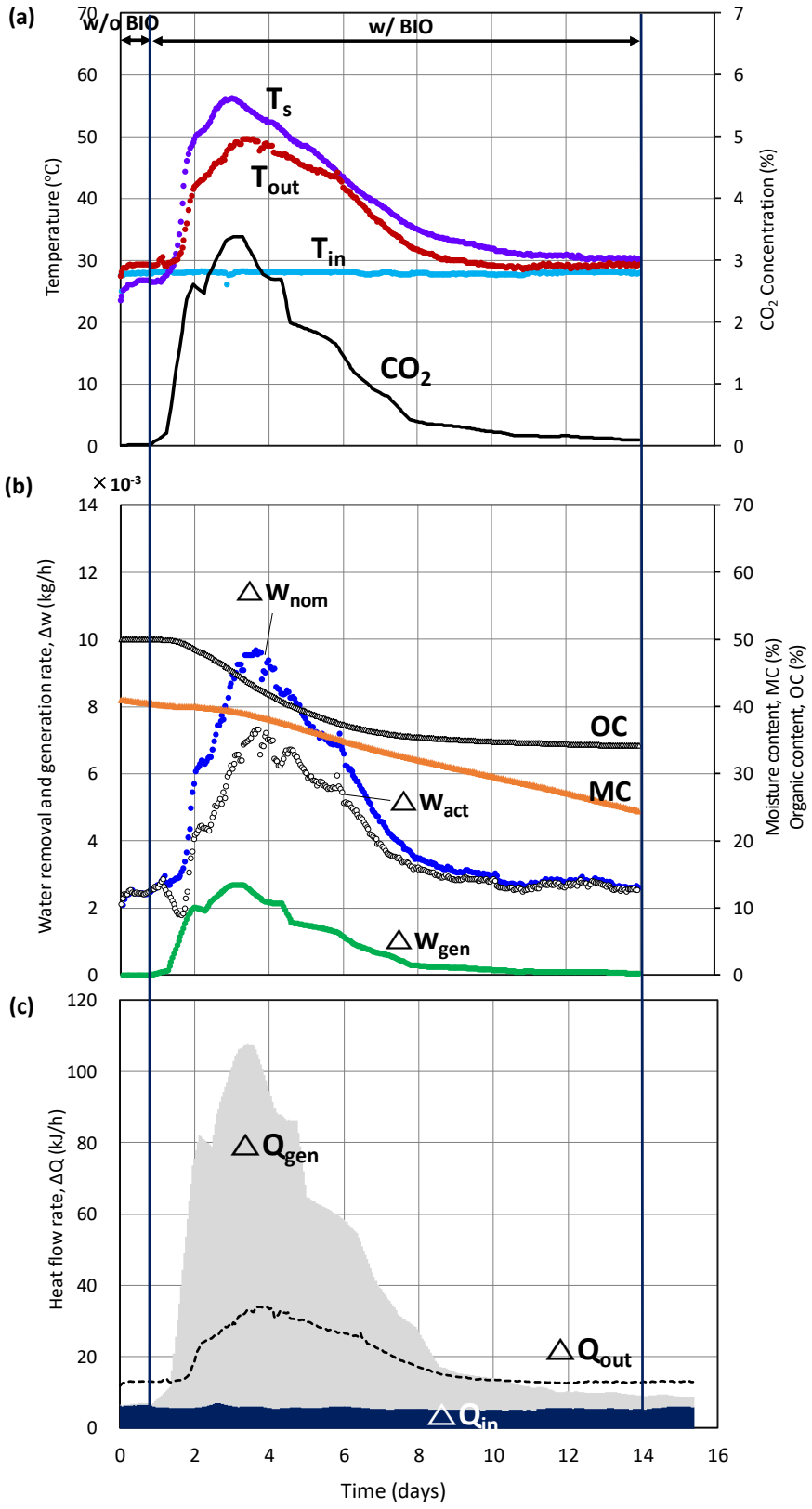

Figure A2-2 Experimental data and model output of run “50-2” (OC 50%, AFR 2 L/min)

(a) Temperature and CO2 concentration profiles (Measured) (b) Rate of water mass changes in balance (Estimated), (c) Heat profiles (Estimated)

Appendix for Chapter 3

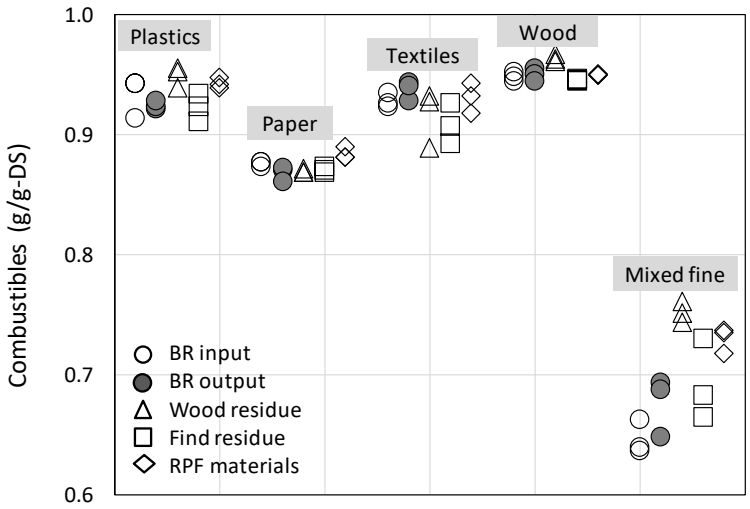

Figure A3-1 Combustible content of waste samples (analyzed in triplicate by each sample)

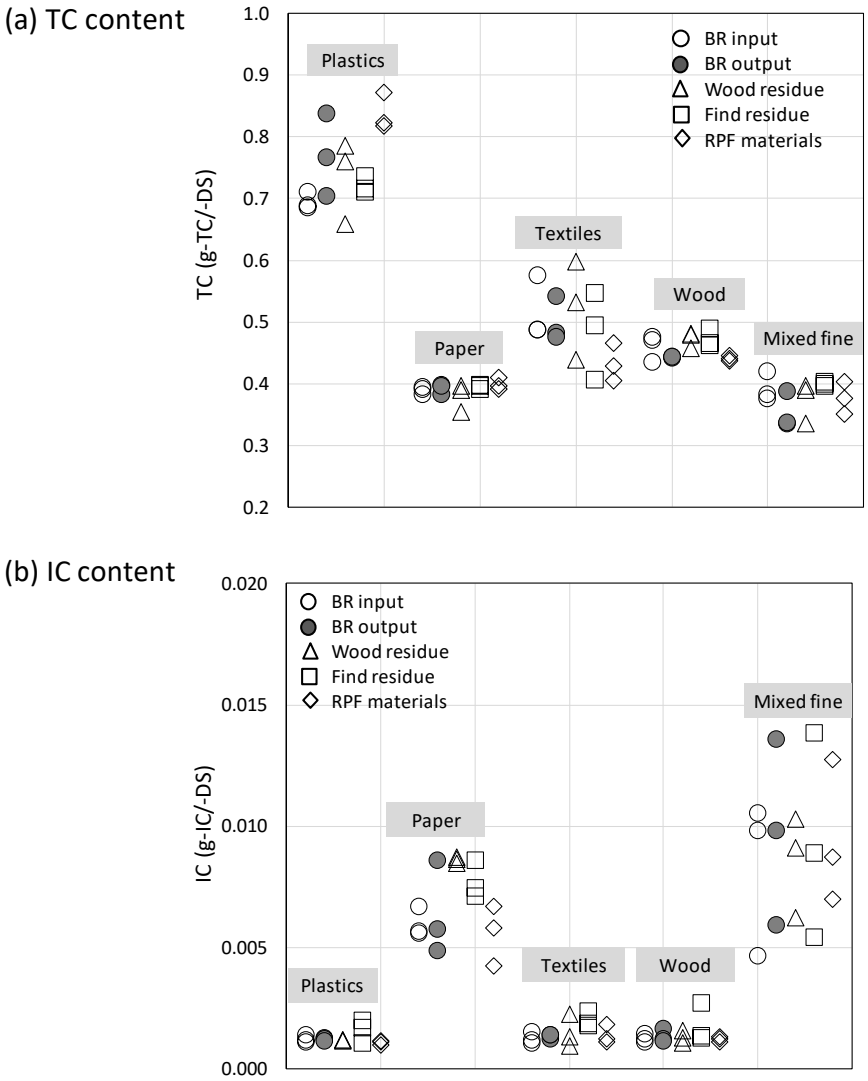

Figure A3-2 TC content and IC content of waste samples (analysed in triplicate by each sample)

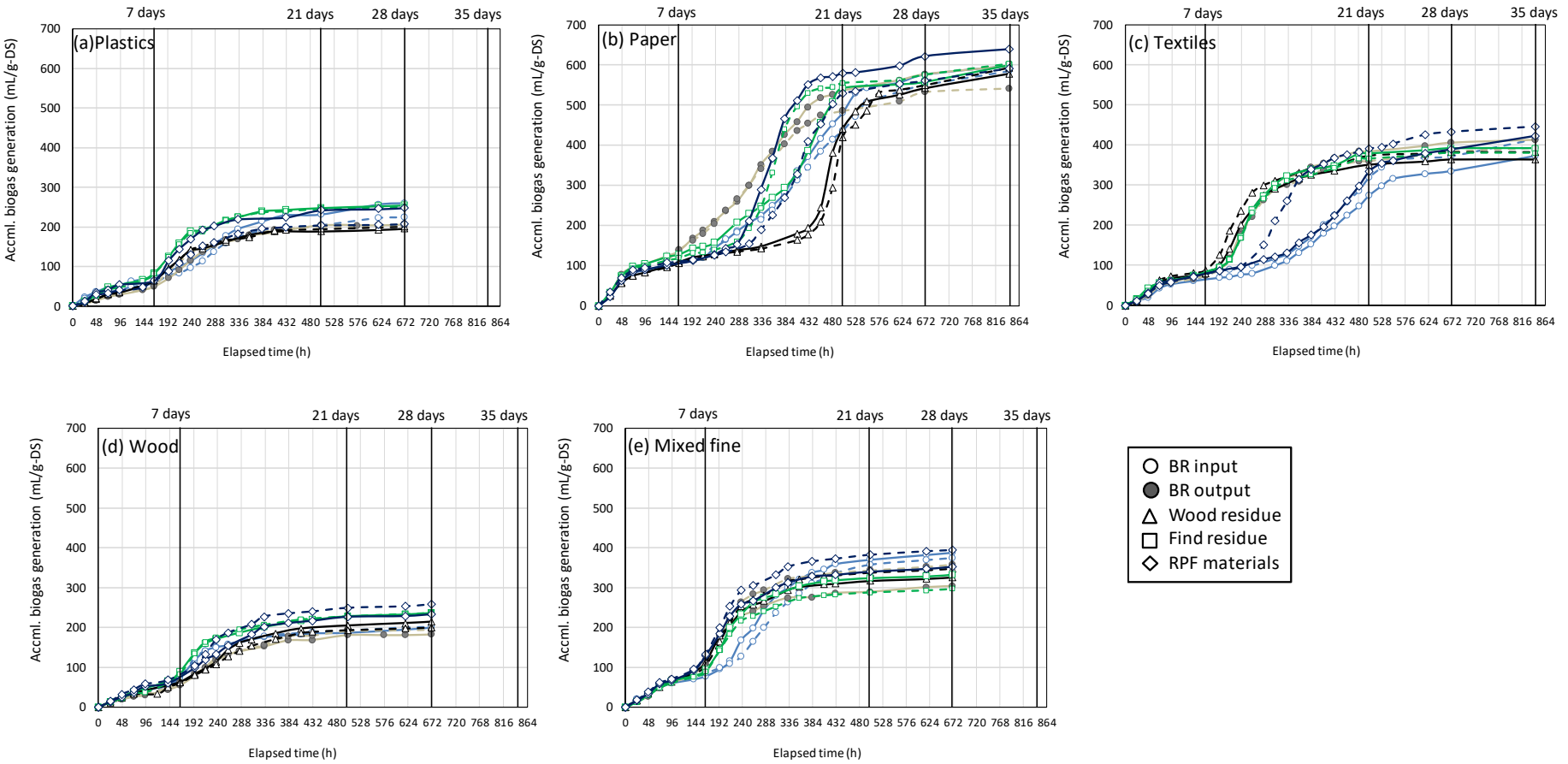

Figure A3-3 Biogas generation rate of waste by each component (analysed in duplicate by waste component of each samples)

(a) Plastics (b) Paper (c) Textiles (d) Wood (e) Mixed fine

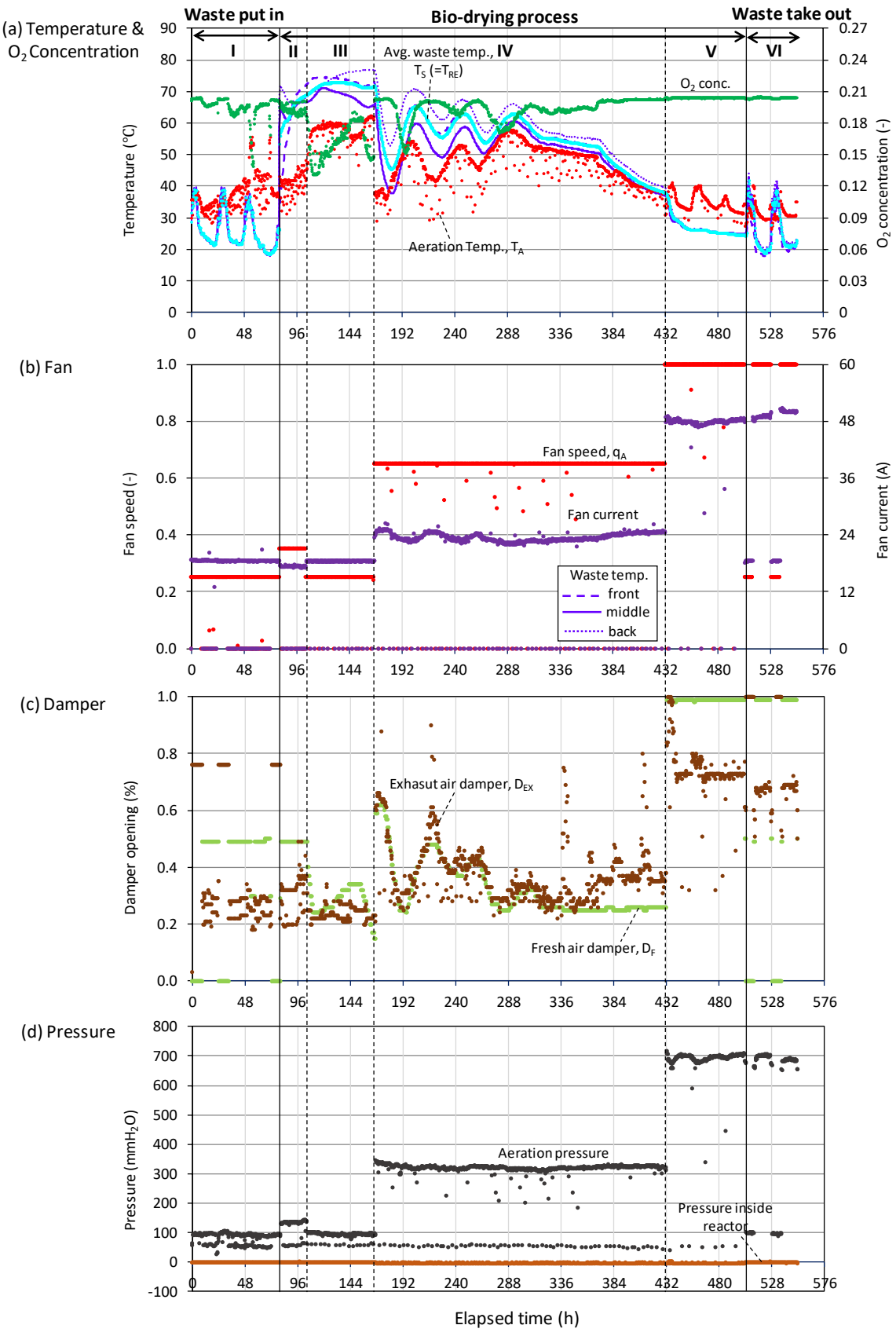

Figure A3-4 Profiles of monitored parameters of biocell reactor (BR3) during bio-drying process (9/17/2018- 10/10/2018)

Appendix for Chapter 4

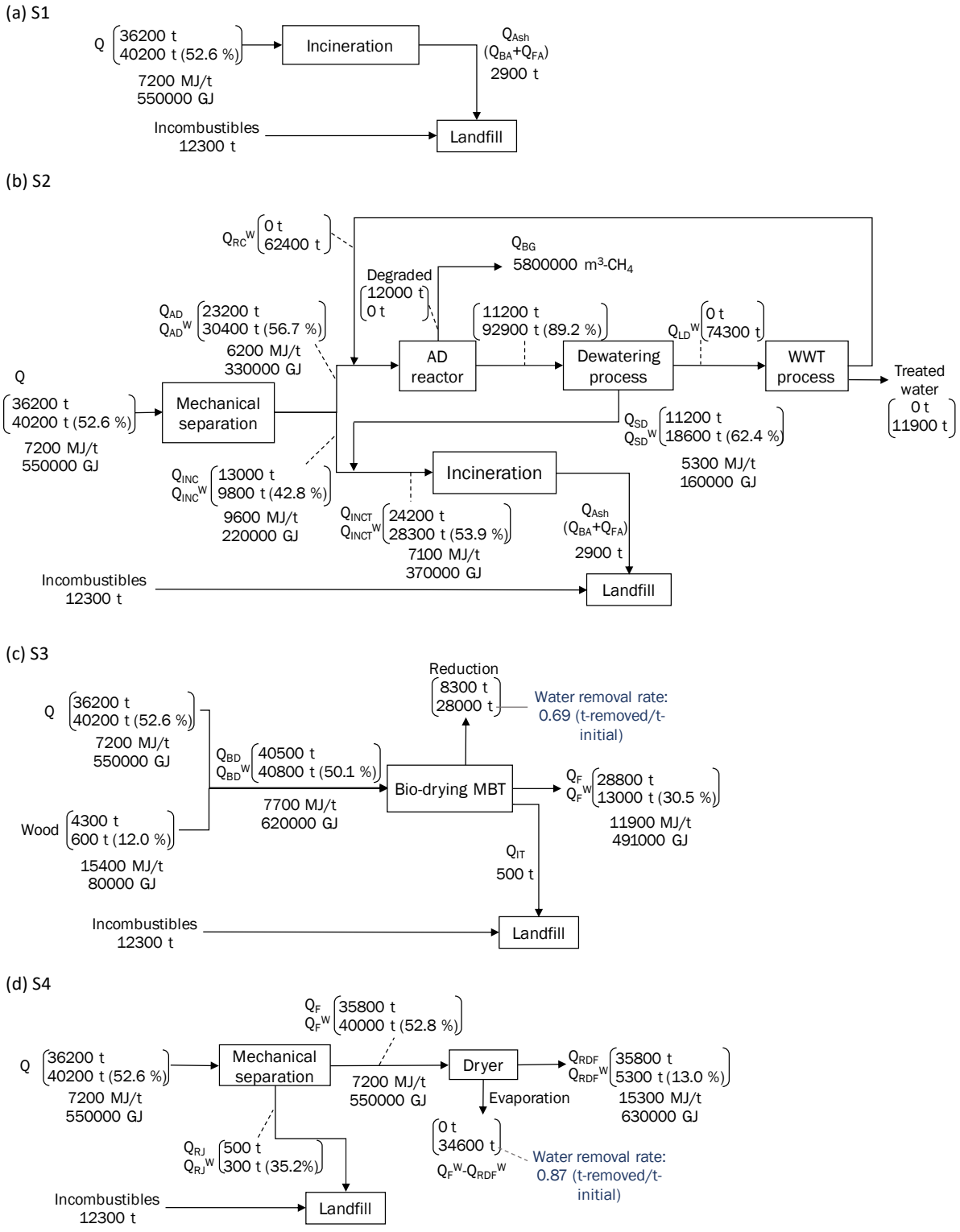

Figure A4-1 Mass flow with energy and moisture content of waste in four systems

Table A4-1 Summary of four systems

(a) Utility consumption and landfill waste

		S1	S2		S3	S4
			Inc.	AD		
Consumption	Electricity (GWh/y), U_E	13.6	9.4	15.6	7.4	22.0
	Fuel (kL/y), U_O	163	112		99	8989
	Water (m^3/y), U_W	45856	31534		5102	
	Alkali chemical (t/y), U_{AC}	446	307			
	Cement (t/y), U_S	37	37			
	Coagulant (t/y), U_C			11		
	Wood (t/y), U_{WD}				4915	
Landfill (t/y), U_{LF}		15158	15158		12778	13070

(b) Energy consumption and generation (Unit: GJ/y)

		S1	S2		S3	S4
			Inc.	AD		
Generation	Electricity recovery	272415	186154	162132	391918	501936
Consumption	Electricity	-128354	-88266	-146448	-70005	-207543
	Fuel	-6335	-4356		-3824	-346024
	Water	-614	-422		-68	
	Alkali chemical	-990	-681			
	Cement	-140	-140			
	Coagulant			-109		
	Wood				-8	
Net		135982	92288	15575	318012	-51632
Landfill		-9566	-9566		-8064	-8248

(c) CO_2 emission (Unit: t-C/y)

		S1	S2		S3	S4
			Inc.	AD		
Generation	Electricity recovery	3733	2551	2222	5370	6878
Consumption	Electricity	-1759	-1210	-2007	-959	-2844
	Fuel	-116	-79		-74	-6652
	Water	-8	-6		-1	
	Alkali chemical	-133	-92			
	Cement	-8	-8			
	Coagulant			-2		
	Wood				-121	
Net		1709	1156	213	4216	-2618
Landfill		-133	-133		-112	-115

Acknowledgments

Foremost, my most sincere gratitude goes to my supervisor Professor Toshihiko Matsuto for his continuous support of my Ph.D. study and research for the last three years. His patience, motivation, and unwavering enthusiasm kept me constantly engaged with my research. His insightful and thorough guidance helped me in all the time of research and writing of this thesis.

Besides my supervisors, I would also like to extend my thanks to the rest of my thesis committee: Professor Kazuei Ishii, and Professor Toshifumi Igarashi, for their encouragement, comments, and suggestions in completion of this thesis.

My sincere thanks also go to Associate Professor Yasumasa Tojo, Assistant Professor In-Hee Hwang, Mr. Takayuki Matsuo for supporting and encouraging me to move forward during my doctoral course. They always gave a hand whenever I was struggled or had difficulties in research. Thanks also go to laboratory secretary Ms. Shimoda and Ms. Yokono for their kind help. And I thank all my fellow mates in the Laboratory of Solid Waste Disposal Engineering: Zihao Guan, Rintaro Kikkawa, Kyohei Gonda, Takaaki Soga, Hisashi Takahashi, Hisashi Utsuno, Hajime Kusakabe, Masaya Yokokawa, Kouta Wada, for their friendship and kindness. One of the greatest memories I have is going hiking to Mt. Tarumae with you guys.

I wish to express my gratitude to Professor Dong-Hoon Lee of the University of Seoul for motivating me to study abroad and giving me the opportunity.

I am deeply grateful to the Graduate school of Engineering and e3 program and the Ministry of Education, Culture, Sports, Science, and Technology (MEXT), Japan for financial support of this research.

Last but not the least, I would like to give special thanks to my parents (Ki-Won Ham, Young-Hee Kim), siblings (Jin-Yong, Boo-Yong, and Eun-Yong) and my new family-in-law for their love, affection, and encouragement which enable me to keep moving forward without hesitation and concerns. Finally, I acknowledge my fiancée, Won-Kyu Kim, who has been giving me infinite love, trust, and support. I could not have come this far without you. I cannot wait to spend the rest of my life with you.

Geun-Yong Ham